Simulating Dark Matter and Galaxies

Ben Moore, Institute for Theoretical Physics, University of Zurich

- Old results from dark matter simulations + code comparison
- How do galaxies get there baryons?
- The imprint of reionisation on the Local Group
- Hydrodynamical code comparison

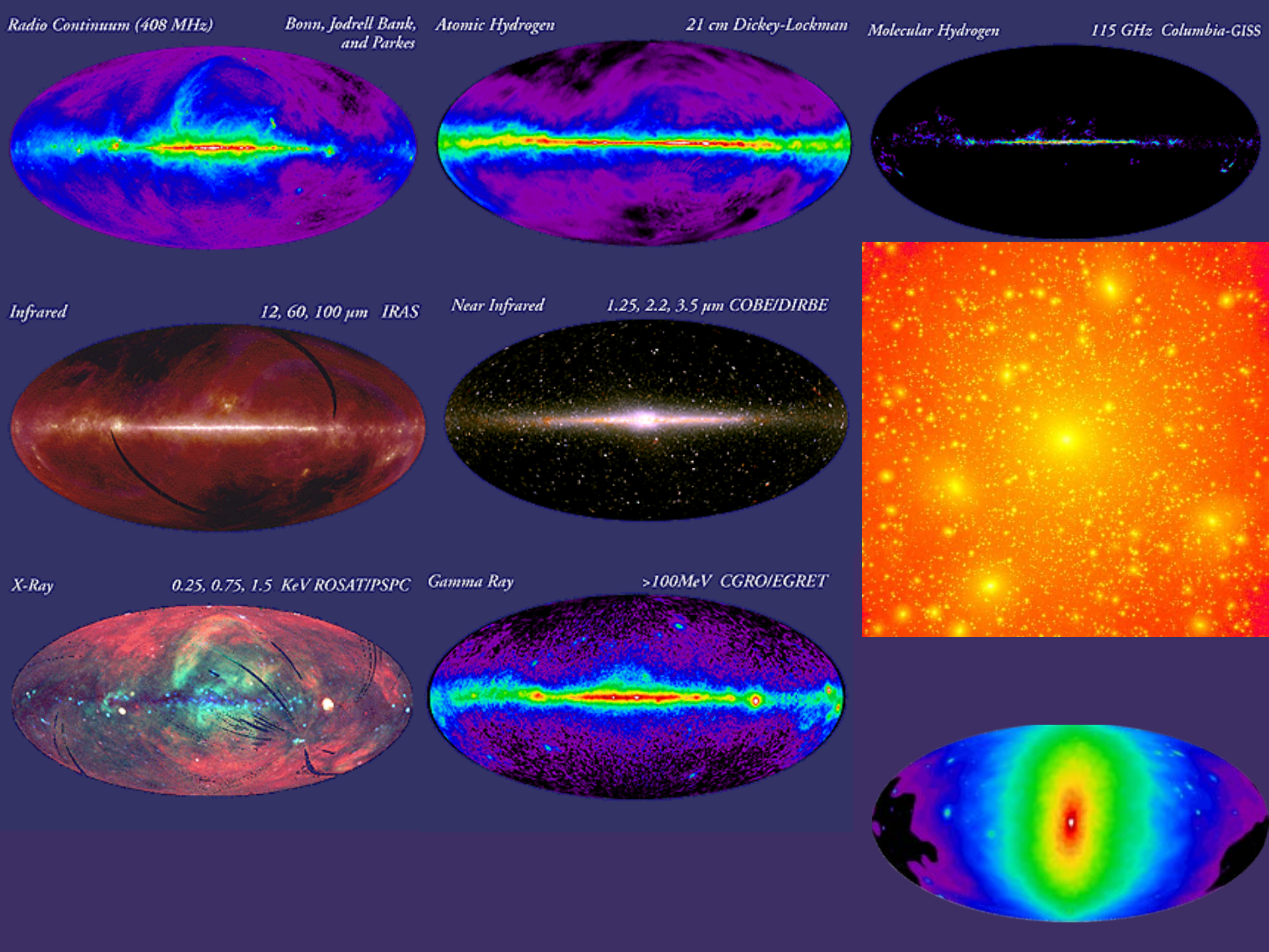
Radio Continuum (408 MHz)
Bonn, Jodrell Bank, and Parkes
Atomic Hydrogen
21 cm Dickey-Lockman
Molecular Hydrogen
115 GHz Columbia-GISS
Infrared
12, 60, 100 μm IRAS
Near Infrared
1.25, 2.2, 3.5 μm COBE/DIRBE
X-Ray
0.25, 0.75, 1.5 KeV ROSAT/PSPC
Gamma Ray
>100MeV CGRO/EGRET

The N-body technique

The collisionless Boltzmann equation is the fundamental equation of a collisionless system

$$\frac{\partial f}{\partial t} + v \cdot \frac{\partial f}{\partial r} - \nabla\Phi \cdot \frac{\partial f}{\partial v} = 0$$

Where $f = (x, y, z, v_x, v_y, v_z)$ is the phase space density.
This can be combined with Poissons equation to completely describe a gravitating system

$$\nabla^2\Phi = 4\pi G\rho$$

Where $\rho = \int f d^3v$

Solving these equations using finite difference techniques is impractical therefore solve the equations of motions of N particles directly. The N particles are a Monte-Carlo realisation of the true initial conditions.

$$\frac{dr}{dt} = v, \quad \frac{dv}{dt} = -\nabla\Phi$$

$$\Phi = -\sum_{i \neq j} \frac{Gm_j}{\left(\left|r_j - r_i\right|^2 + \varepsilon^2\right)^{1/2}}$$

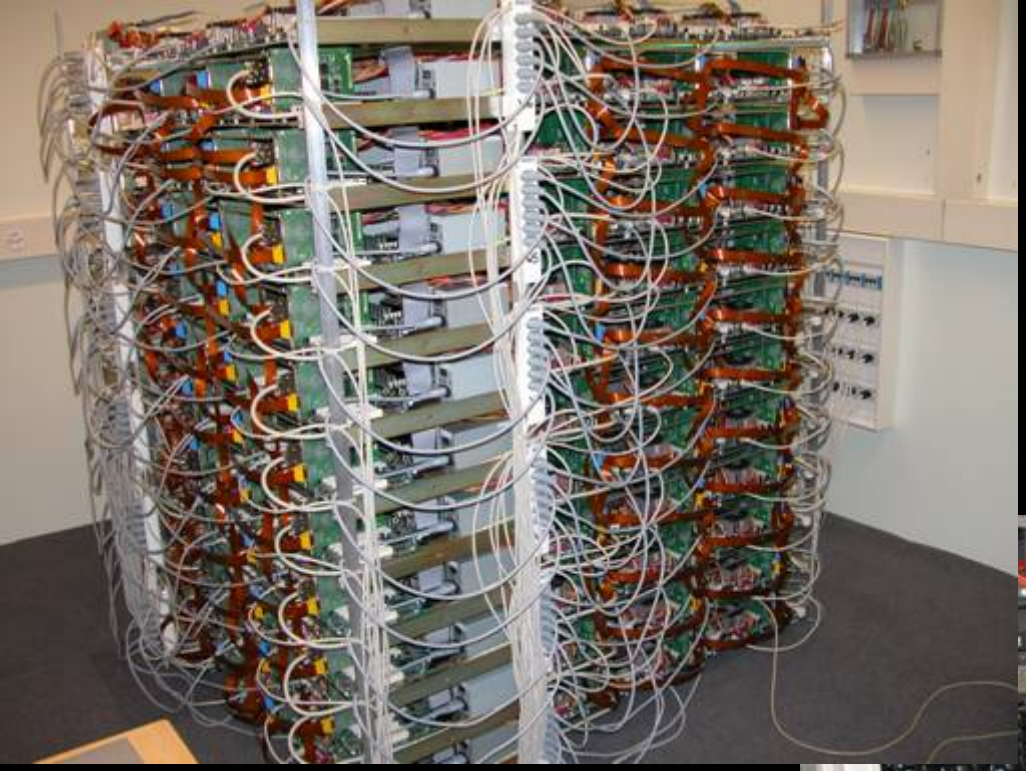

zBox2 (2006)

500 quad Opteron 852's, 580Gb memory, 65Tb disk, 3d-SCI low latency network.

zBox1: (Stadel & Moore 2002)

288 AMD MP2200+ processors, 144 Gigs ram

Compact, easy to cool and maintain

Very fast Dolphin/SCI interconnects - 4 Gbit/s, microsecond latency

A teraflop supercomputer for $500,000

Roughly one cubic meter, one ton and requires 40 kilowatts of power

R = 6.0 Mpc

z = 10.155

The formation of a cold dark matter halo.

This movie shows the density of dark matter in physical coordinates so that you can see the expansion of the universe.

a = 0.090

diemand 2003

Stable for about 10^70 Gyrs

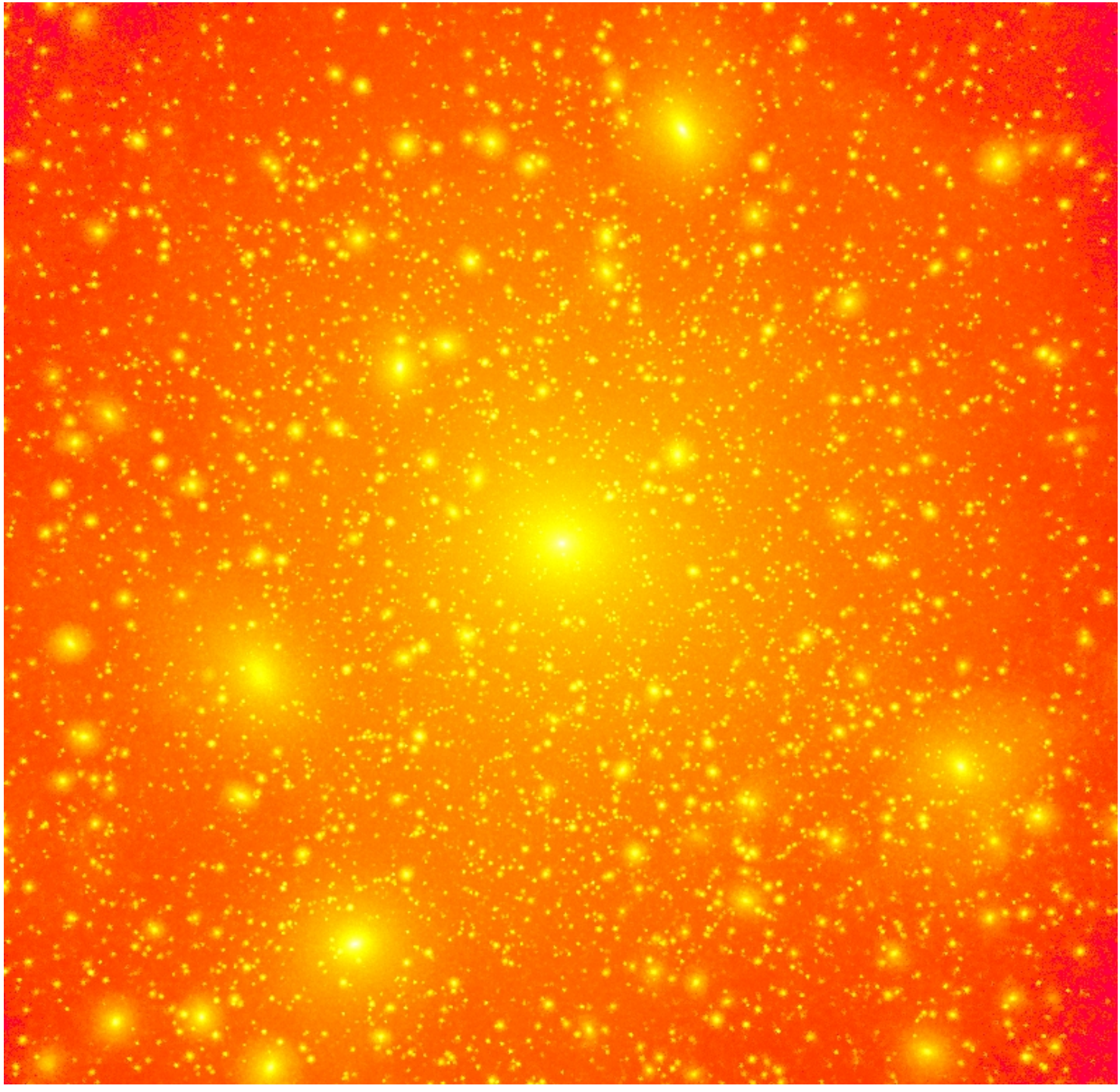

Density profiles and derivatives – ART, GRAPE, GADGET, PKDGRAV, TPM

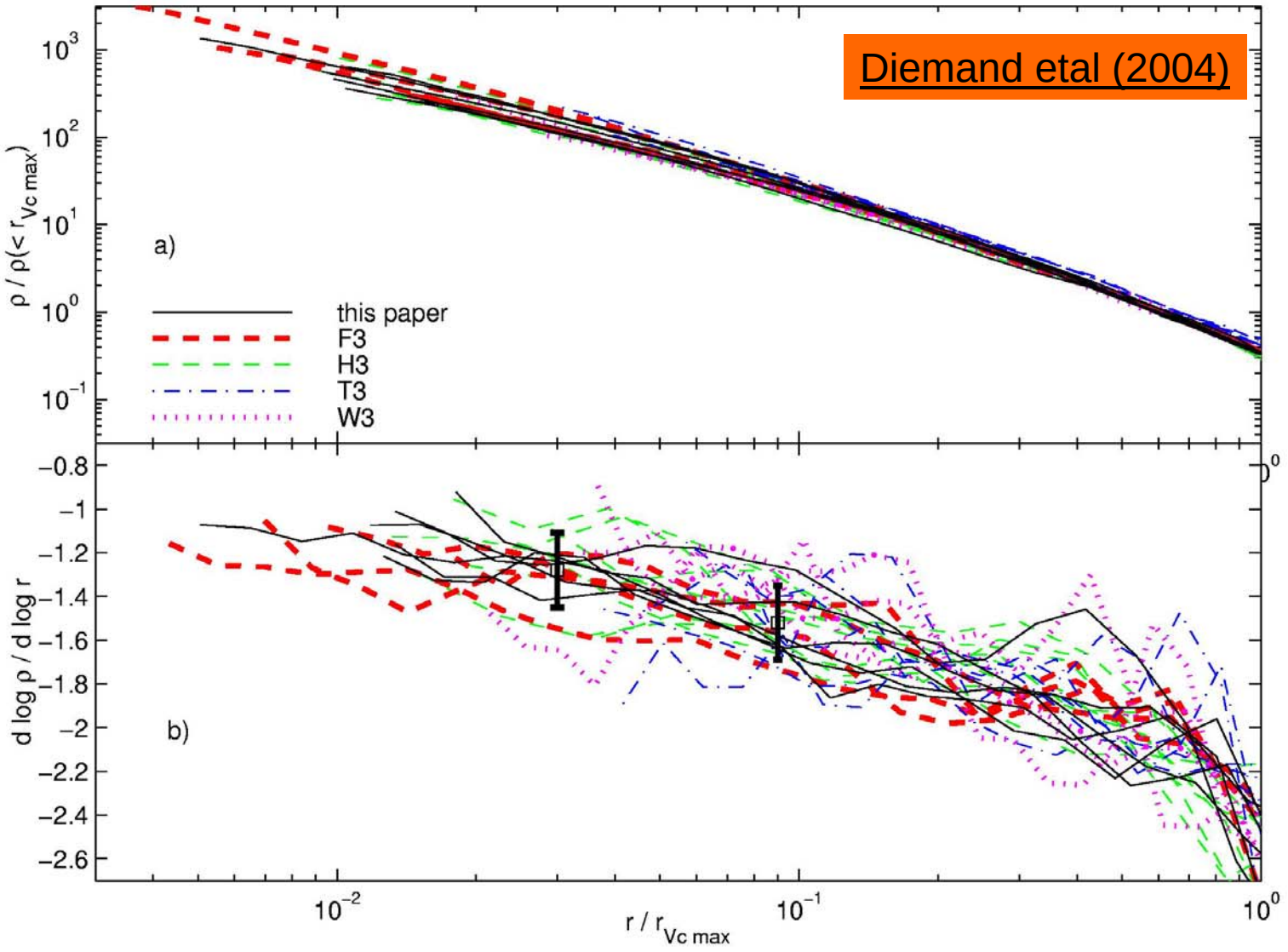

Figure 5. Panel (a): Density profiles of cluster simulated by different groups Normalized to the radius were the circular velocity peaks r_{Vcmax} and to $\rho(< r_{\mathrm{Vcmax}})$: Six cluster from this paper (solid lines), four from Fukushige et al. (2003) (thick dashed lines), eight from Hayashi et al. (2003) (thin dashed lines), six from Tasitsiomi et al. (2003) (dashed dotted lines)' four from Wambsganss et al. (2003) (dotted lines). Despite the different codes, parameters and initial conditions used the results are very similar. Panel (b): Logarithmic slope for the profiles from (a). Points with error bars give the averages at 0.03 and 0.09 r_{Vcmax} and a scatter of 0.15 (see Table 4).

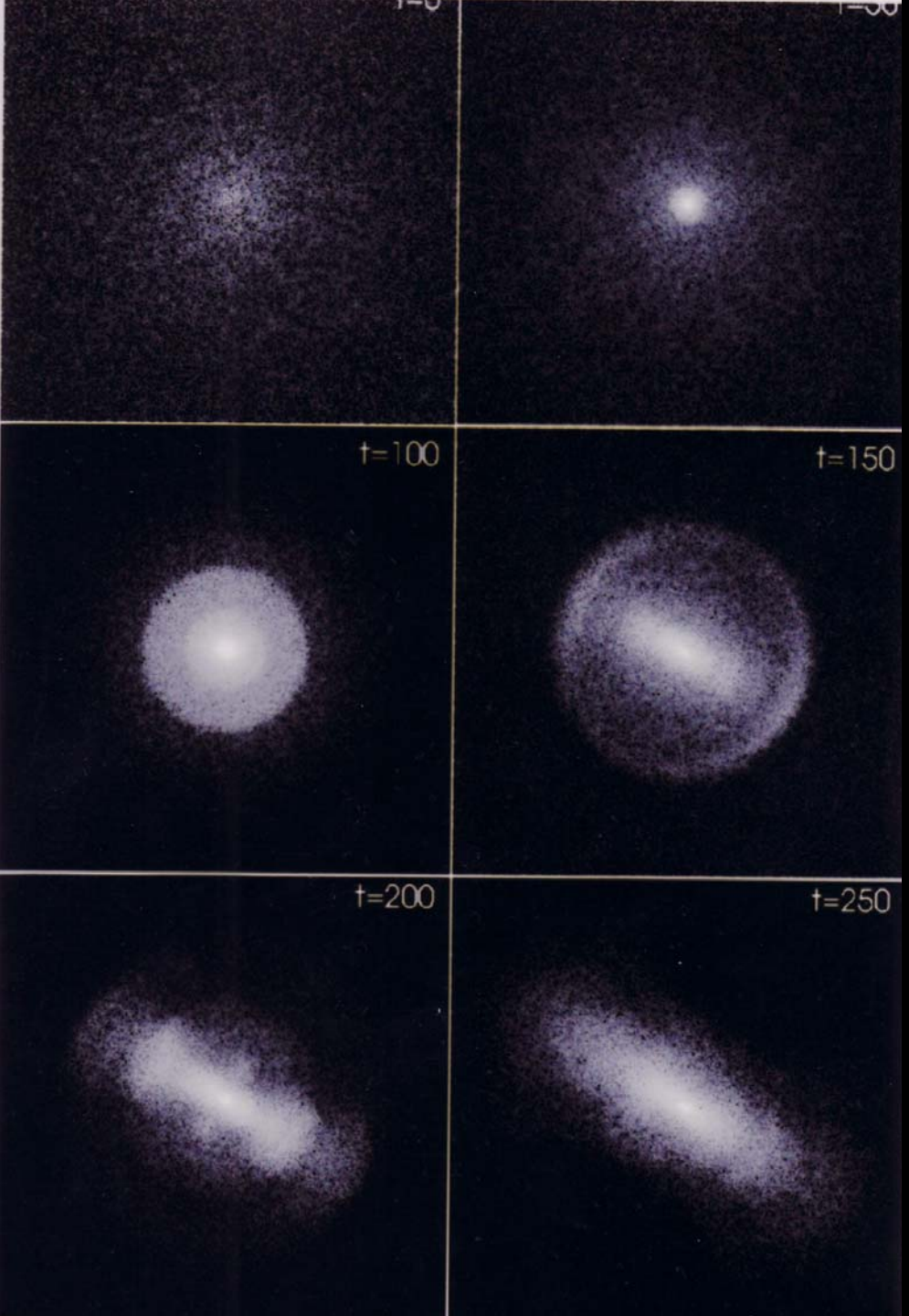

Historically the first n-body simulations were carried out to study the collapse of a cloud of stars. (van Albada 1968)

With 100 stars these authors found structures similar to elliptical galaxies.

However very cold collapses lead to a radial orbit instability and the system forms a prolate bar.

Numerical simulations show that k.e./p.e.>0.2 in order to suppress this instability.

Do real dark matter halos form triaxial structures??

Universal density profiles from spherical collapse simulations with different initial radial profiles... (Hansen etal in preparation)

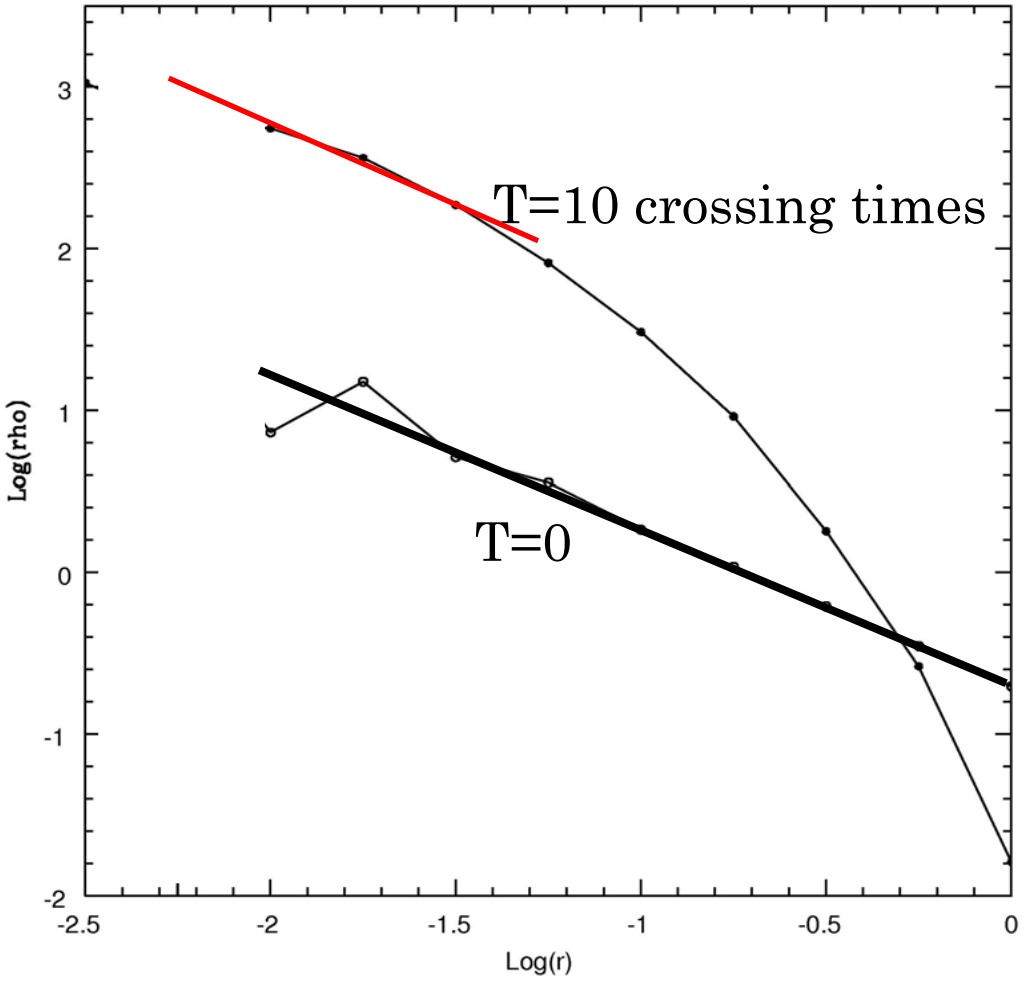

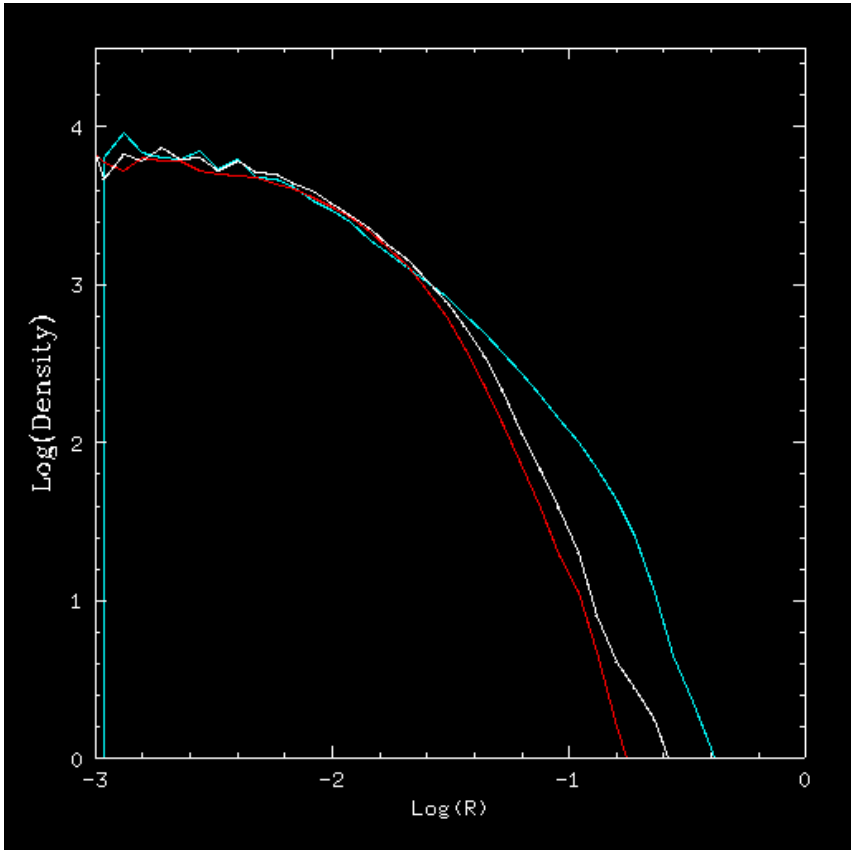

Bolatto, Blitz etal (2001)

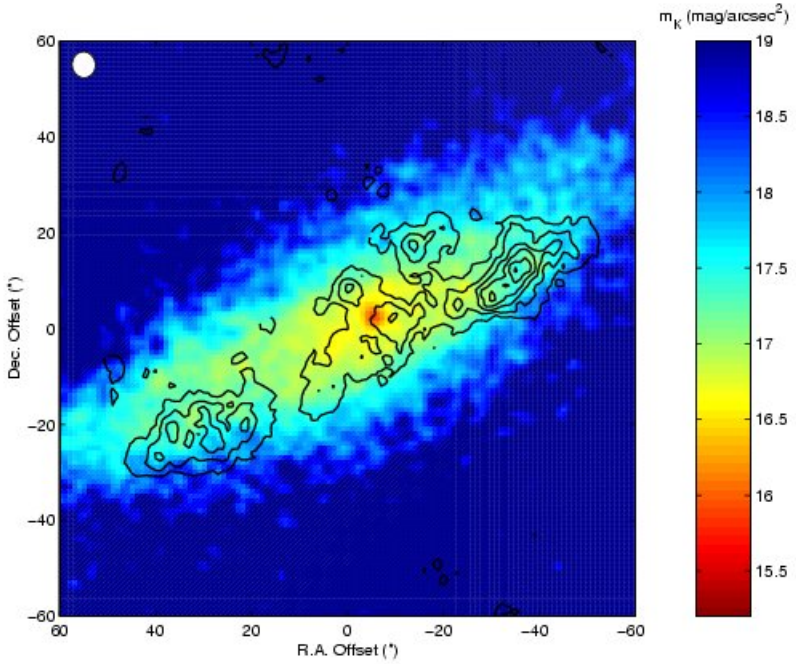

Fig. 1.— 2MASS K–band image of NGC 4605 with integrated intensity CO contours overlaid. The RMS of the integrated intensity data is ~ 130 mJy beam^{-1} km s^{-1} (~ 450 mK km s^{-1}). The contours start at 3σ and increase in steps of 4σ to 3 Jy beam^{-1} km s^{-1}. The offsets are with respect to NGC 4605's center, at $\alpha_{J2000} = 12^{\rm h}40^{\rm m}00\overset{\rm s}{.}0$, $\delta_{J2000} = 61°36'31''$. The synthesized beam is shown in the upper left corner.

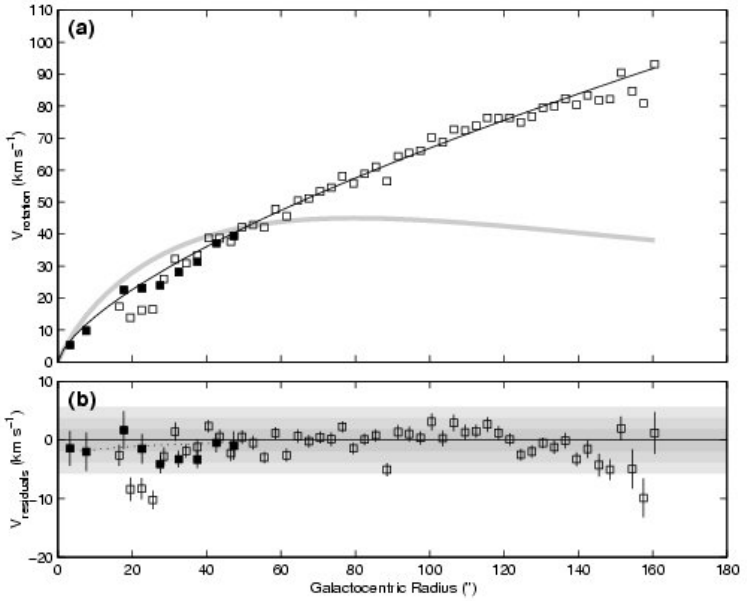

Fig. 5.— Combined CO and Hα rotation curve of NGC 4605 after removing the maximal disk. The key to symbols and lines is the same as in Fig. 4. The few data points missing had $v_c < v_{disk}$, yielding imaginary v_{halo}. Plot (a) shows the new outer halo fit for $r \in [40'', 140'']$, $\rho \propto r^{-0.65}$, and the fact that the maximal disk is dynamically dominant inside $r \sim 50''$. Plot (b) shows the residuals after removing the outer halo fit. The gray regions indicate 1σ, 2σ, and 3σ departures from the fit. There is no evidence for a break in the power law (i.e., a core) after the disk is removed.

Confrontation of rotation curves with predictions from numerical simulations

DeBlok, McGaugh, Rubin & Bosma (2002)

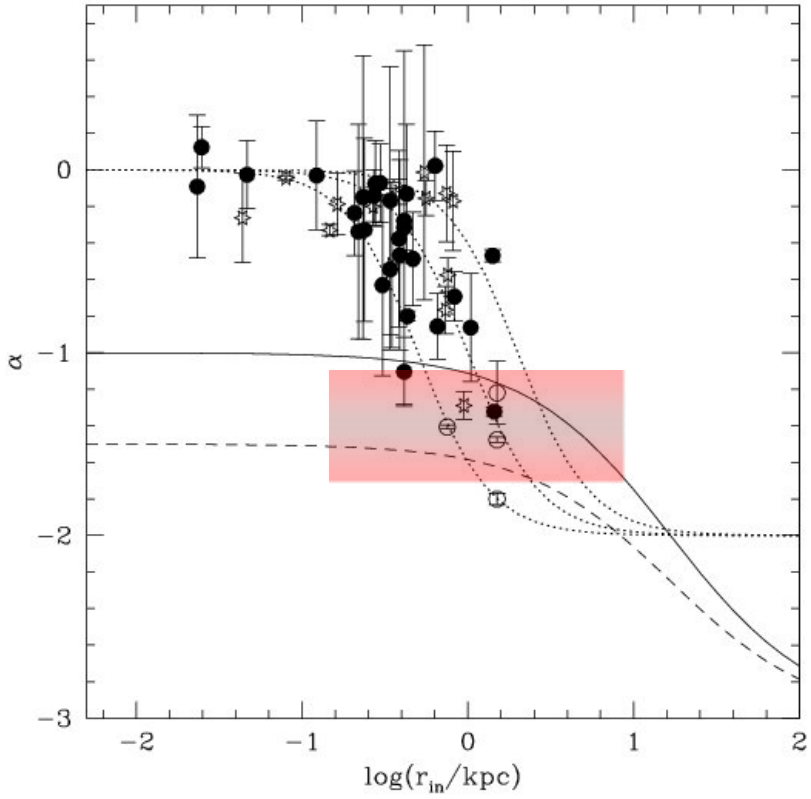

Swaters, Madore, van den Bosch & Balcells (2002)

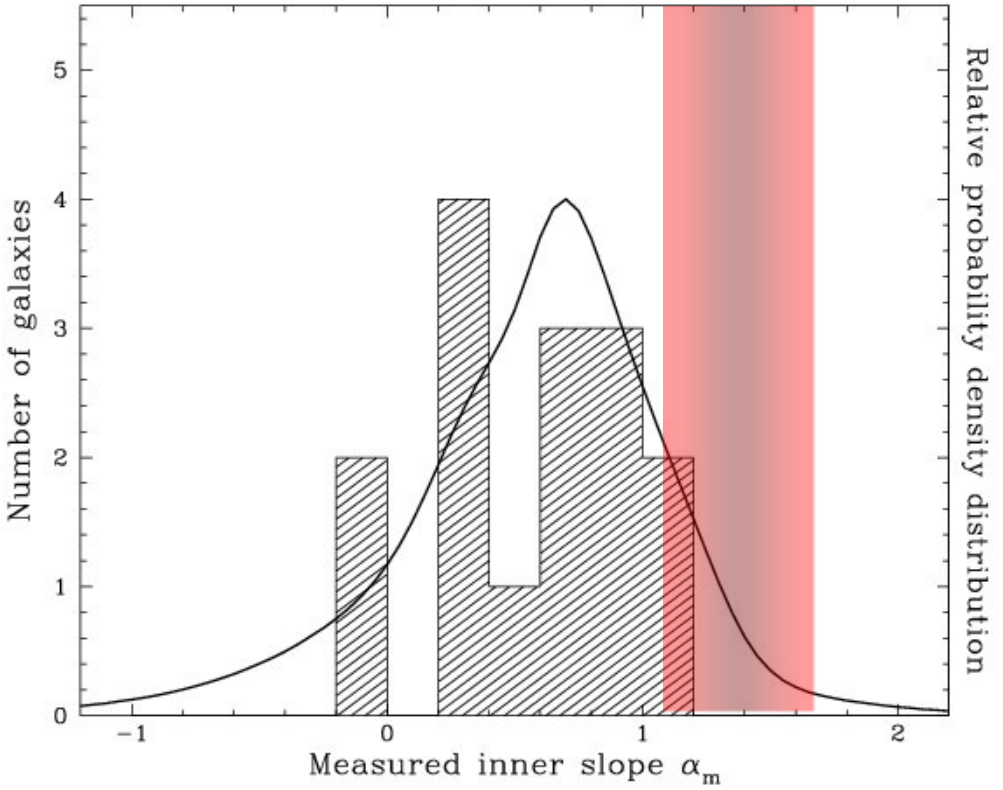

Bars heat core? Not all galaxies are barred i.e. M33. Bars are long lived.

Triaxility? CDM haloes are round, should observe 50% galaxies with steeper cusps.

Predictions of CDM on the scales of galaxies and clusters

Cusps vs cores

Still a problem, data better fit by cores.

No really good solutions as yet

Bars don't do it

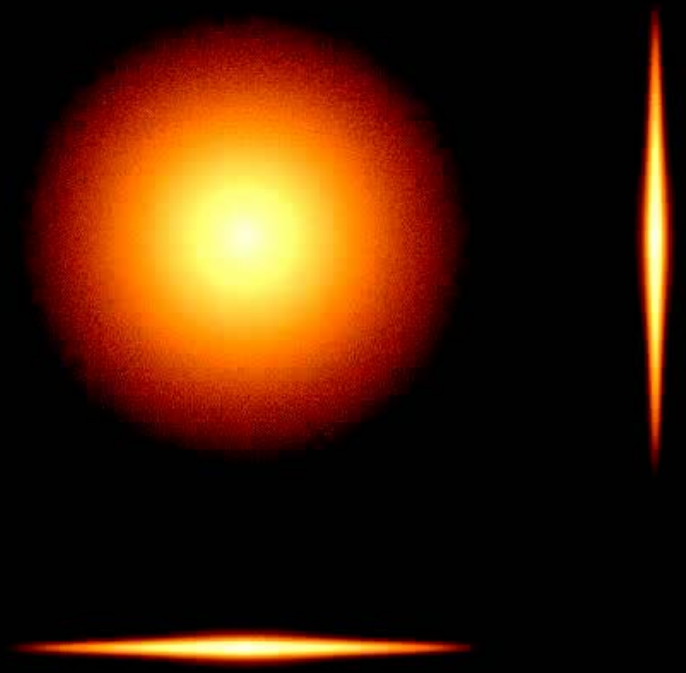

Dark matter substructures

Reionisation may work really well

Warm dark matter even better

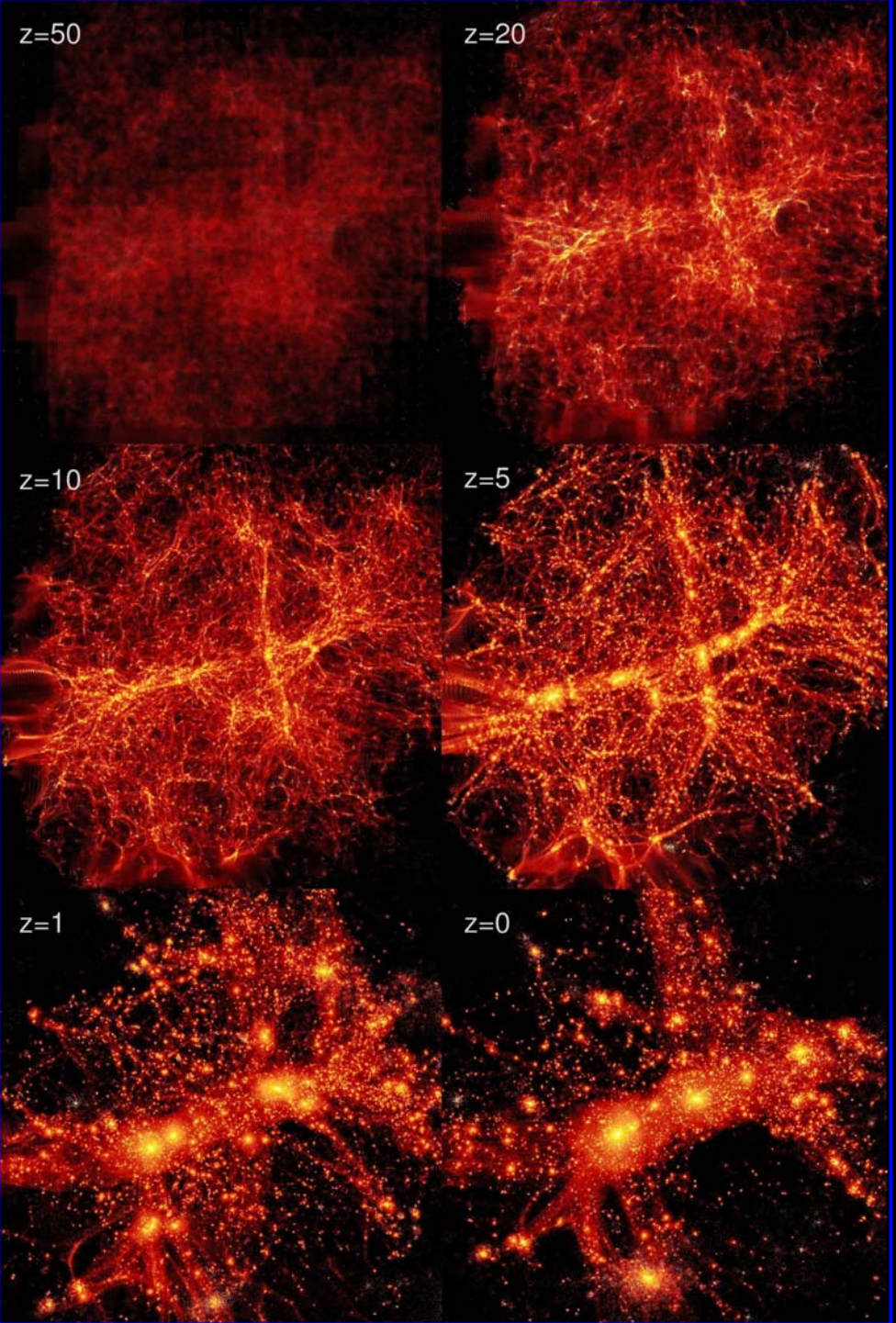

The formation and future of the Local Group of galaxies

Which galaxy merges with the MW first?

Sagittarius

Large Magellanic Cloud

M31

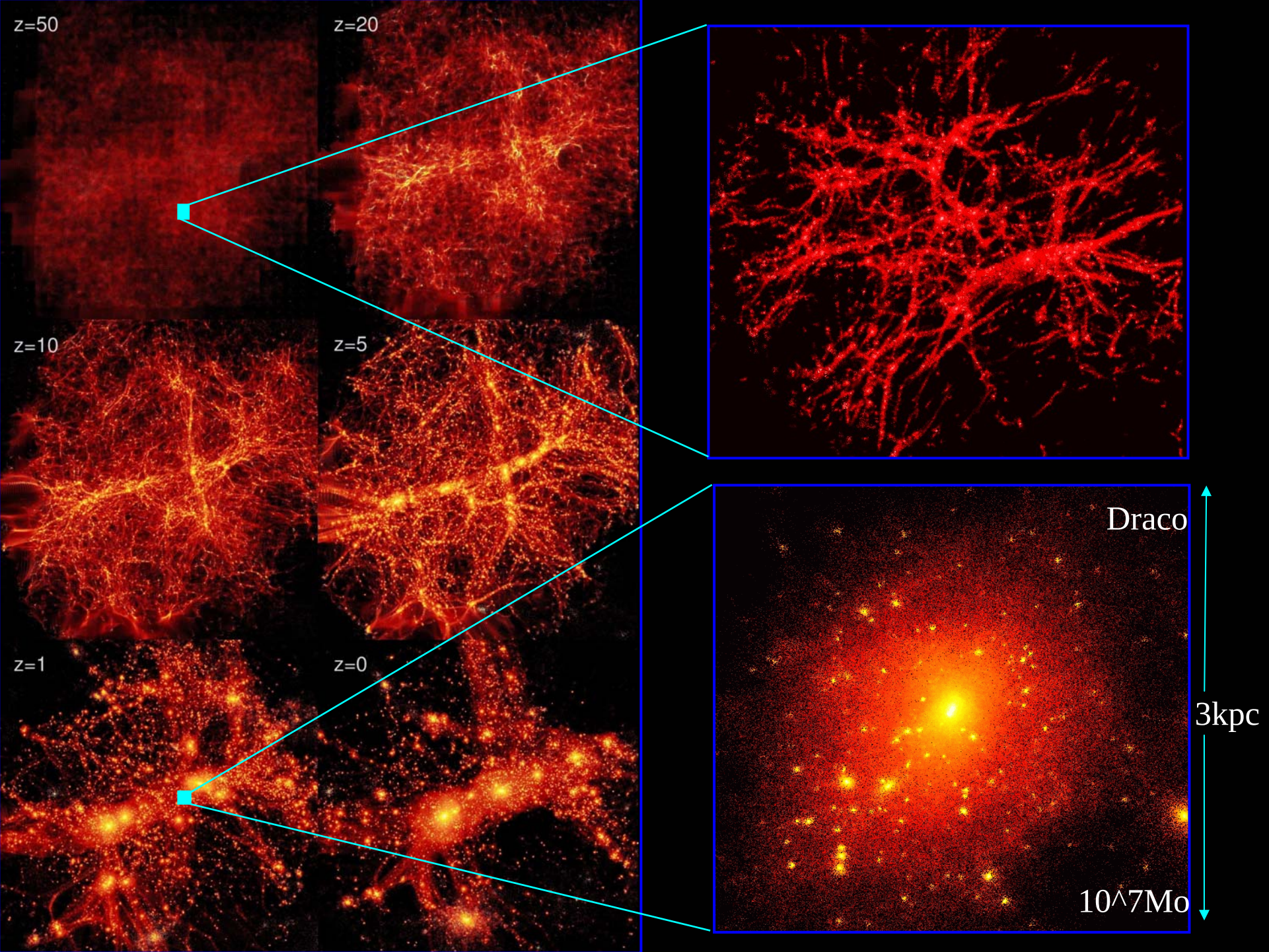
z=50
z=20
z=10
z=5
z=1
z=0
Draco
3kpc
10^7Mo

A dynamical fossil in the Ursa Minor dwarf spheroidal galaxy

Jan T. Kleyna[1], Mark I. Wilkinson[2], Gerard Gilmore[3], N. Wyn Evans[4],

[1,2,3,4]*Institute of Astronomy, Madingley Road,Cambridge, CB3 OHA, UK*

[1]*kleyna@ast.cam.ac.uk;* [2]*markw@ast.cam.ac.uk;* [3]*gil@ast.cam.ac.uk;* [4]*nwe@ast.cam.ac.uk*

ABSTRACT

The nearby Ursa Minor dwarf spheroidal (UMi dSph) is one of the most dark matter dominated galaxies known, with a central mass to light ratio $M/L \sim 70$. Somewhat anomalously, it appears to contain morphological substructure in the form of a second peak in the stellar number density. It is often argued that this substructure must be transient because it could not survive for the > 10 Gyr age of the system, given the crossing time implied by UMi's 8.8 km s^{-1} internal velocity dispersion. In this paper, however, we present evidence that the substructure has a cold kinematical signature, and argue that UMi's clumpiness could indeed be a primordial artefact. Using numerical simulations, we demonstrate that substructure is incompatible with the cusped dark matter haloes predicted by the prevailing Cold Dark Matter (CDM) paradigm, but is consistent with an unbound stellar cluster sloshing back and forth within the nearly harmonic potential of a cored dark matter halo. Thus CDM appears to disagree with observation at the least massive, most dark matter dominated end of the galaxy mass spectrum.

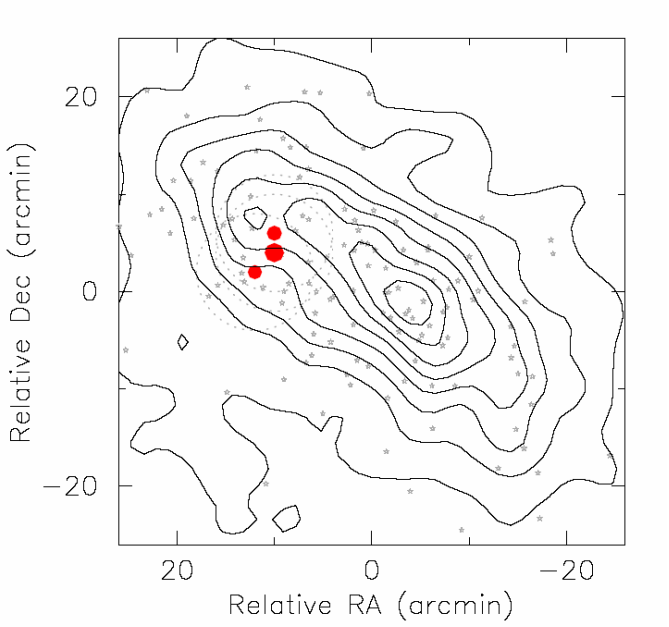

Kleyna etal modelled the cold clump of stars as an unbound system which disperses in a cuspy potential. Oscillates as a "coherent" system in a core. (All orbital frequencies the same)

Goerdt et al 2006

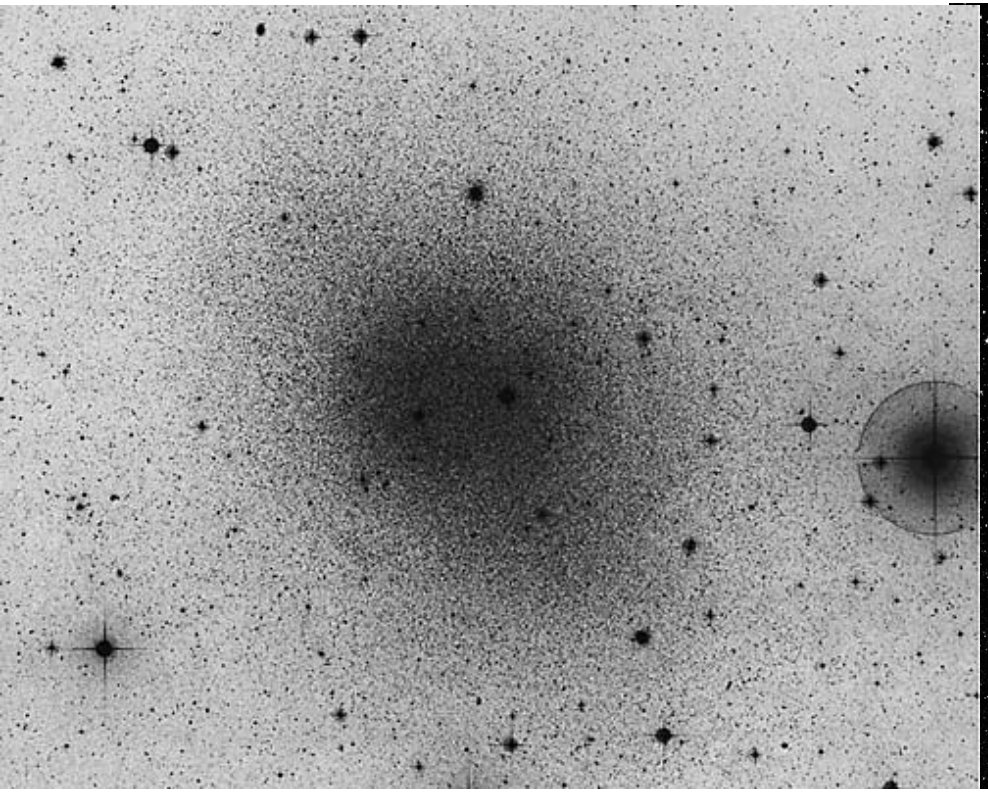

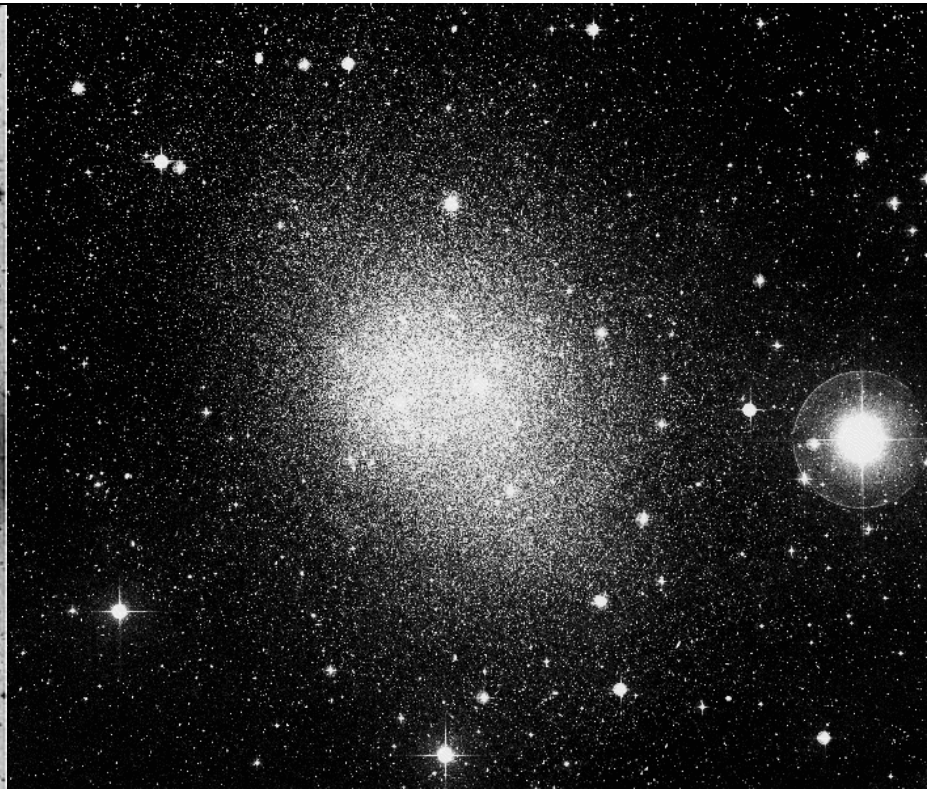

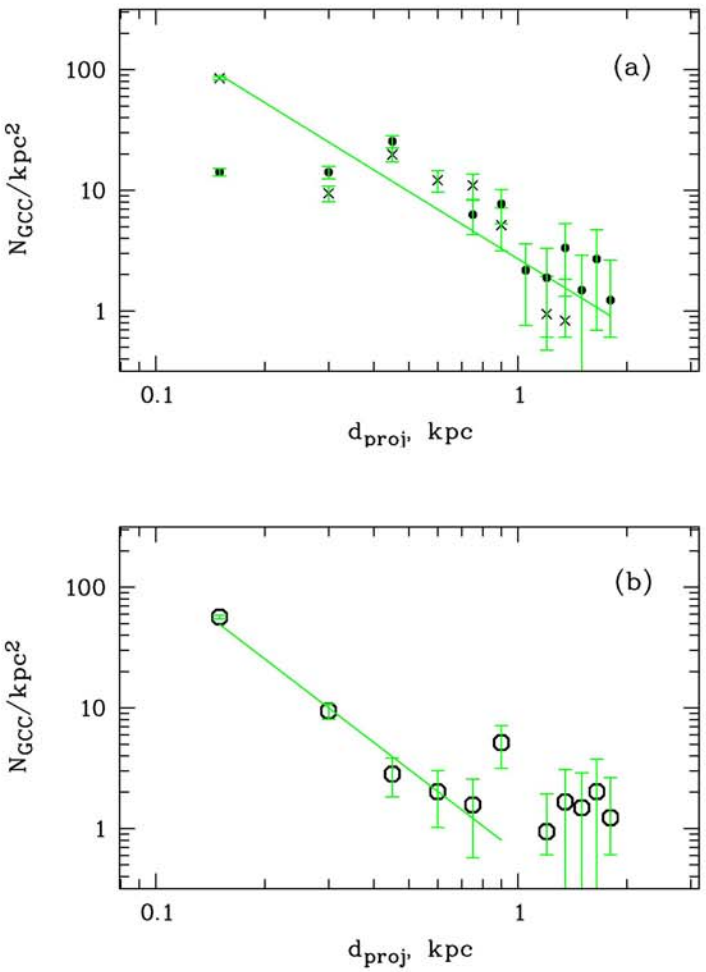

Fig. 7. Radial distribution of GCCs in dIrr galaxies *(panel a)* and dSph galaxies *(panel b)*. The sample of GCCs in dIrrs is divided into blue GCCs with $(V-I)_0 < 0.75$ *(dots)* and red GCCs $(V-I)_0 > 0.75$ *(crosses)*. Plotted here is the logarithm of the surface density of GCCs per square kpc (evaluated in 0.15-kpc bins) vs. the logarithmic projected distance from the galaxy center, in kpc.

galaxies seems to flatten out beyond ~ 1 kpc galactocentric distance. Hence, the fit includes only the inner part of the GCC population. The profiles of the GCC population in dIrr galaxies do not show a flattening at large galactocentric distances.

These values are in good agreement with those found for globular cluster systems in elliptical ($x = 0.8 - 2.6$, Puzia et al. 2004) and dwarf elliptical galaxies ($x = 1.6 \pm 0.4$, Durrell et al. 1996). Moreover, Harris (1986) found $x = 3.5 \pm 0.5$ for the combined spatial distribution of globular clusters in NGC 147, NGC 185 and NGC 205. Minniti et al. (1996) constructed a composite dwarf elliptical galaxy from all early-type dwarf galaxies in the Local Group and computed $x = 2.1$.

4.4. Structural Parameters

Under the superb spatial resolution of HST/WFPC2, typical globular clusters (Harris 1996) begin to be resolved for galaxies less distant than $D \sim 10$ Mpc. Using our King-profile approximation routine we measure structural parameters for all our sample GCCs. Figure 8 shows half-light radii, r_h, and core radii, r_c of GCCs as a function of their projected galactocentric distance. Both panels show a trend of increasing half-light and core radius as a function of increasing galactocentric distance. These correlations are however driven by the outermost GCCs. Spectroscopy is necessary to measure their radial velocities and test whether these objects are genuine globular clusters or resolved background galaxies. If we consider GCCs with projected distances less than ~ 1 kpc to avoid potential contamination by background sources (see Fig. 7b), we find only tentative evidence for a r_c–$d_{\rm proj.}$ correlation. With the same radial constraint we find no correlation between half-light radius and galactocentric distance.

Goerdt et al (2006) – sinking globular clusters produce core and stall there

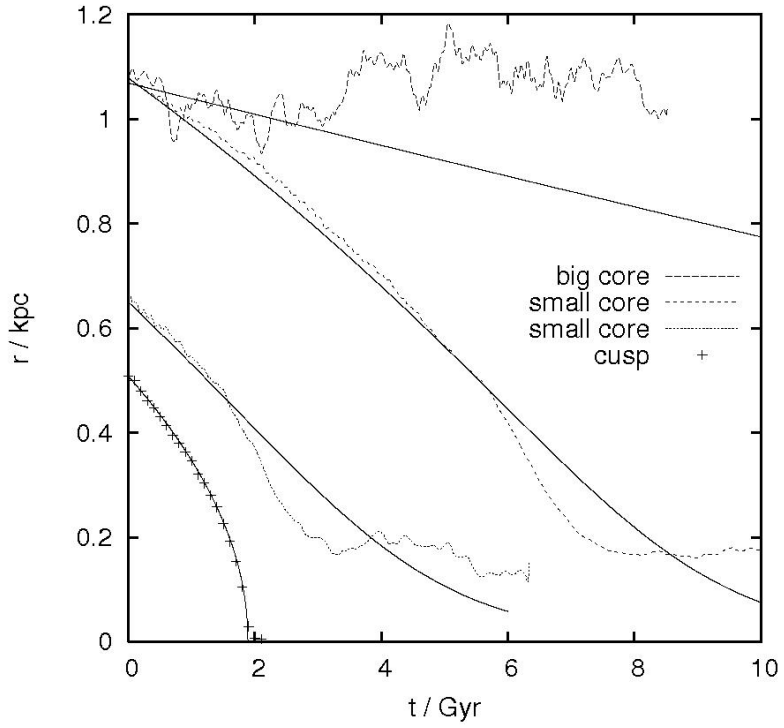

Figure 2. Radial distance of the single globular cluster from the centre of its host halo as a function of time. We start the calculations with the globular at different initial radii for clarity. Solid curves are the analytic estimates, dashed curves are from the numerical simulations.

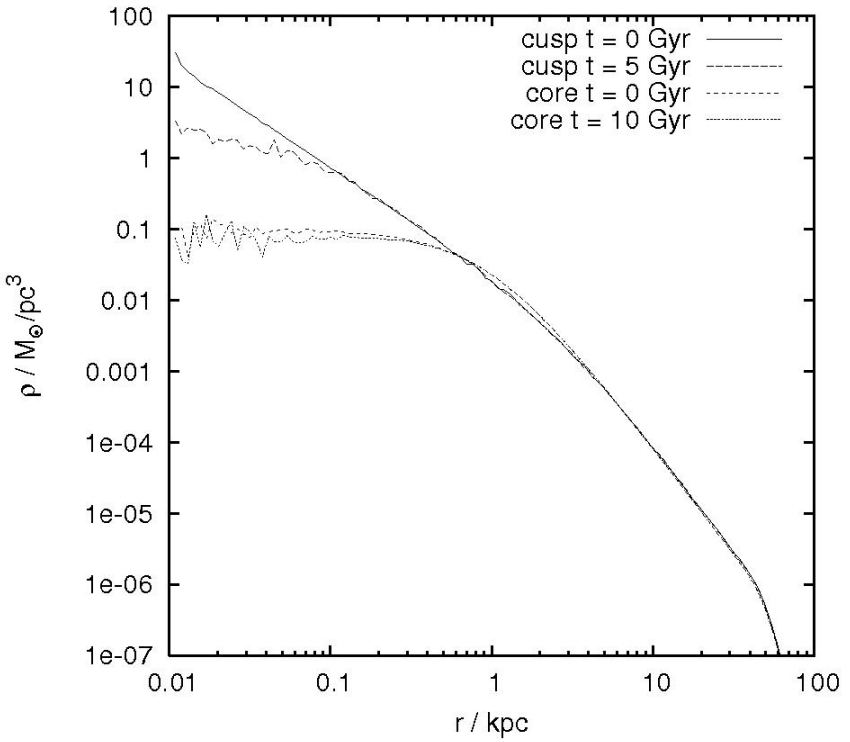

Figure 5. Radial density profile of the dark matter haloes. Only the dark matter is shown, the mass of the globular clusters is neglected. The initial conditions are compared with the final state of the system. An isolated halo, evolved for the same time, has exactly the same density profile as the initial conditions.

Read et al (2006) show that dynamical friction fails due to resonance

Core

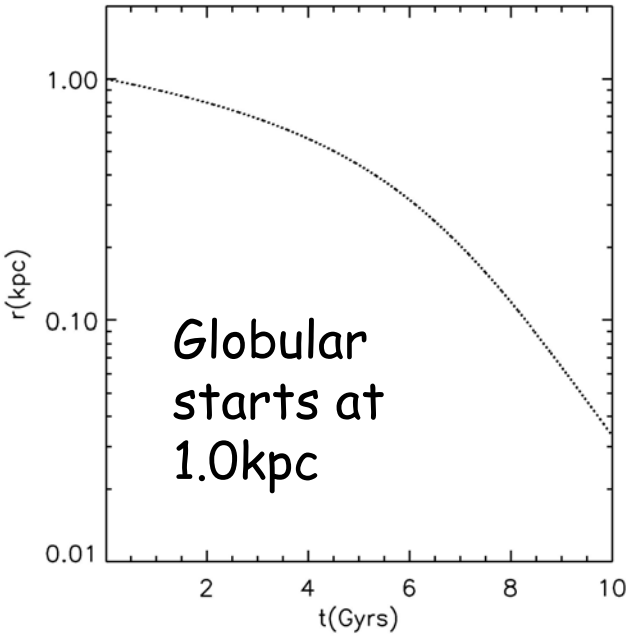
1.00
0.10
0.01
r(kpc)
2
4
6
8
10
t(Gyrs)
Globular
starts at
1.0kpc

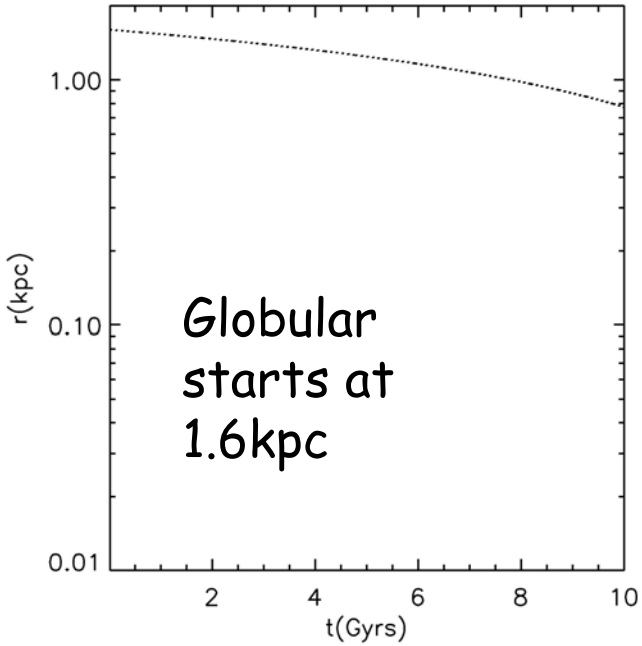
1.00
0.10
0.01
r(kpc)
2
4
6
8
10
t(Gyrs)
Globular
starts at
1.6kpc

NFW

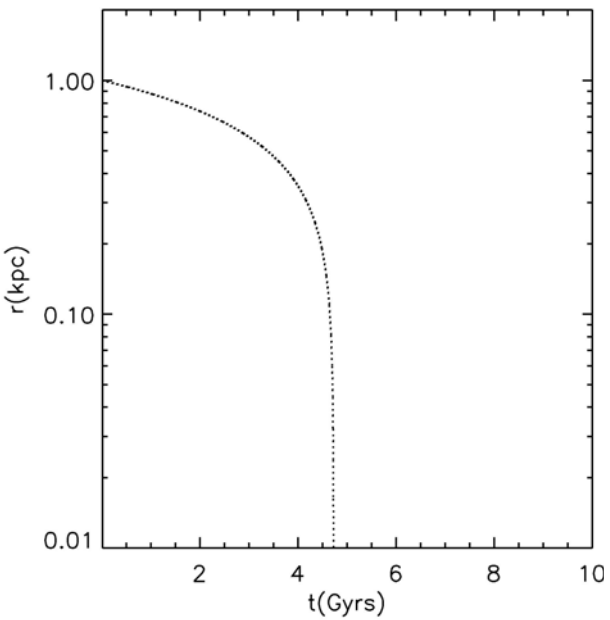
1.00
0.10
0.01
r(kpc)
2
4
6
8
10
t(Gyrs)

The first structures in the universe

Diemand etal (2005) earth mass, parsec scale

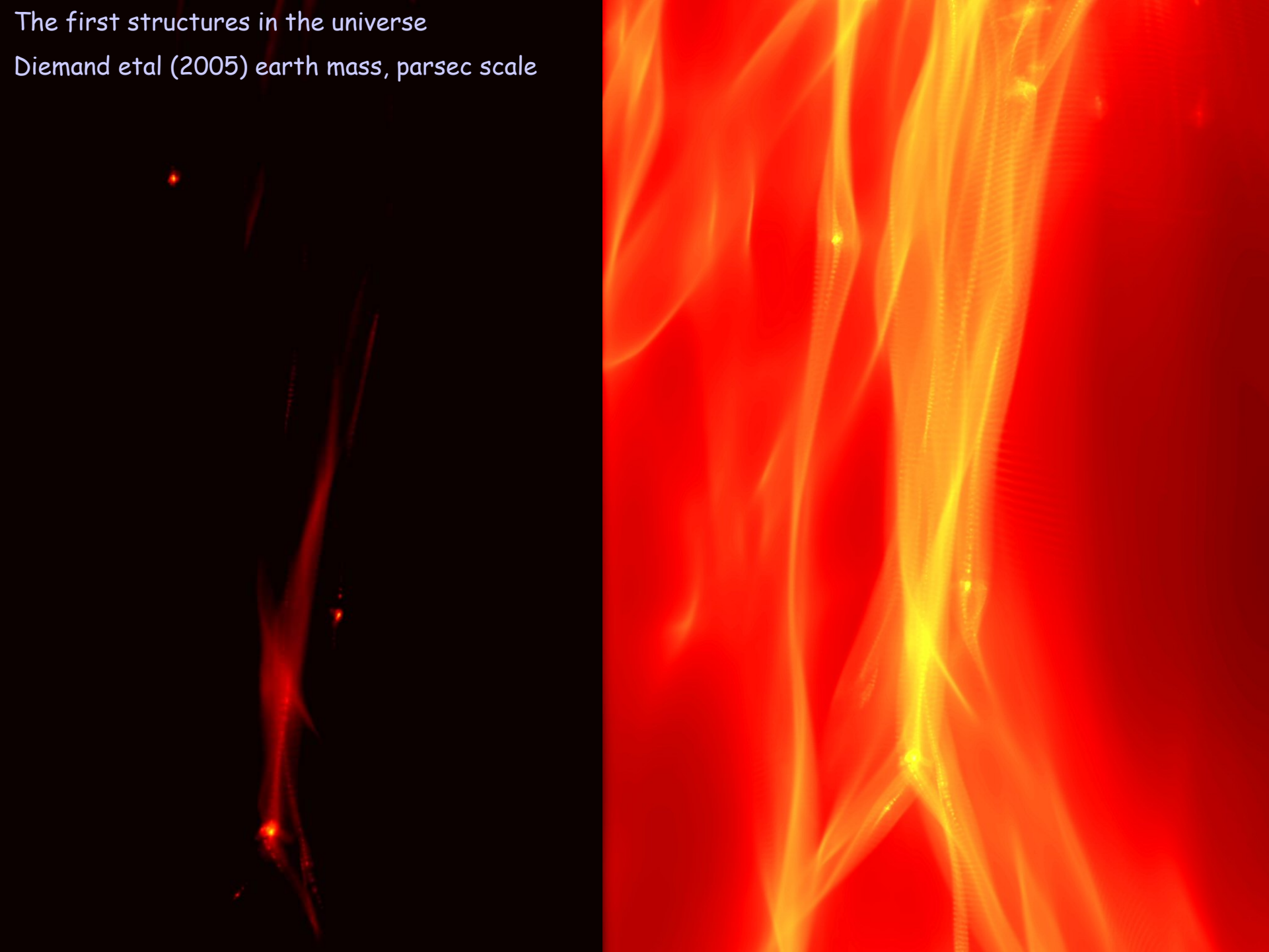

Diemand etal (2005)

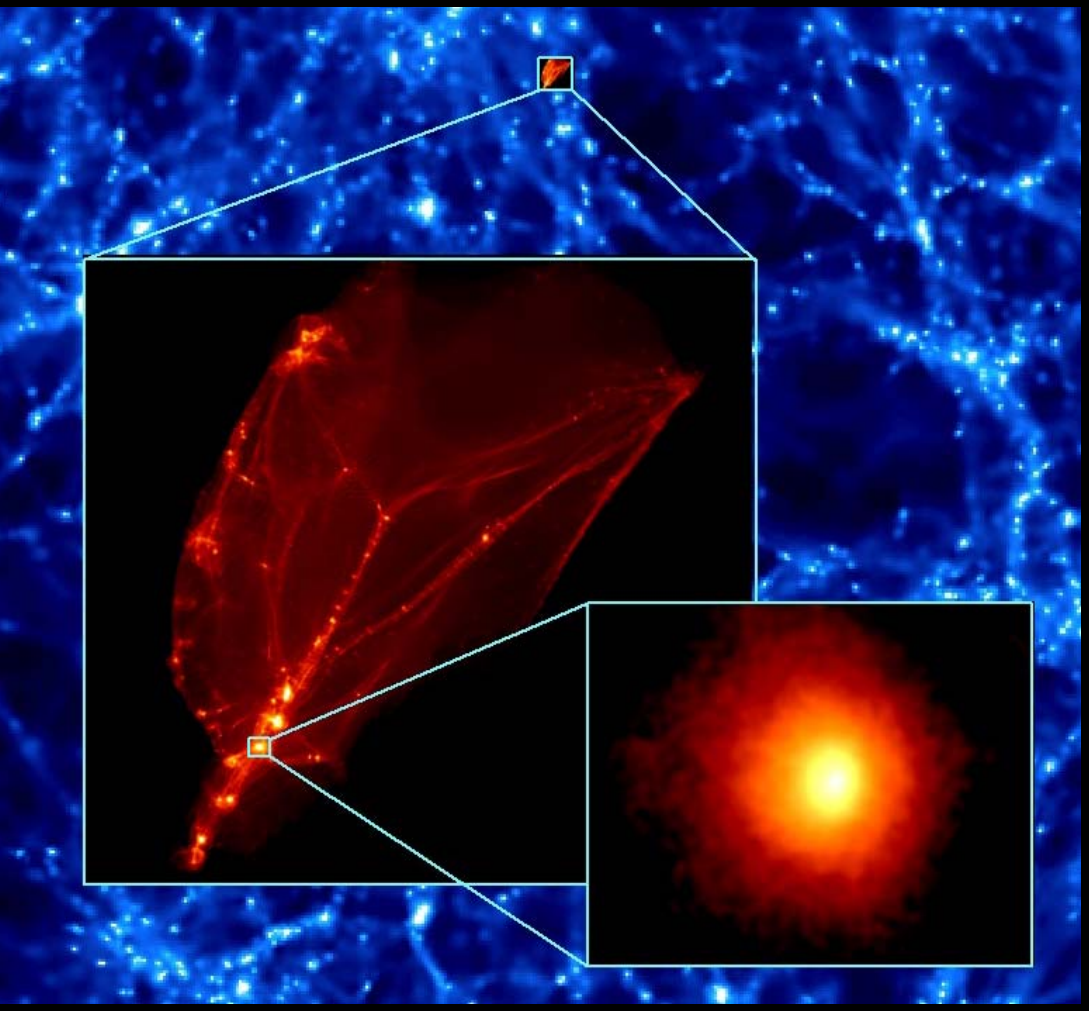

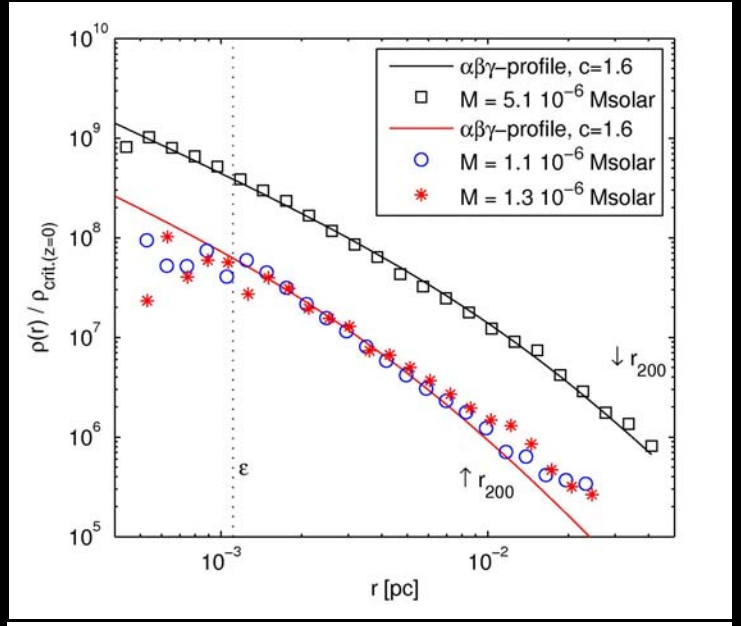

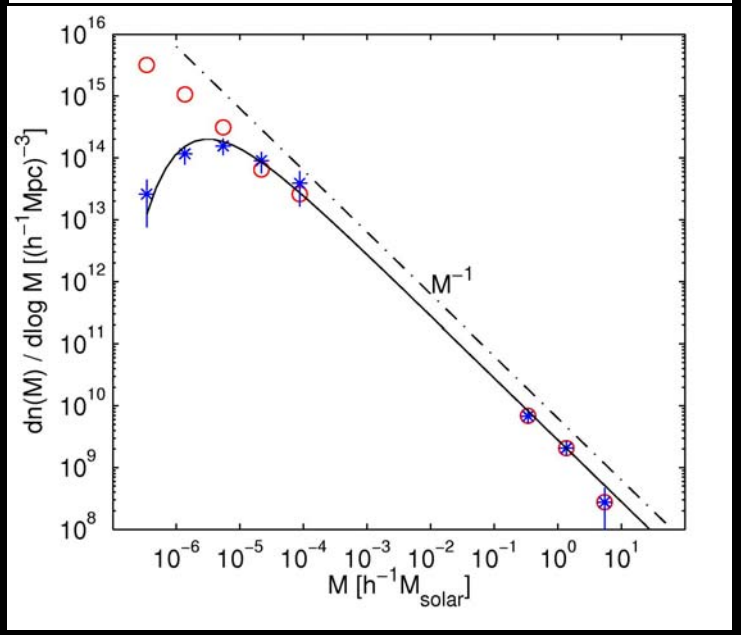

This is the one of the first objects to form in the Universe at z=60. The halo is smooth, has a cuspy density profile, has an earth mass 10^-6Mo and a size of the solar system.
Can be detected as high proper motion gamma-ray sources (Moore et al 2005).

Proper motion of gamma-rays from microhalo sources

Savvas M. Koushiappas
T-6, Theoretical Division, & ISR-1, ISR Division, MS B227,
Los Alamos National Laboratory, Los Alamos, NM 87545, USA; smkoush@lanl.gov

I discuss the prospects of detecting the smallest dark matter bound structures by searching for the proper motion of gamma-ray sources in the upcoming GLAST all sky map. I show that for WIMP dark matter, there should be at least one gamma-ray source with a proper motion greater than 9 arcminutes if more than $\sim 1\%$ of microhalos survive tidal disruption. Such a detection will imply that the kinetic decoupling temperature of the CDM particle must be less than 100 MeV and the mass of the WIMP must be less than 600 GeV.

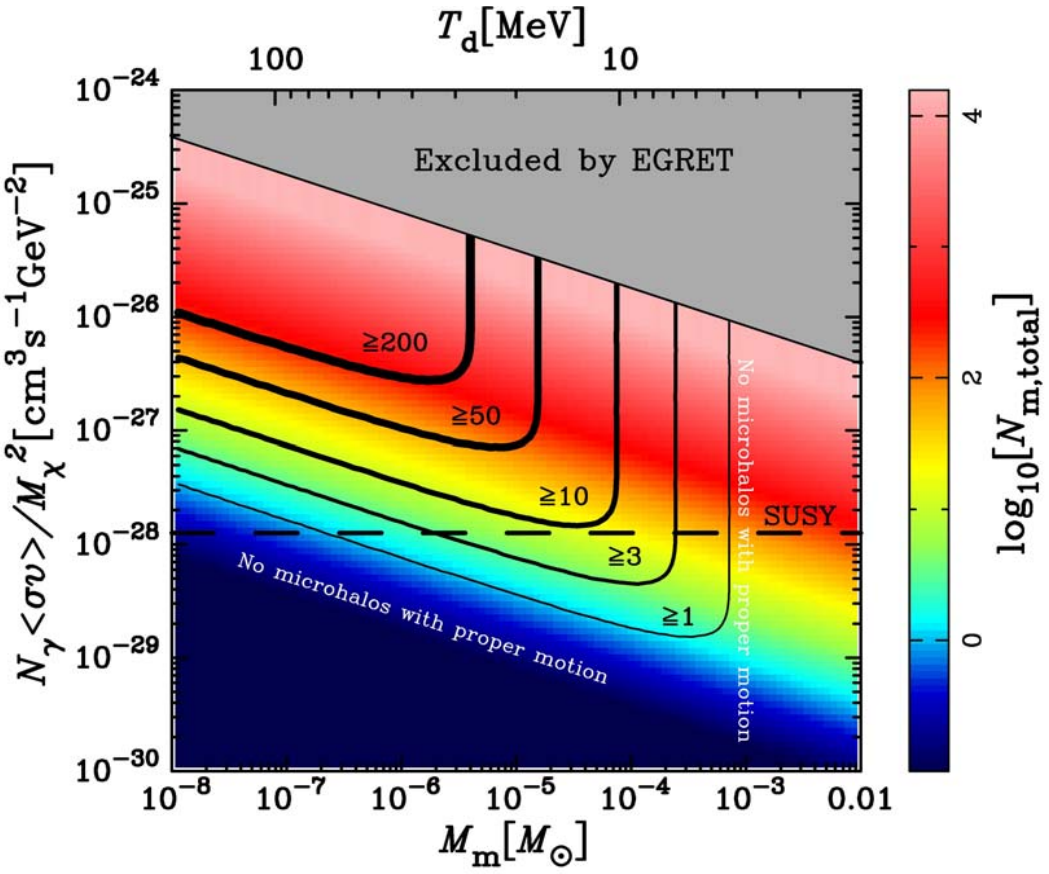

But, Zhao et al claimed that all microhaloes near the sun would be disrupted by encounters with halo stars

The survival and disruption of CDM micro-haloes: implications for direct and indirect detection experiments

Tobias Goerdt[1⋆], Oleg Y. Gnedin[2], Ben Moore[1], Jürg Diemand[3] & Joachim Stadel[1]

1 *Institut für Theoretische Physik, Universität Zürich, Winterthurerstrasse 190, CH-8057 Zürich, Schweiz*
2 *The Ohio State University, Department of Astronomy, 140 W 18th Avenue, Columbus, OH 43210, USA*
3 *University of California, Department of Astronomy and Astrophysics, 1156 High Street, Santa Cruz CA 95064, USA*

Draft version 12 September 2006

ABSTRACT

If the dark matter particle is a neutralino then the first structures to form are cuspy cold dark matter (CDM) haloes collapsing after redshifts $z \approx 100$ in the mass range $10^{-6} - 10^{-3}\,\mathrm{M}_{\odot}$. We carry out a detailed study of the survival of these micro-haloes in the Galaxy as they experience tidal encounters with stars, molecular clouds, and other dark matter substructures. We test the validity of analytic impulsive heating calculations using high resolution N-body simulations. A major limitation of analytic estimates is that mean energy inputs are compared to mean binding energies, instead of the actual mass lost from the system. This energy criterion leads to an overestimate of the stripped mass and underestimate of the disruption timescale since CDM haloes are strongly bound in their inner parts. We show that a significant fraction of material from CDM micro-haloes can be unbound by encounters with Galactic substructure and stars, however the cuspy central regions remain relatively intact. Furthermore, the micro-haloes near the solar radius are those which collapse significantly earlier than average and will suffer very little mass loss. Thus we expect a fraction of surviving bound micro-haloes, a smooth component with narrow features in phase space, which may be uncovered by direct detection experiments, as well as numerous surviving cuspy cores with proper motions of arc-minutes per year, which can be detected indirectly via their annihilation into gamma-rays.

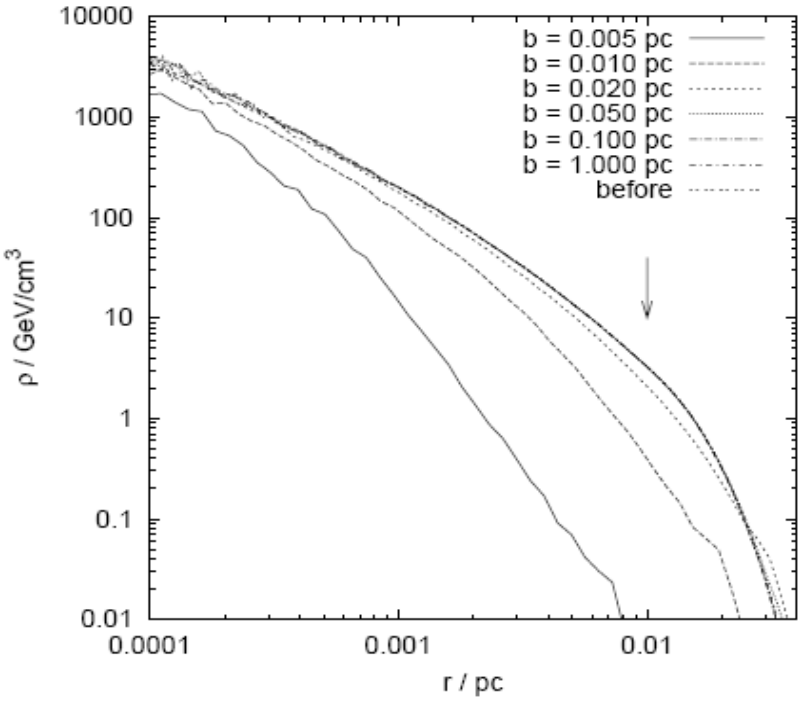

Figure 4. Density profile of the micro-halo in a new equilibrium, after encounters with different impact parameters, b. The arrow indicates the micro-halo radius.

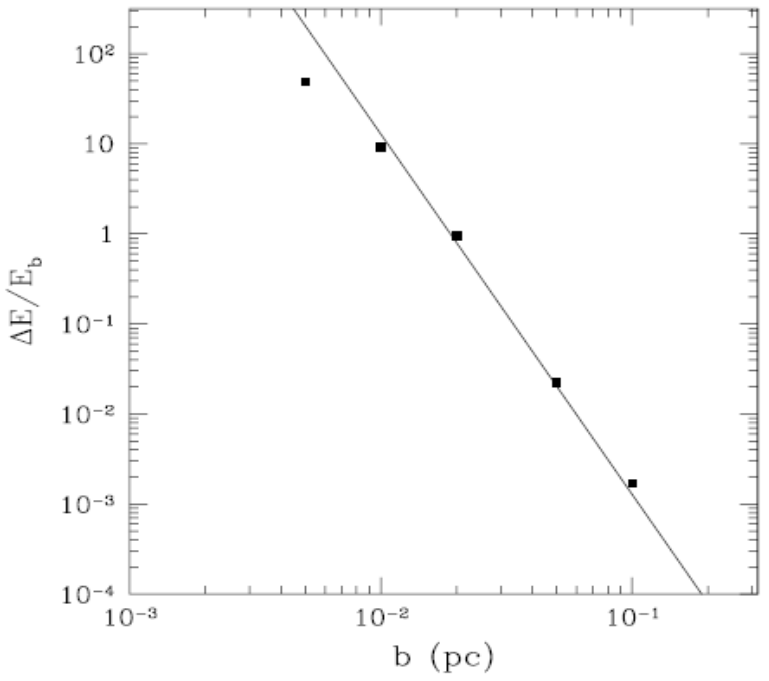

Figure 5. Total energy change of all particles immediately following the perturbation, as a function of impact parameter (*filled squares*) and the analytical prediction in the impulse approximation (*solid line*).

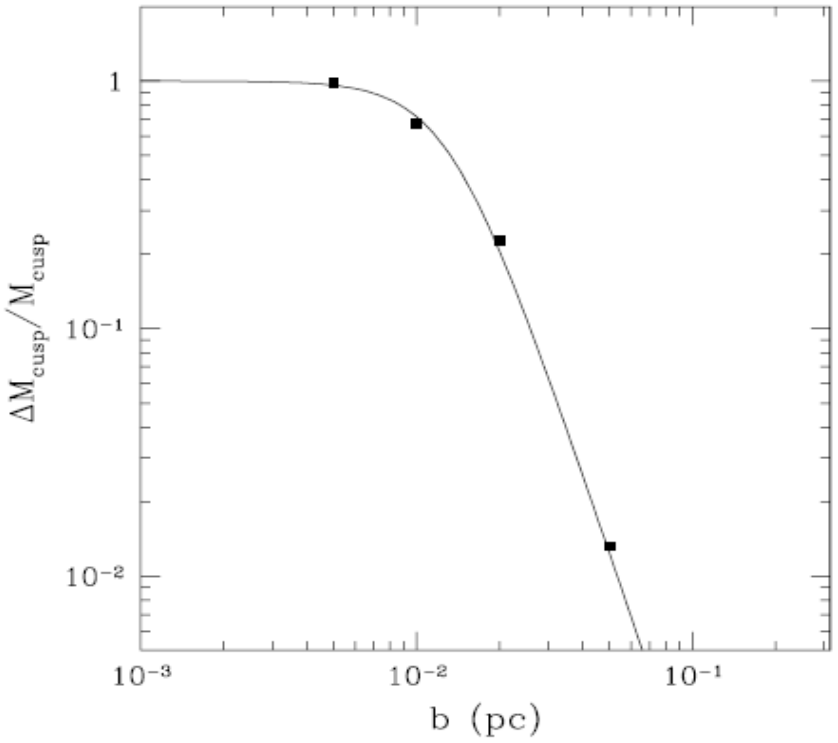

Figure 7. Mass lost inside the scale radius, $r < r_s$, after the potential relaxation, as a function of impact parameter.

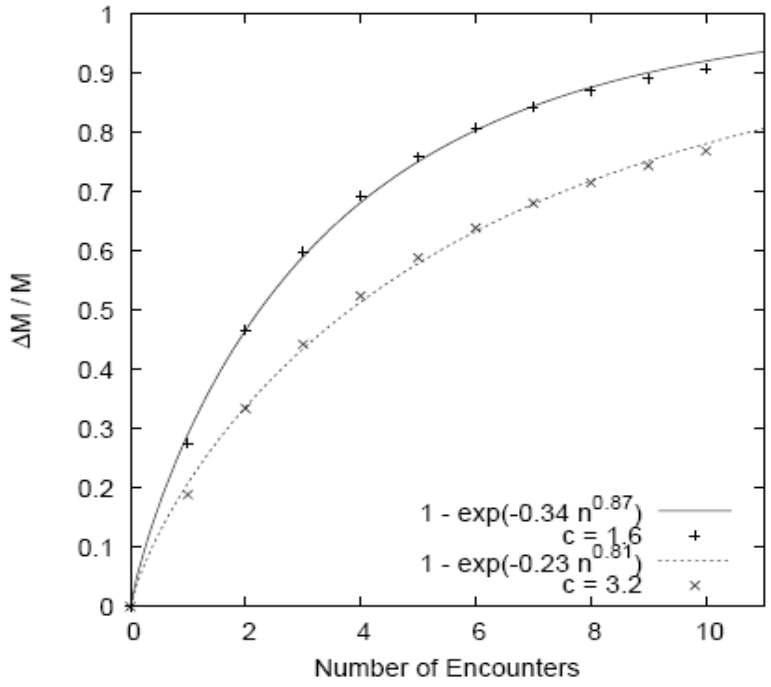

Figure 9. Cumulative mass loss of different micro-haloes after a number of identical encounters with $b = 0.02$ pc.

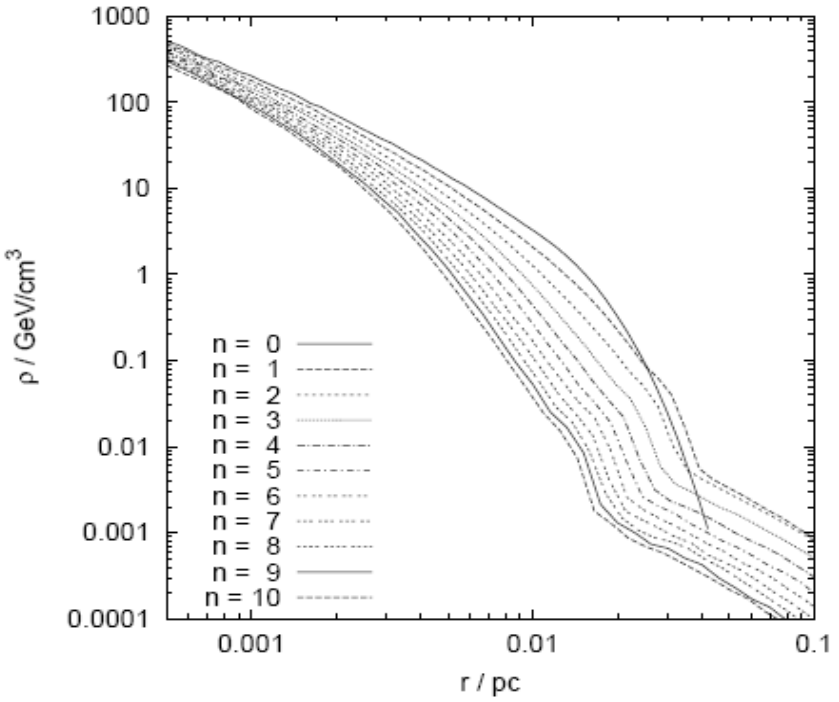

Figure 8. Density profile of the micro-halo after successive encounters with a star with the same mass and orbital parameters ($b = 0.02$ pc), marked by the encounter number n.

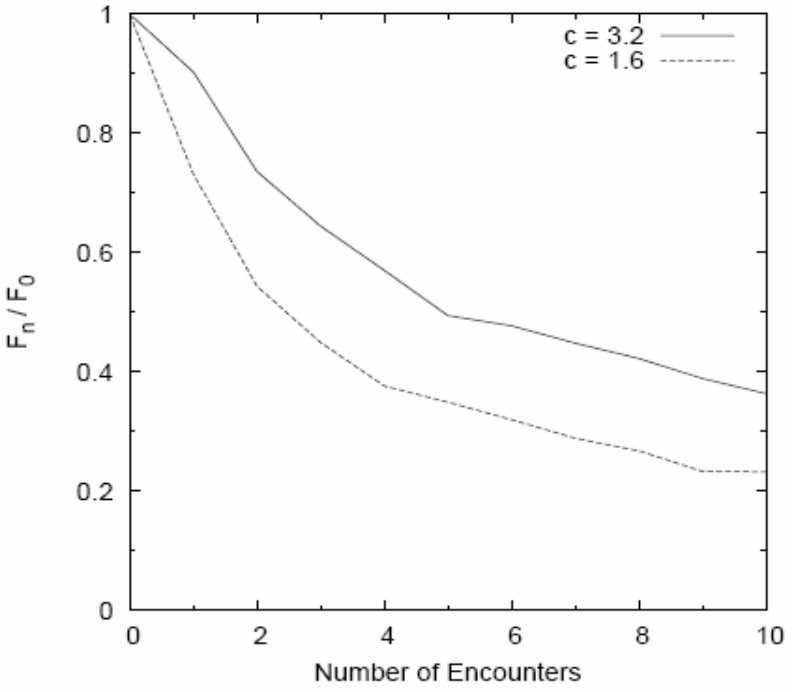

Figure 10. The relative flux of annihilation products from different micro-haloes after a given number of encounters. The typical mass loss from a halo would lead to a decrease in flux of between a factor of two or three.

Kazantzidis etal (2004)

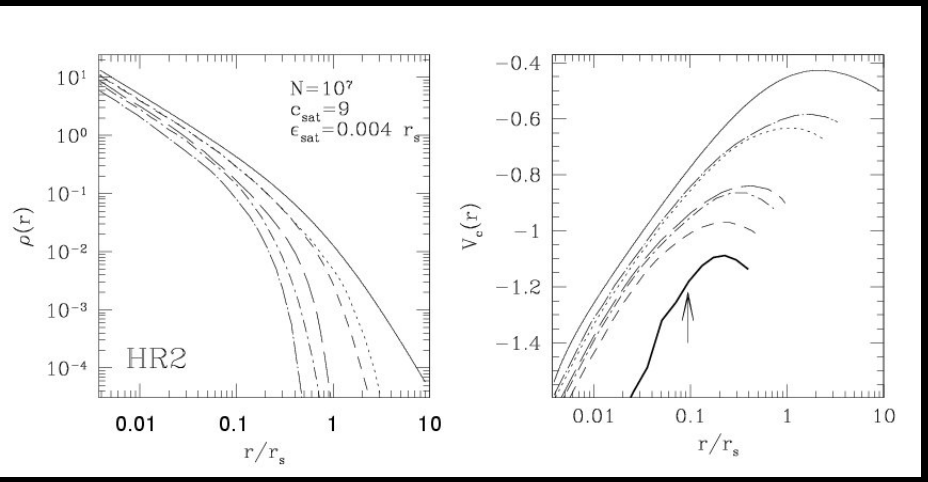

t=0.00 Gyr

Summary of microhalo survival:

Lose>90% of there mass due to tidal heating, encounters with stars, substructure

Cores survive intact.

Satellites, dark and light

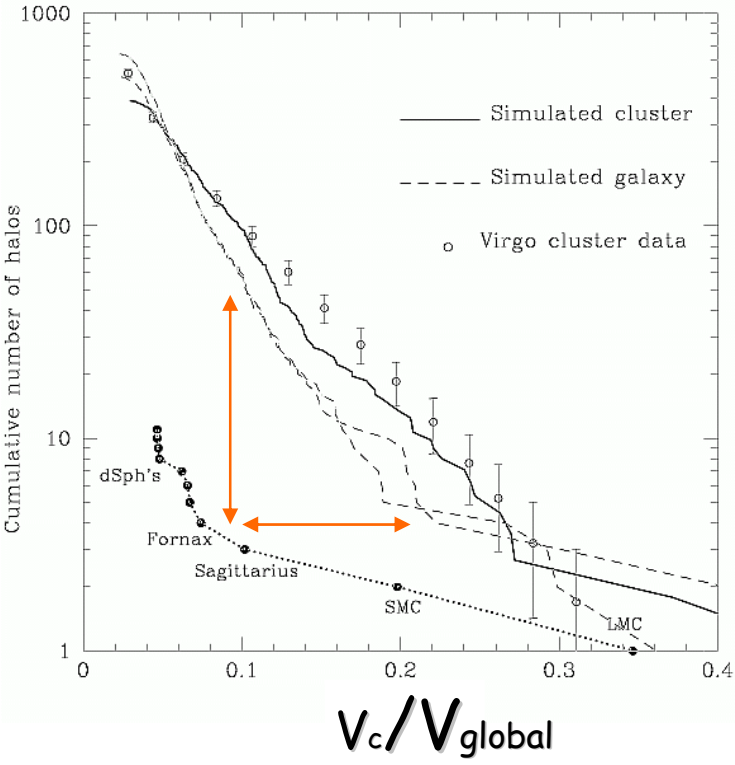

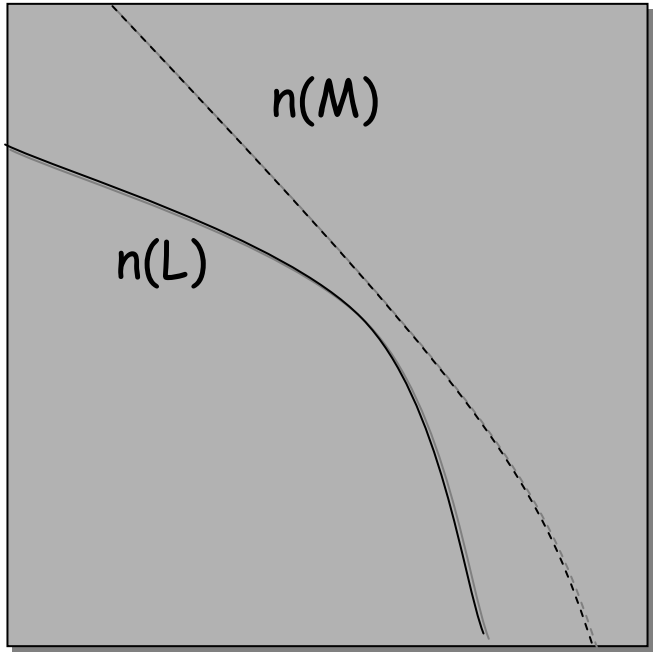
n(M)
n(L)

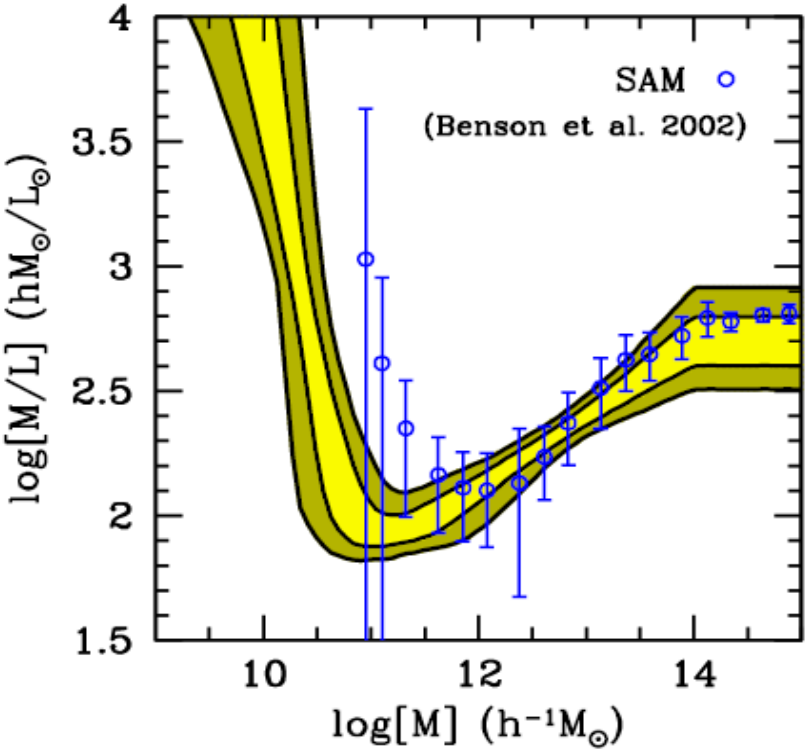
SAM
(Benson et al. 2002)
log[M/L] (hM⊙/L⊙)
log[M] (h⁻¹M⊙)
4
3.5
3
2.5
2
1.5
10
12
14

The Milky Way's satellite population in a ΛCDM universe

Felix Stoehr[1], Simon D. M. White[1], Giuseppe Tormen[2], Volker Springel[1]
[1] *Max-Planck-Institut für Astrophysik, Karl-Schwarzschild-Str. 1, 85748 Garching bei München, Germany*
[2] *Dipartimento di Astronomia, Universita di Padova, vicolo dell'Osservatorio 5, 35122 Padova, Italy*
Email: felix@mpa-garching.mpg.de, swhite@mpa-garching.mpg.de, tormen@pd.astro.it, volker@mpa-garching.mpg.de

MNRAS, accepted, July 23, 2002

ABSTRACT
We compare the structure and kinematics of the 11 known satellites of the Milky Way with high resolution simulations of the formation of its dark halo in a ΛCDM universe. In contrast to earlier work, we find excellent agreement. The observed kinematics are exactly those predicted for stellar populations with the observed spatial structure orbiting within the most massive "satellite" substructures in our simulations. Less massive substructures have weaker potential wells than those hosting the observed satellites. If there is a halo substructure "problem", it consists in understanding why halo substructures have been so inefficient in making stars. Suggested modifications of dark matter properties (for example, self-interacting or warm dark matter) may well spoil the good agreement found for standard Cold Dark Matter.

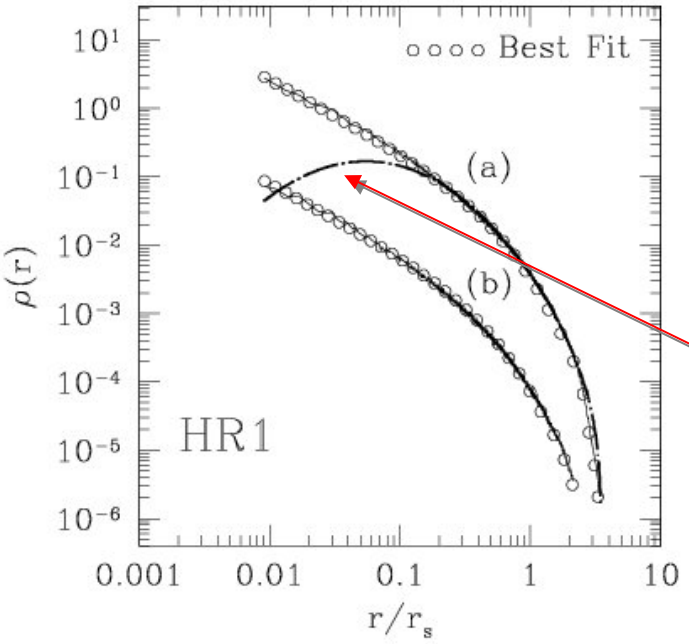

$$\sigma_{\rm p}^2(R) = \frac{2}{I(R)} \int_R^{r_{\rm t}} \left(1 - \beta \frac{R^2}{r^2}\right) \frac{\rho\, \sigma_{\rm r}^2(r,\beta)\, r}{\sqrt{r^2 - R^2}}\, {\rm d}r$$

Stoehr etal density profile…

Kazantzidis etal (2004)

t=0.00 Gyr

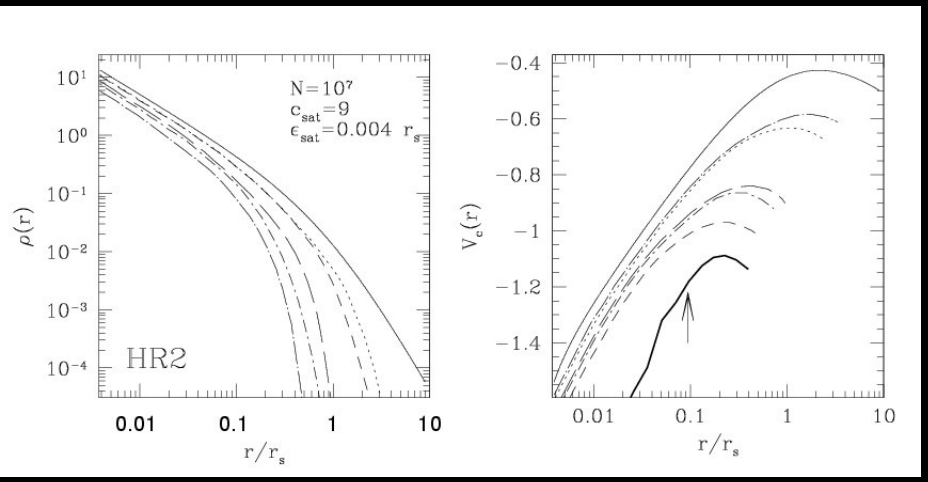

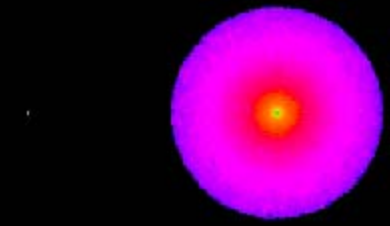

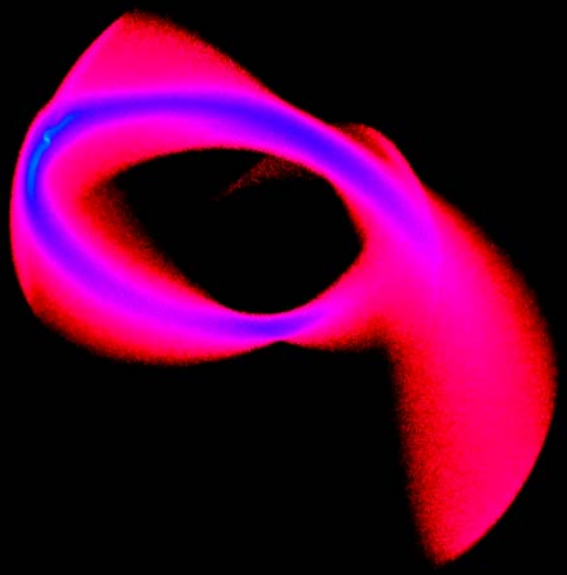

Chiara Mastropietro et al.

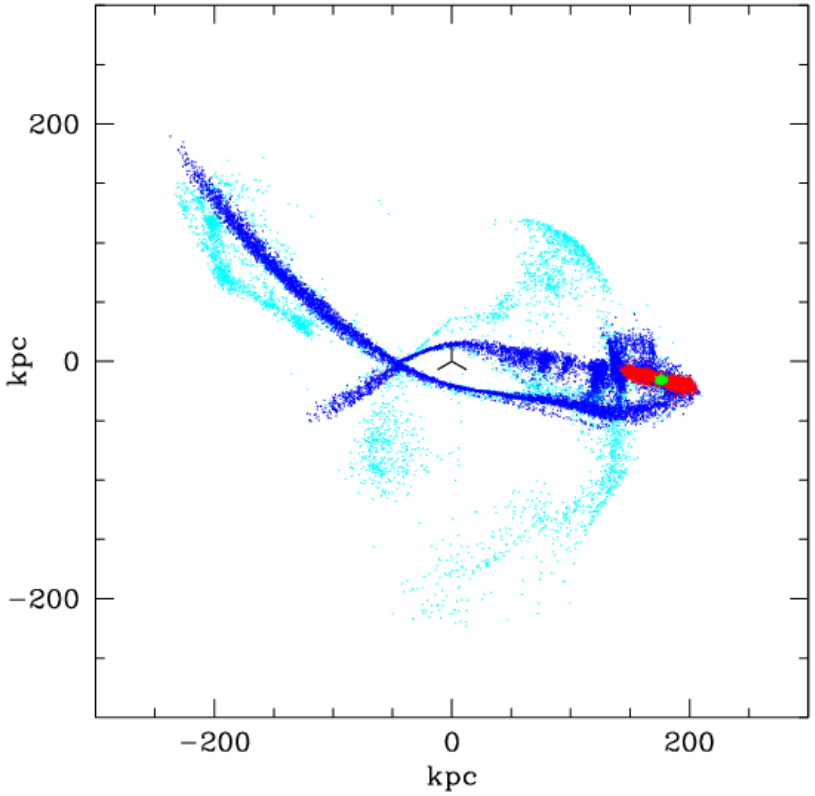

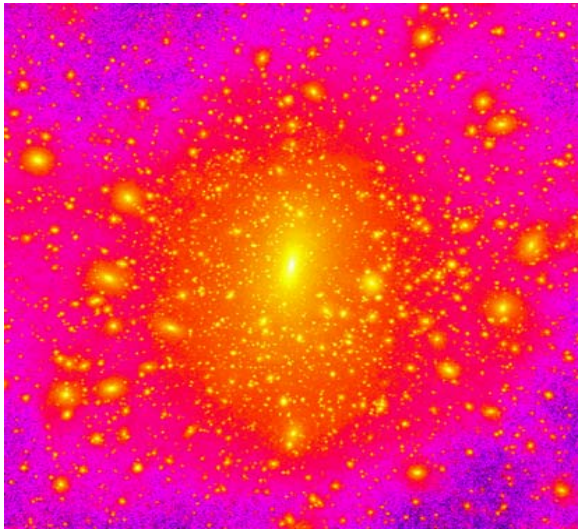

RESOLUTION

Fornax like cuspy halos in a 5:1 orbit within a galactic potential

Three different mass resolutions ($N=10^5,10^6,10^7$)

Softening = 50pc

1) Clear difference in the evolution of the bound satellite mass between low and high resolution runs.

2) Timescales over which the satellite looses 99.9% converge between the highest resolution cases.

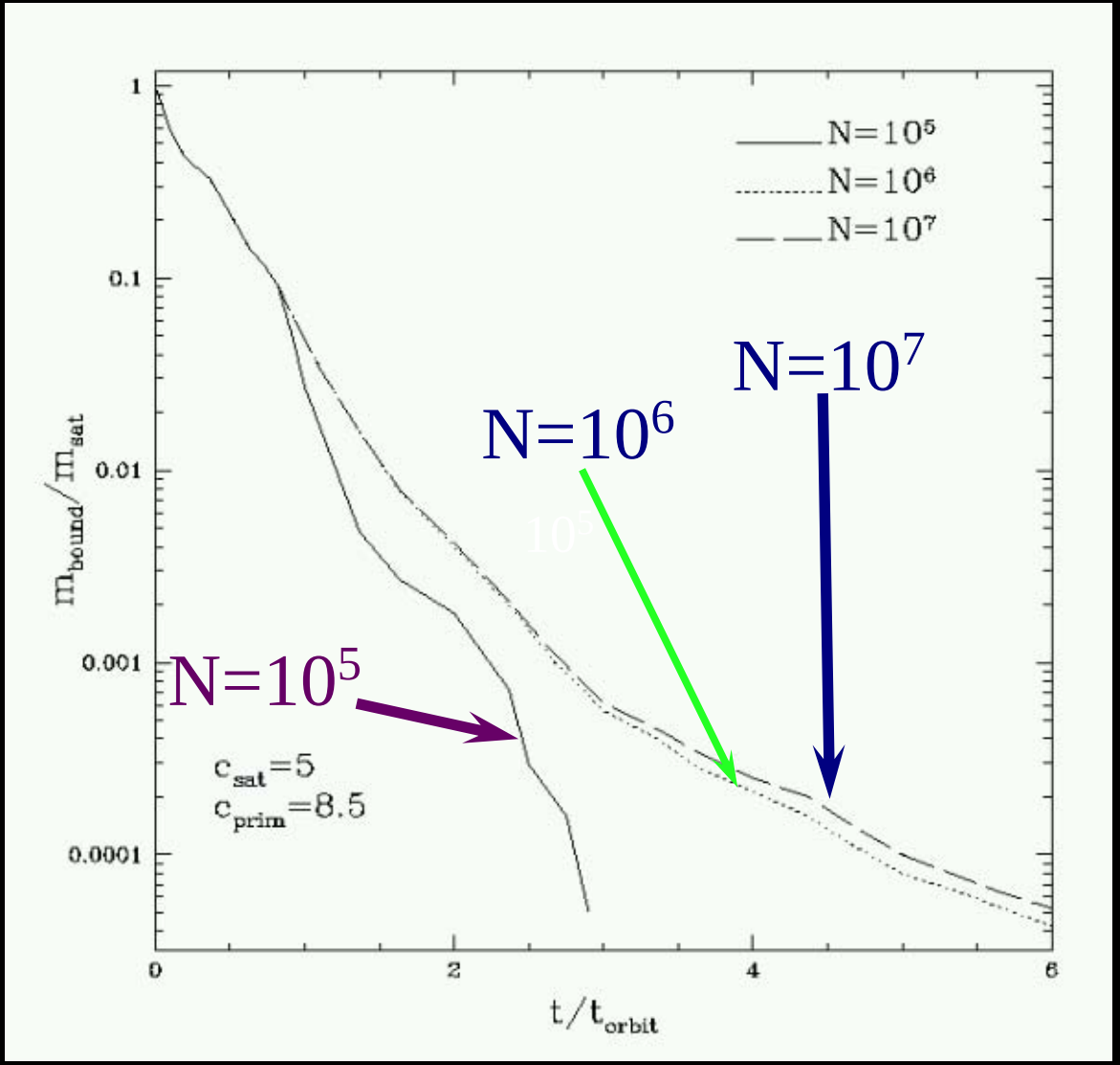

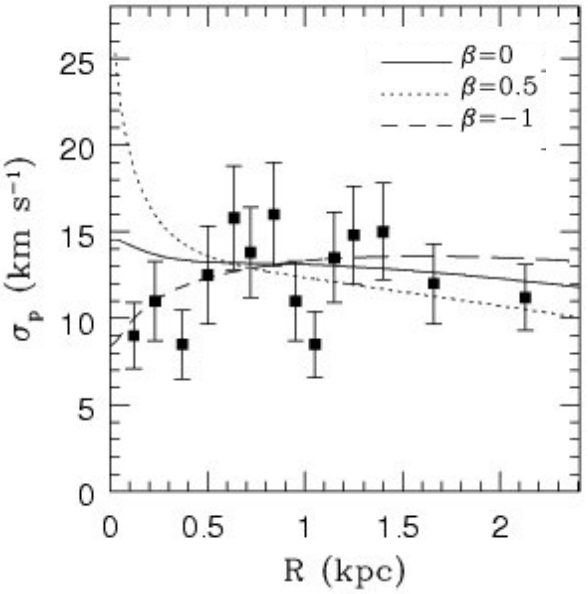

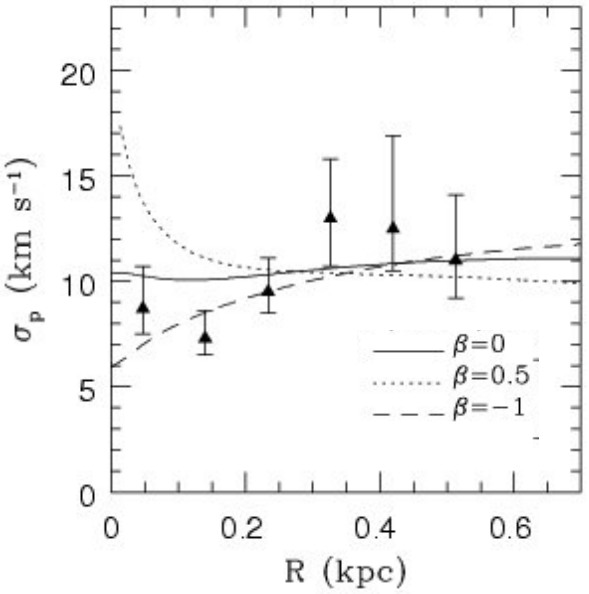

$$\sigma_{\rm p}^2(R) = \frac{2}{I(R)} \int_R^{r_{\rm t}} \left(1 - \beta \frac{R^2}{r^2}\right) \frac{\rho\, \sigma_{\rm r}^2(r,\beta)\, r}{\sqrt{r^2 - R^2}}\, {\rm d}r$$

Can only embed dSph's in CDM halos with Vc<25km/s → can't embed observed satellites in most massive dark matter substructures. (Not a simple mass cut-off to star-formation.)

All observed stellar dispersion profiles with many stars and careful background subtraction are flat. Consistent with exponential sub-dominant light distribution embedded in dark matter cusp.

Hiding satellites behind reionisation

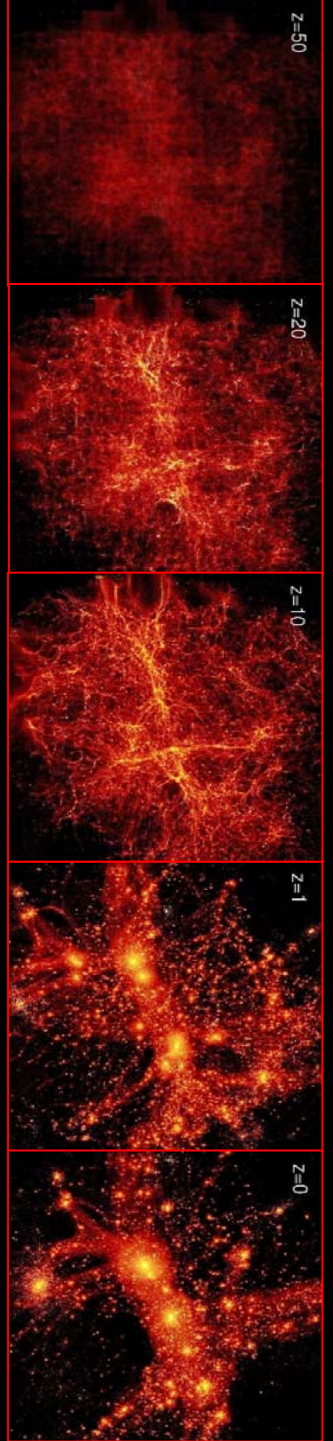

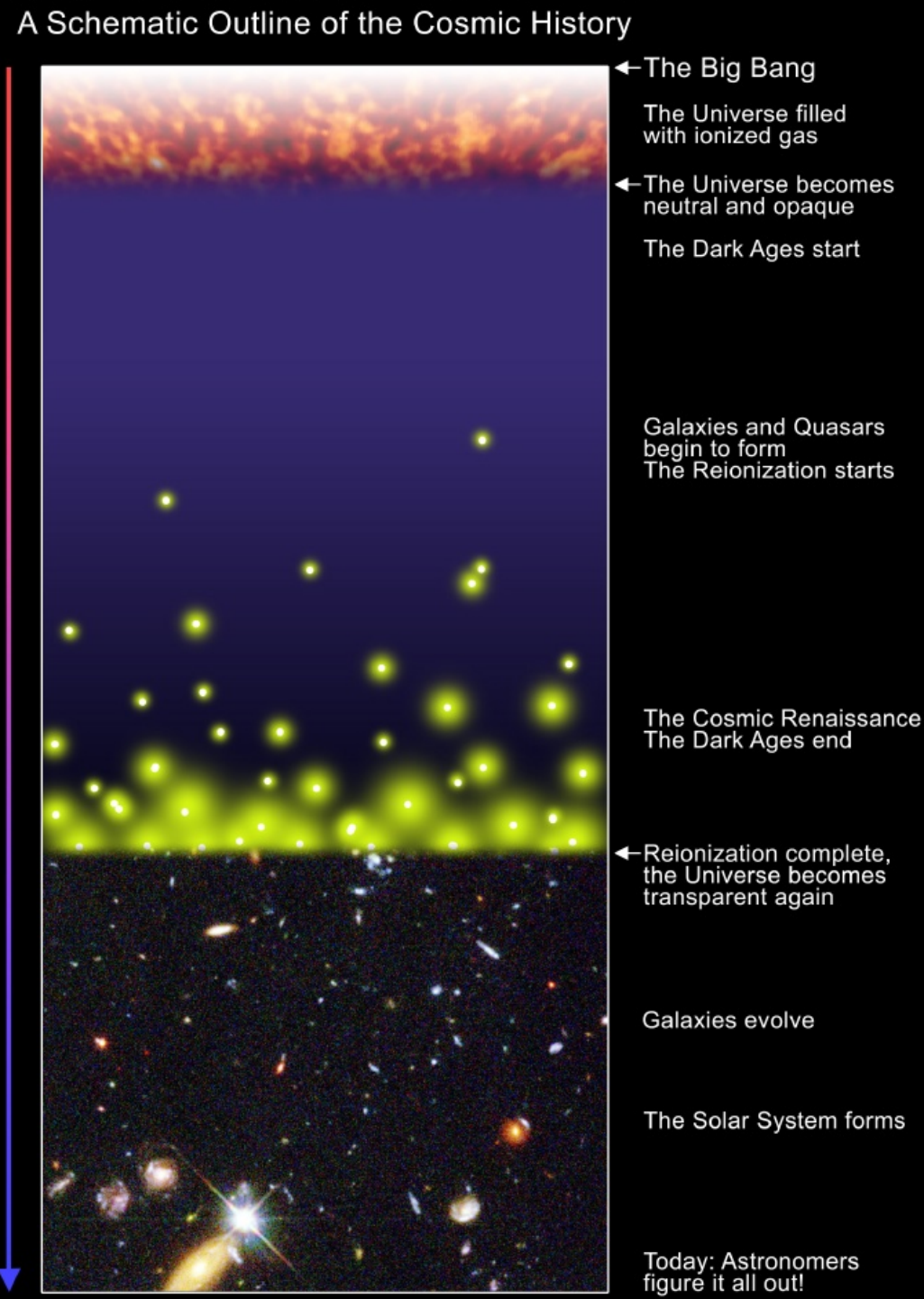

Mon. Not. R. Astron. Soc. **000**, 1–18 (2005) Printed 29 June 2005 (MN LATEX style file v2.2)

The distribution and kinematics of early high-σ peaks in present-day haloes: implications for rare objects and old stellar populations

Jürg Diemand[1,2⋆], Piero Madau[1], Ben Moore[2]
1*Department of Astronomy and Astrophysics, University of California, Santa Cruz, CA 95064.*
2*Institute for Theoretical Physics, University of Zürich, Winterthurerstrasse 190 ,CH-8057 Zürich, Switzerland.*

29 June 2005

ABSTRACT

We show that the hierarchical assembly of cold dark matter haloes preserves the memory of the initial conditions. Using N-body cosmological simulations, we demonstrate that the spatial distribution and kinematics of objects that formed within early galactic haloes (old stars, satellite galaxies, globular clusters, black holes etc.) depends only on the rarity of the peak in which they formed. Matter from the rarer peaks of the primordial density field ends up more concentrated and falling off more steeply with radius compared to the overall mass distribution, it has a lower velocity dispersion, moves on more radial orbits and has a more elongated shape. Population II stars that form in cold dark matter dominated proto-galaxies that were 2.5σ peaks end up with a half light radius of 16.9 kpc, falling off as $r^{-3.5}$ with an anisotropy varying from isotropic in the inner halo to nearly radial at the halo edge. This agrees well with the kinematics of halo red giant stars recently observed by Battaglia et al. (2005).

The red regions marked at z=10 are the ≈100 halos that have already collapsed and could form stars. These regions are then traced to the final time where most of these halos have merged into the galaxy with about 10 satellites surviving in the final halo.

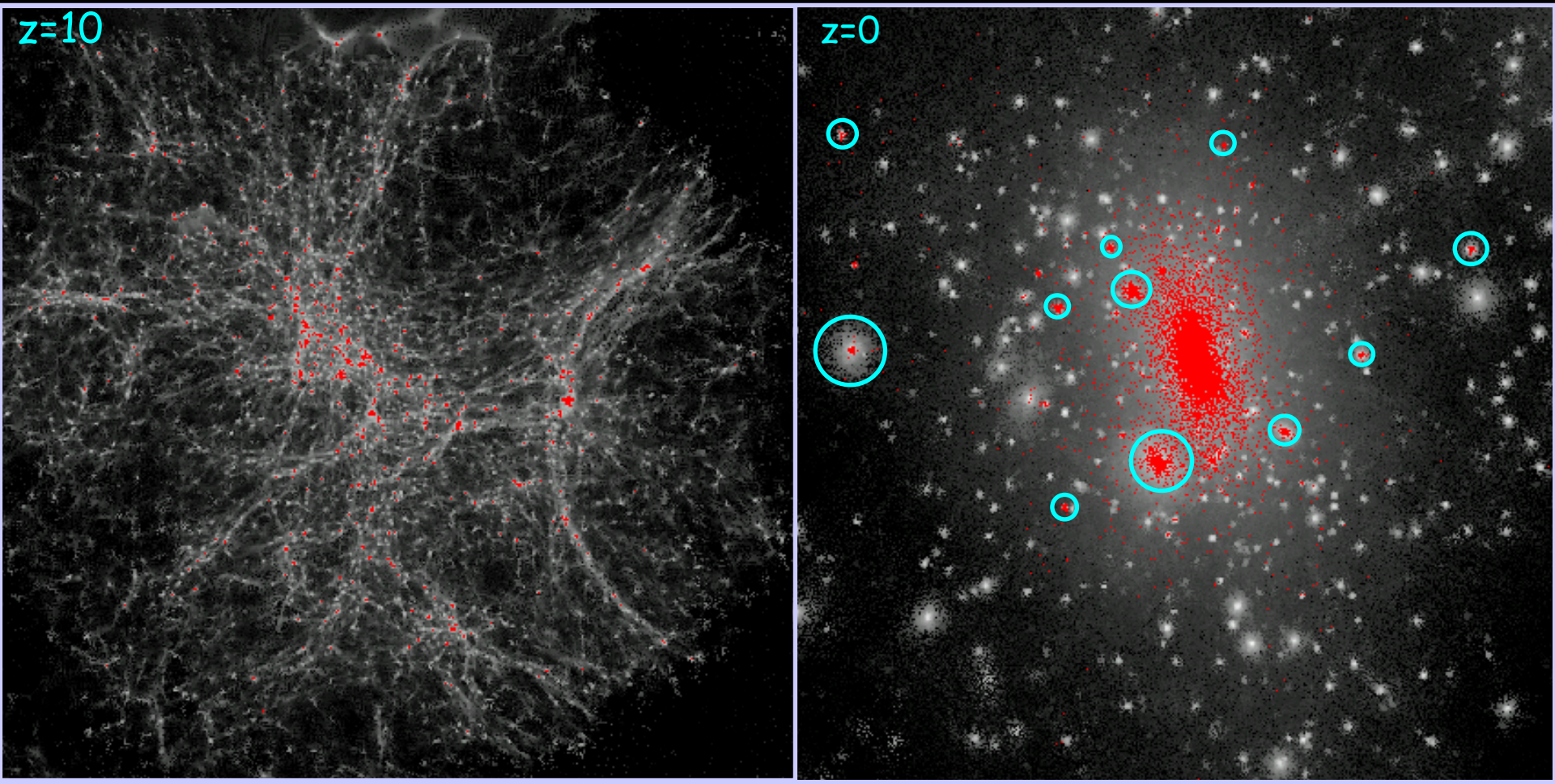

Moore etal (1998, 2001), White & Springel (2000), Diemand et al. (2005)

...showed that the rare peaks have a r^-3 distribution

Most of the satellites remain dark since they could not cool gas after re-ionisation.

Mon. Not. R. Astron. Soc. **000**, 1–10 (2004) Printed 16 October 2005 (MN LATEX style file v2.2)

Globular clusters, satellite galaxies and stellar haloes from early dark matter peaks

Ben Moore[1⋆], Juerg Diemand[2], Piero Madau[2], Marcel Zemp[1,3] & Joachim Stadel[1]

1. *Institute for Theoretical Physics, University of Zürich ,CH-8057 Zürich, Switzerland*
2. *Department of Astronomy and Astrophysics, University of California, Santa Cruz, CA 95064, USA*
3. *Institute of Astronomy, ETH Zürich, ETH Honggerberg HPF D6, CH-8093, Zürich, Switzerland*

16 October 2005

$$M_{\rm H} \approx 10^8 \left[(1+z)/10\right]^{-3/2} M_\odot \ \text{(virial temperature } 10^4\,\text{K)},$$

Kauffmann etal (1993), Bullock etal (2000), Cote etal (2000), White & Springel (2000), Barkana & Loeb (2001), Moore (2001), Tully etal (2002), Benson etal (2002) Somerville etal (2003), Kravtsov (2004). Kravtsov & Gnedin (2005), Diemand (2005), Gnedin & Kravtsov (2006).

ABSTRACT

The Milky Way contains several distinct old stellar components that provide a fossil record of its formation. We can understand their spatial distribution and kinematics in a hierarchical formation scenario by associating the proto-galactic fragments envisaged by Searle and Zinn (1978) with the rare peaks able to cool gas in the cold dark matter density field collapsing at redshift $z > 10$. We use hierarchical structure formation simulations to explore the kinematics and spatial distribution of these early star-forming structures in galaxy haloes today. Most of the proto-galaxies rapidly merge, their stellar contents and dark matter becoming smoothly distributed and forming the inner Galactic halo. The metal-poor globular clusters and old halo stars become tracers of this early evolutionary phase, centrally biased and naturally reproducing the observed steep fall off with radius. The most outlying peaks fall in late and survive to the present day as satellite galaxies. The observed radial velocity dispersion profile and the local radial velocity anisotropy of Milky Way halo stars are successfully reproduced in this model. If this epoch of structure formation coincides with a suppression of further cooling into lower sigma peaks then we can reproduce the rarity, kinematics and spatial distribution of satellite galaxies as suggested by Bullock et al. (2000). Reionisation at $z = 12 \pm 2$ provides a natural solution to the missing satellites problem. Measuring the distribution of globular clusters and halo light on scales from galaxies to clusters could be used to constrain global versus local reionisation models. If reionisation occurs contemporary, our model predicts a constant frequency of blue globulars relative to the host halo mass, except for dwarf galaxies where the average relative frequencies become smaller.

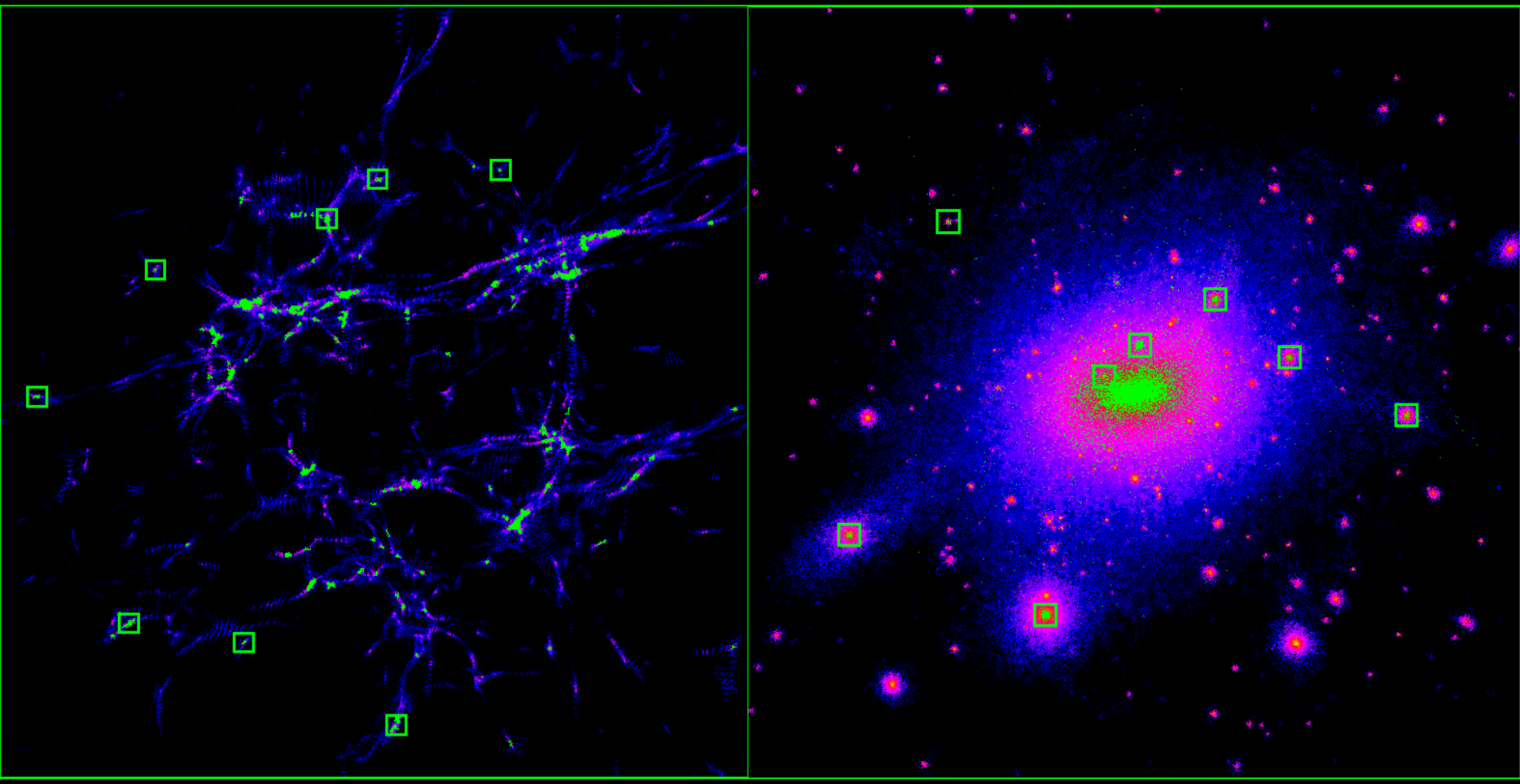

z=10

z=0

The only rare peaks that survive are those that form furthest from the forming galaxy. These are the progenitors of the dSph satellites.

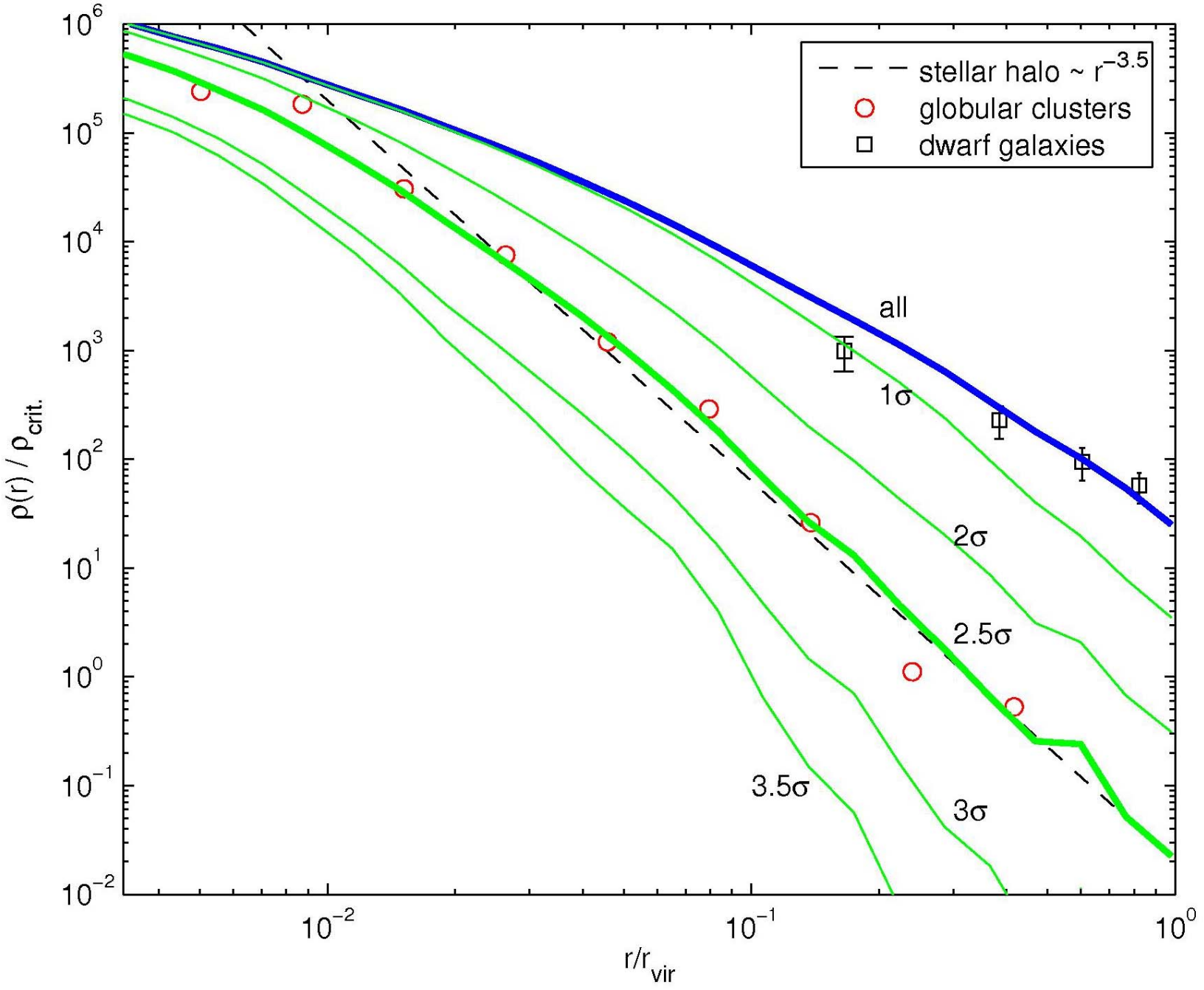
stellar halo ~ r^-3.5
globular clusters
dwarf galaxies
all
1σ
2σ
2.5σ
3σ
3.5σ
ρ(r) / ρcrit.
r/rvir
10^6
10^5
10^4
10^3
10^2
10^1
10^0
10^-1
10^-2
10^-2
10^-1
10^0

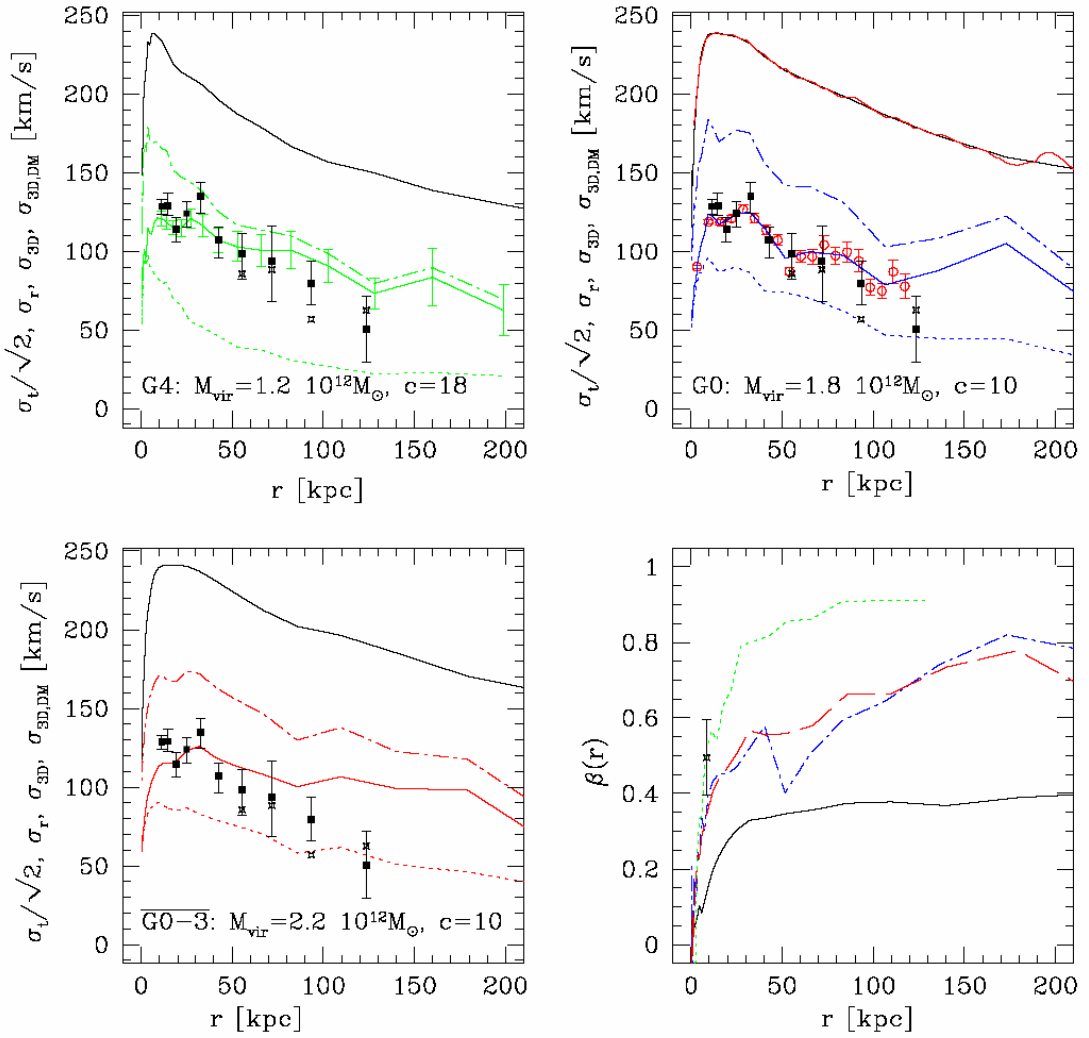

Data points are observations of the stellar velocity dispersions of halo stars by Battaglia et al (2005).

Stars which form in the rare early dark matter peaks have similar spatial and kinematical properties (Diemand etal).

Figure 12. Kinematics of our model stellar haloes compared with observations of Milky Way halo stars. The simulated CDM haloes are rescaled to give a local circular velocity of 220 km/s after taking adiabatic contraction into account (see text for details). The lower right panel shows the anisotropy profiles $\beta(r) = 1 - \sigma_t(r)/2\sigma_r(r)^2$ for the average of G0 to G4 (dashed line for the stars and solid for the dark matter) and for the stars in G0 (dashed-dotted) and G4 (dotted). The data point is the local halo anisotropy from Chiba & Beers (2000). The lines in the other three panels show (from bottom to top) the stellar $\sigma_t/\sqrt{(2)} \simeq \sigma_\theta \simeq \sigma_\phi$ (dotted), σ_r (solid) and σ_{3D} (dashed-dotted). The uppermost lines are the 3D velocity dispersion profile of the dark matter, note that it is much larger and smoother than the stellar σ_{3D}. To illustrate the fluctuations in the stellar dispersions, σ_r and $\sigma_{3D,DM}$ in halo G0 are plotted twice: once using our usual choice of 30 logarithmic bins to the virial radius and also using smaller linear bins (open circles with error bar for σ_r, another solid line for $\sigma_{3D,DM}$). The points are σ_r of the Milky Way halo from Battaglia et al. (2005) with (squares) and without (stars) the contribution from the satellite galaxies.

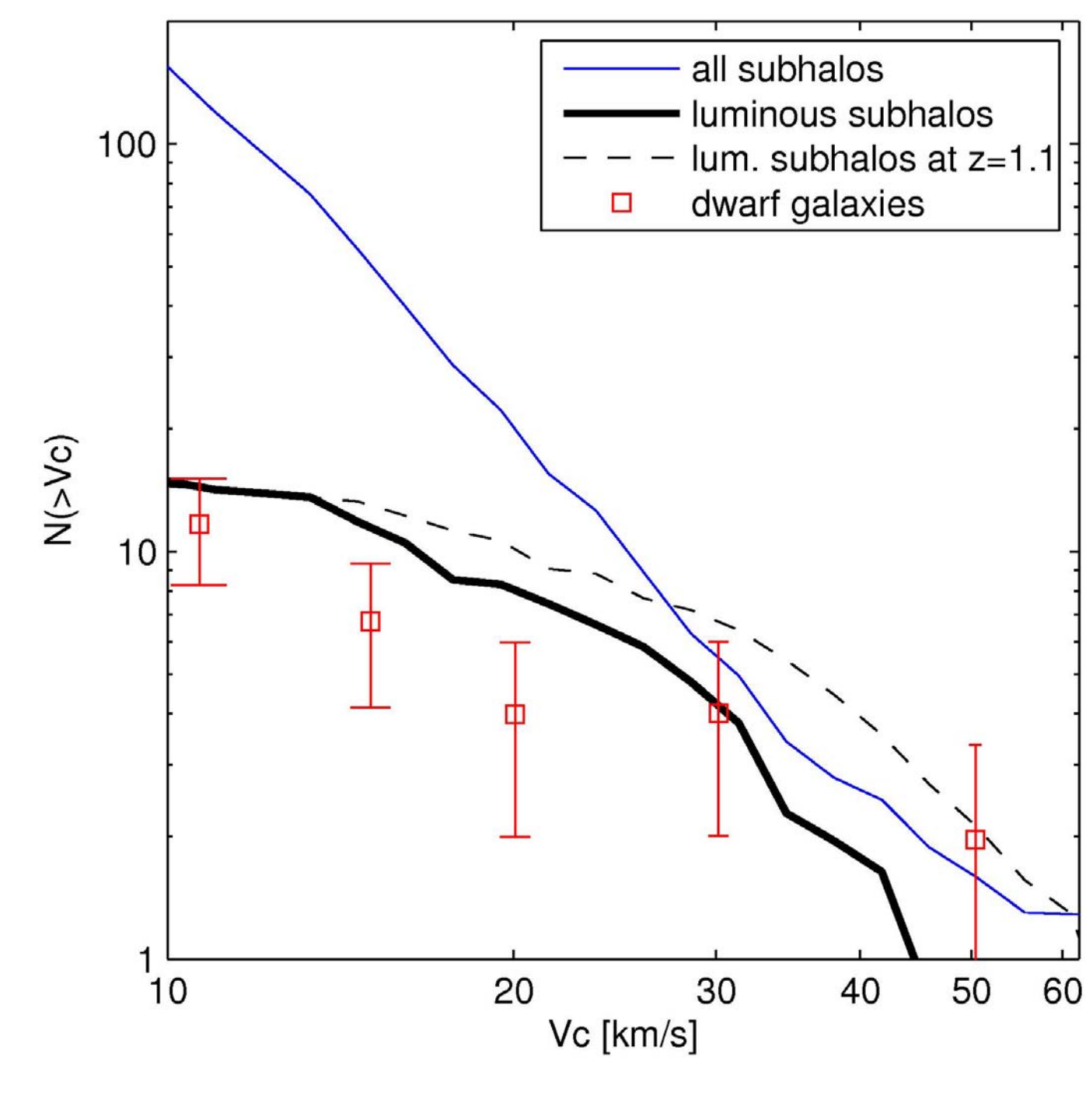
all subhalos
luminous subhalos
lum. subhalos at z=1.1
dwarf galaxies
100
10
1
N(>Vc)
10
20
30
40
50
60
Vc [km/s]

What about changing the nature of dark matter?

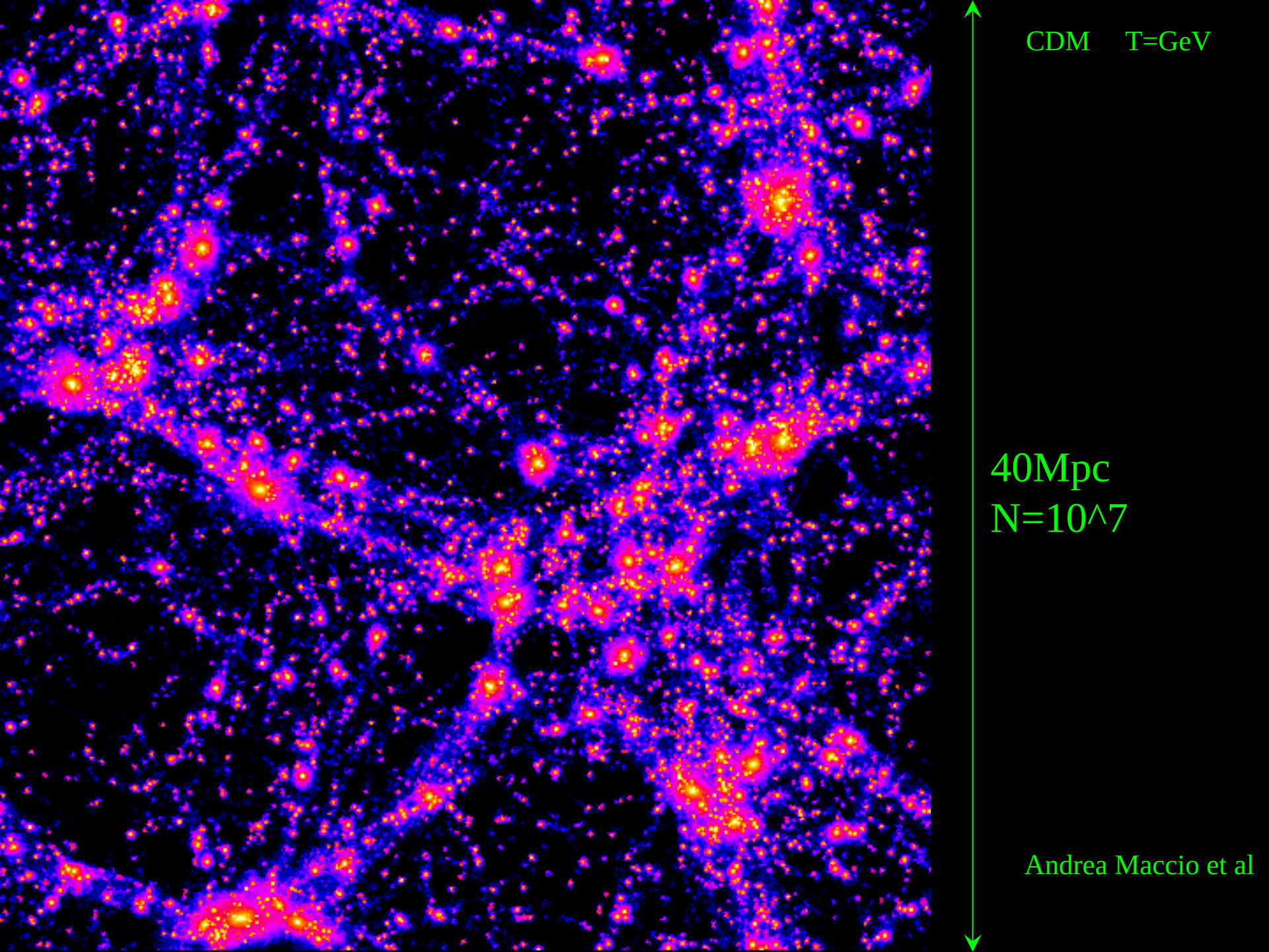
CDM T=GeV
40Mpc
N=10^7
Andrea Maccio et al

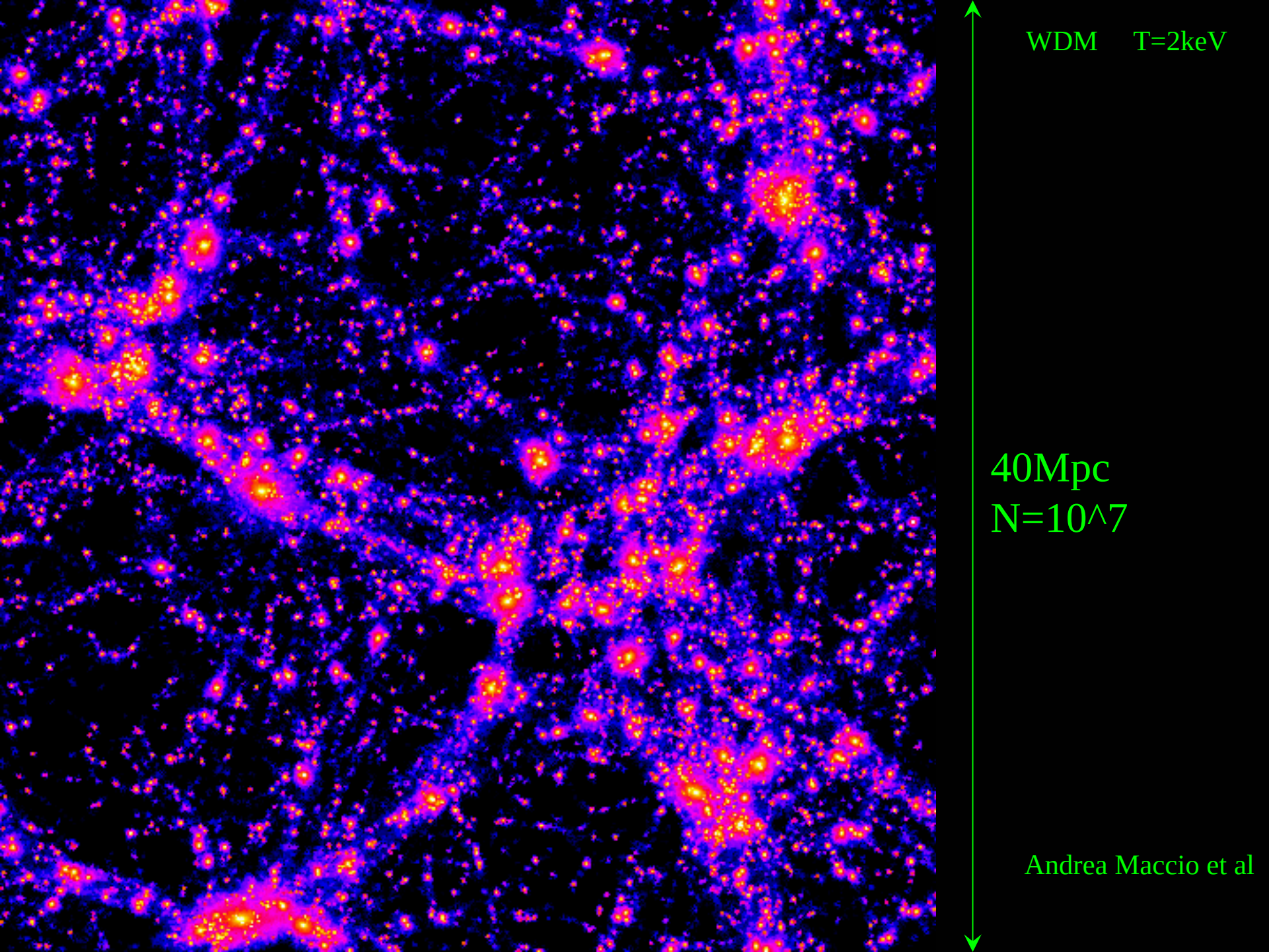
WDM T=2keV
40Mpc
N=10^7
Andrea Maccio et al

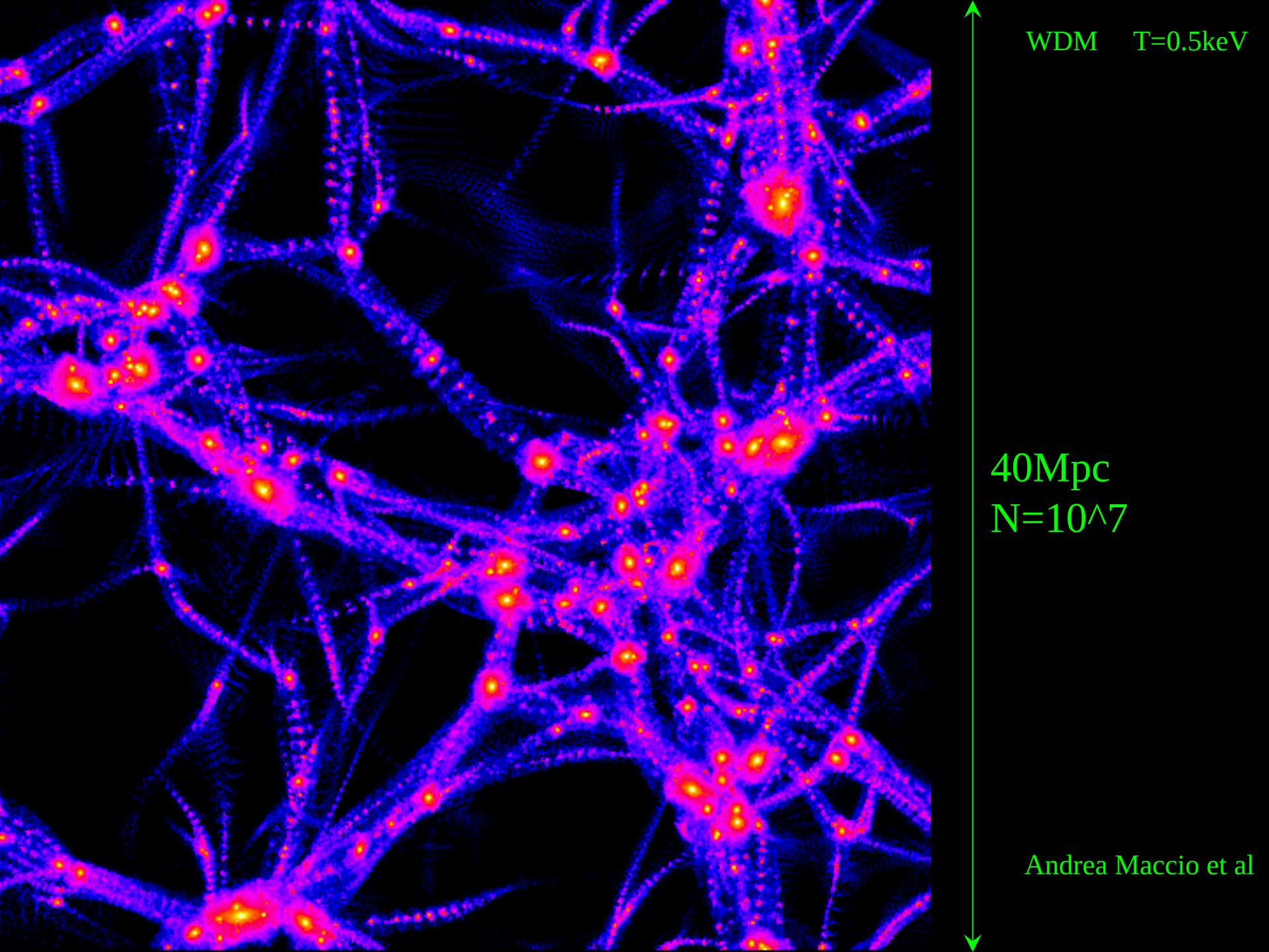
WDM T=0.5keV
40Mpc
N=10^7
Andrea Maccio et al

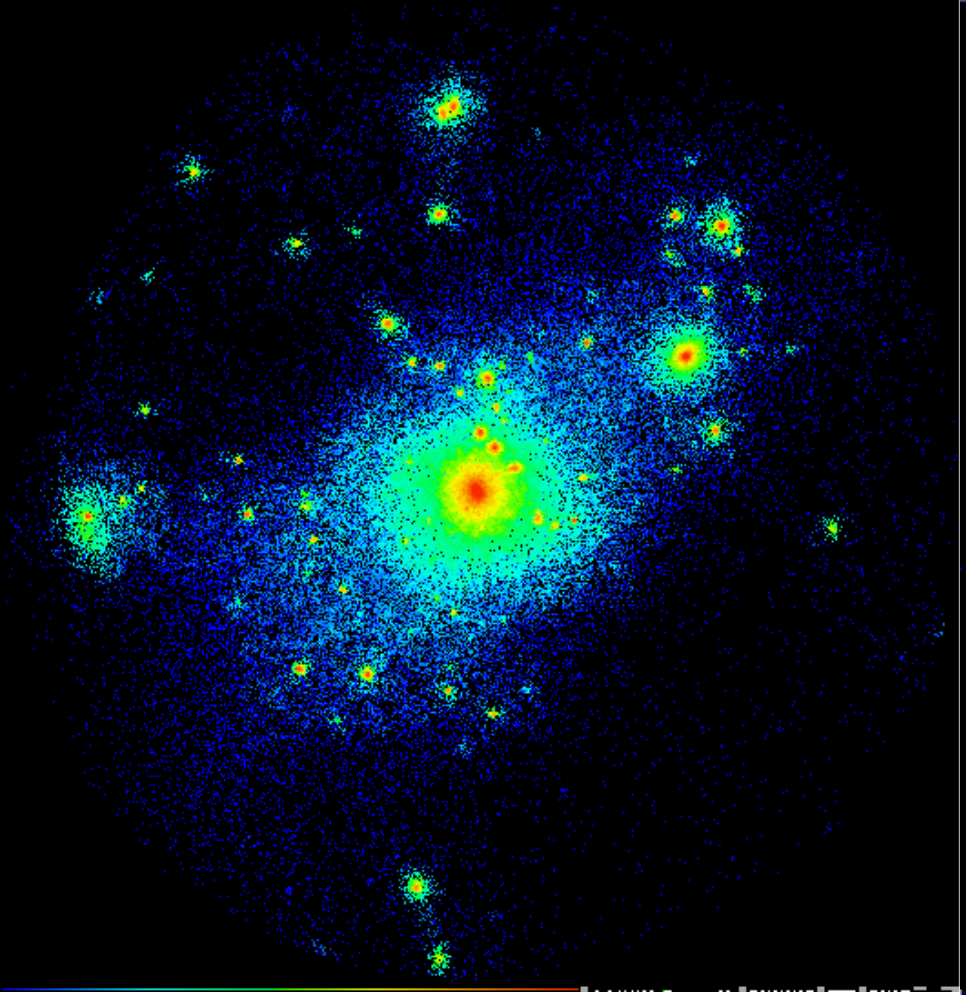

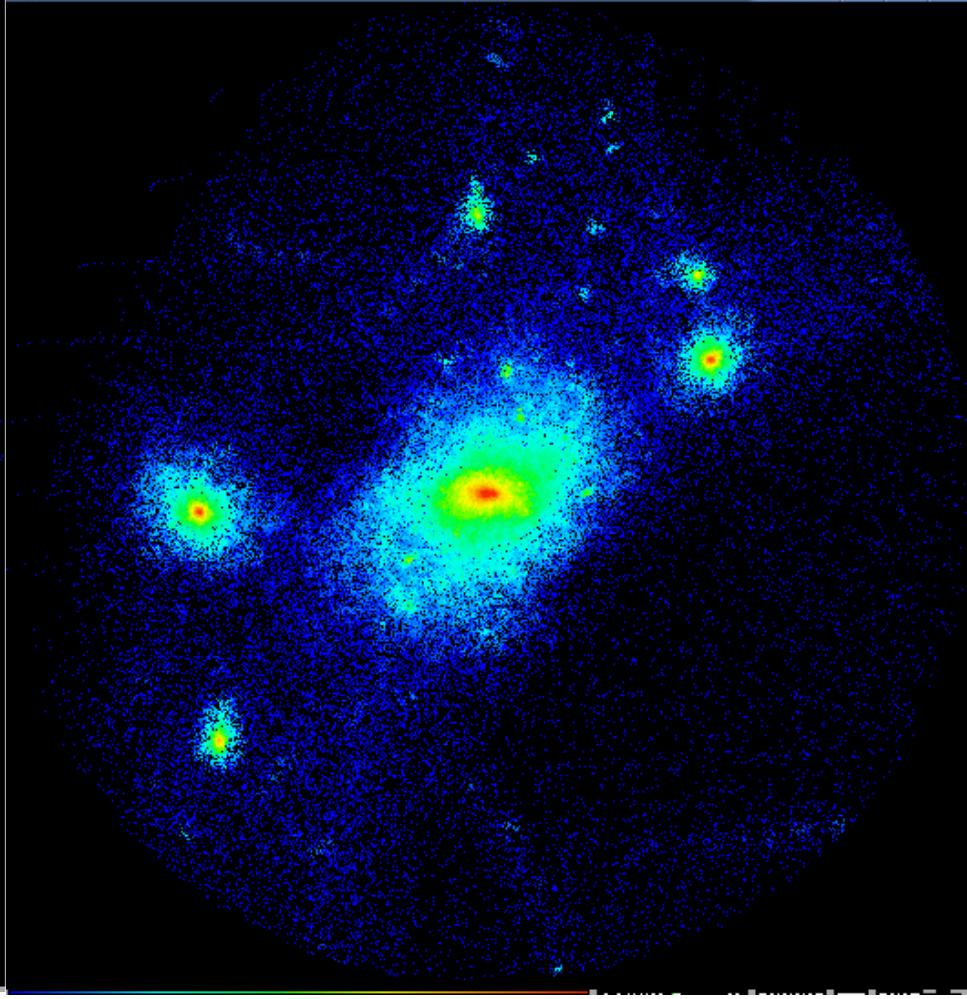

Andrea Maccio et al

$$R_{>\,\mathrm{eq}} \approx 0.2(\Omega_X h^2)^{1/3}\left(\frac{1.5}{g_X}\right)^{1/3}\left(\frac{\mathrm{keV}}{m_X}\right)^{4/3}\ \mathrm{Mpc}\ .$$

$$r_c > 32\left(\frac{10\ \mathrm{km\ s^{-1}}}{\sigma}\right)^{1/2}\left(\frac{\mathrm{keV}}{m_X}\right)^{2}\ \mathrm{pc}$$

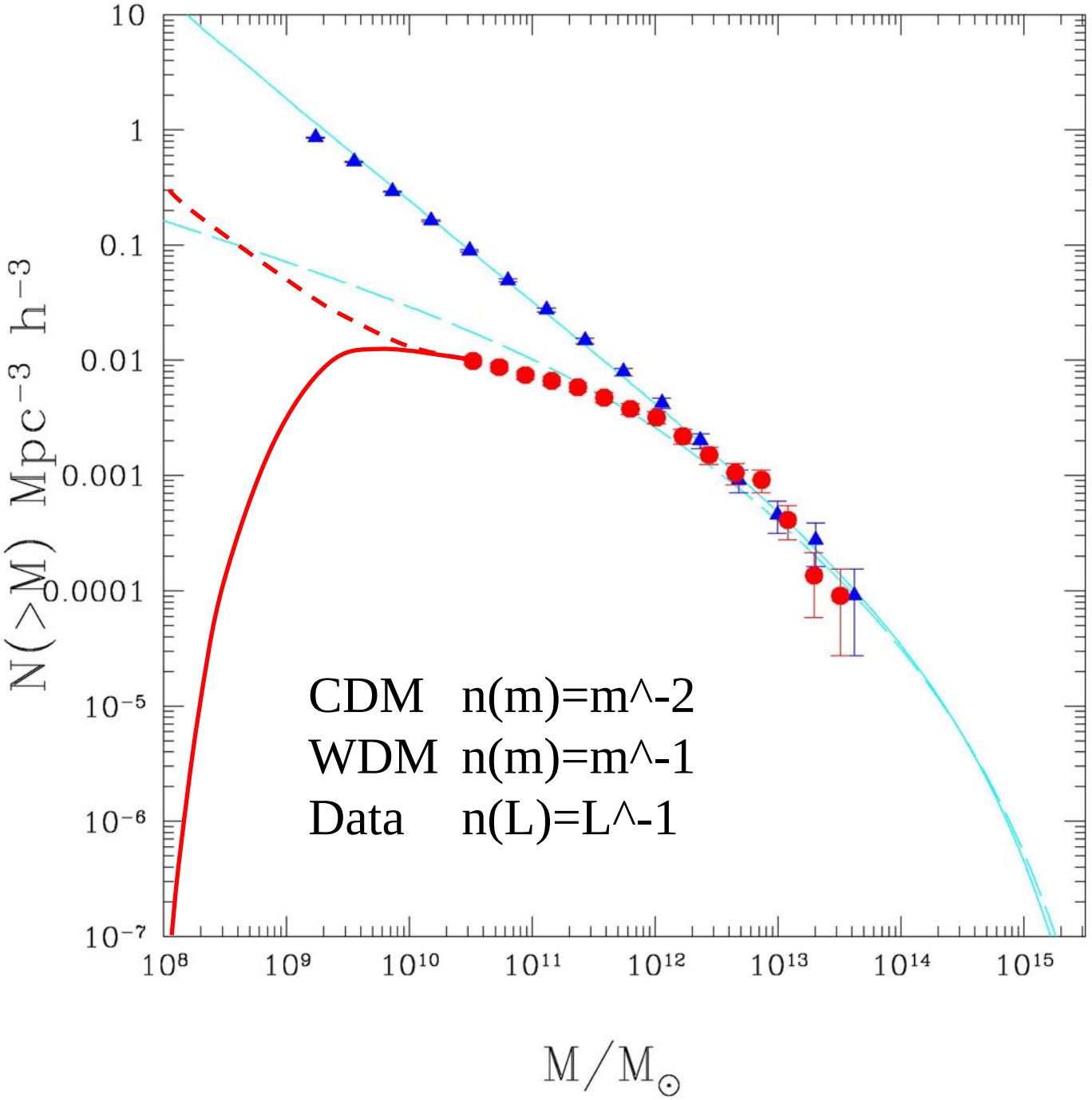
10
1
0.1
0.01
0.001
0.0001
10^{-5}
10^{-6}
10^{-7}
$N(>M)$ Mpc^{-3} h^{-3}
10^8
10^9
10^{10}
10^{11}
10^{12}
10^{13}
10^{14}
10^{15}
$M/M_\odot$
CDM n(m)=m^-2
WDM n(m)=m^-1
Data n(L)=L^-1

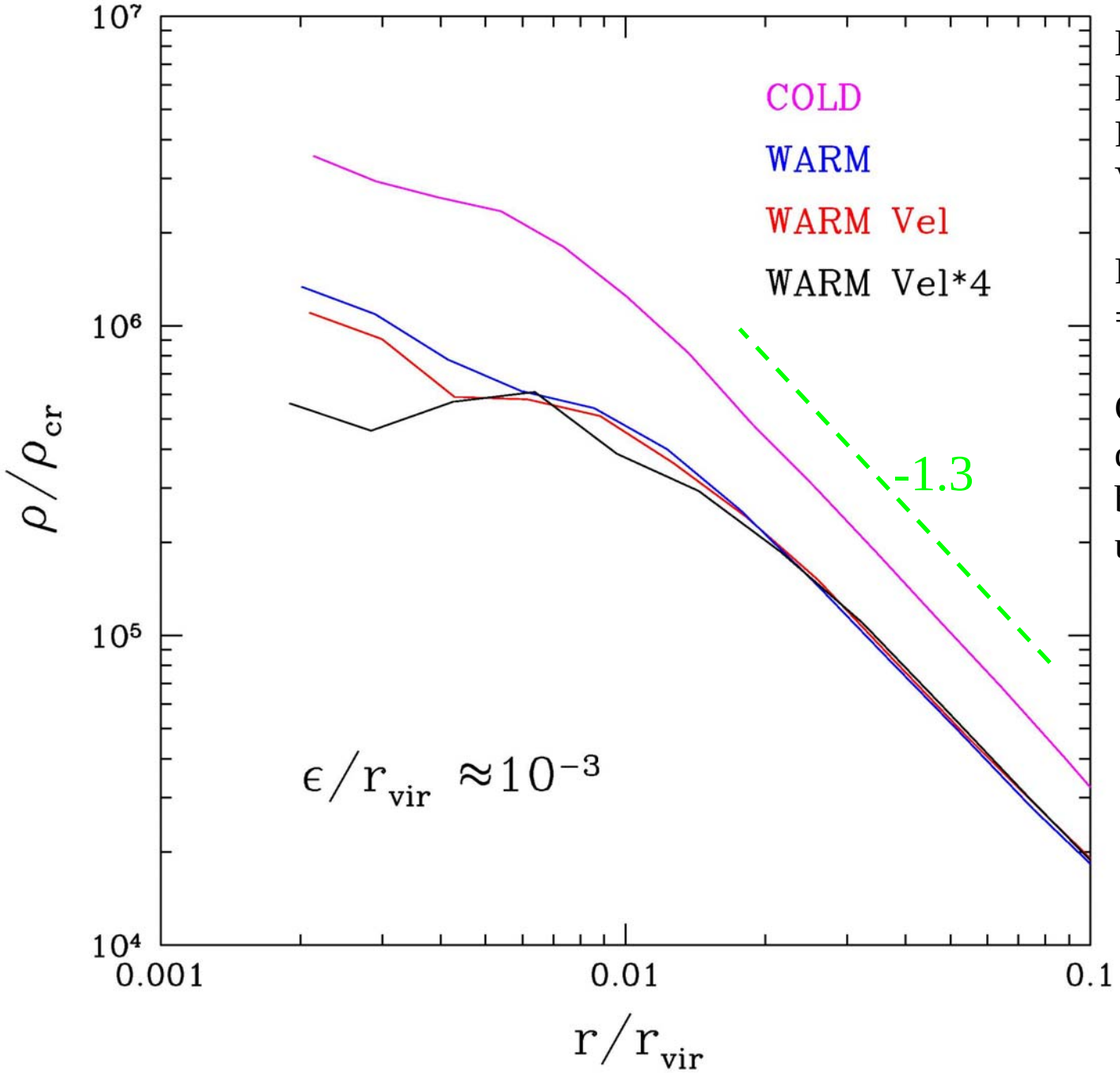

Halo mass=10^8Mo
N=10^7
R_200=80kpc
V_peak=50km/s

Resolve to 0.5%R_200 =800pc>core

Confirm that mean density of halo is lower but central cusp unchanged.

Andrea Maccio et al

- **Gas accretion and evidence for a Galactic cooling flow**

The measured distribution of "spin" parameter in CDM halos

$$\lambda = \frac{J\sqrt{|E|}}{GM^{5/2}}$$

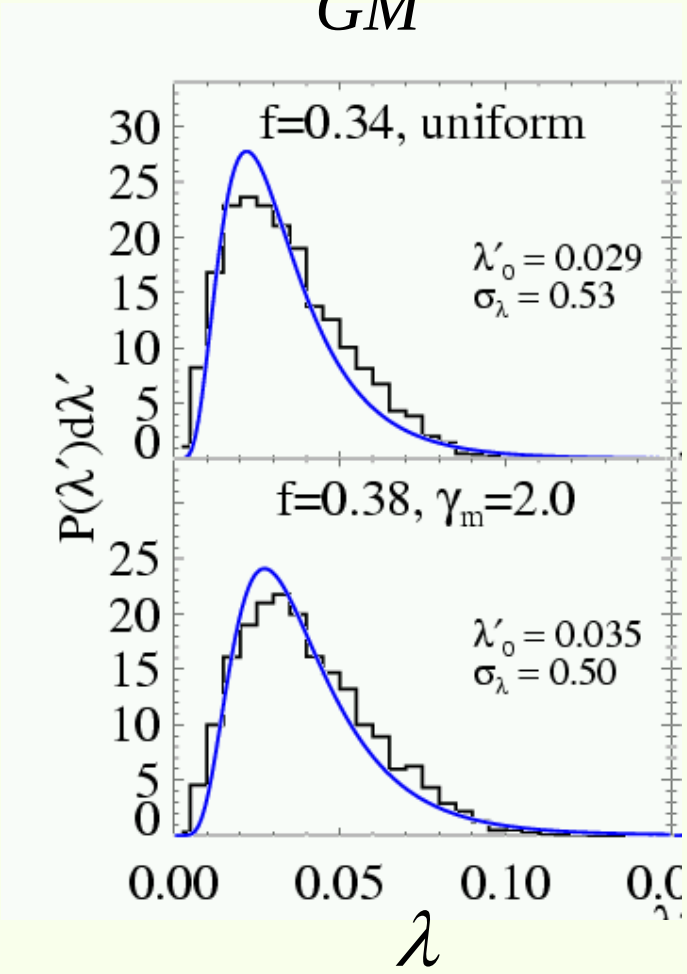

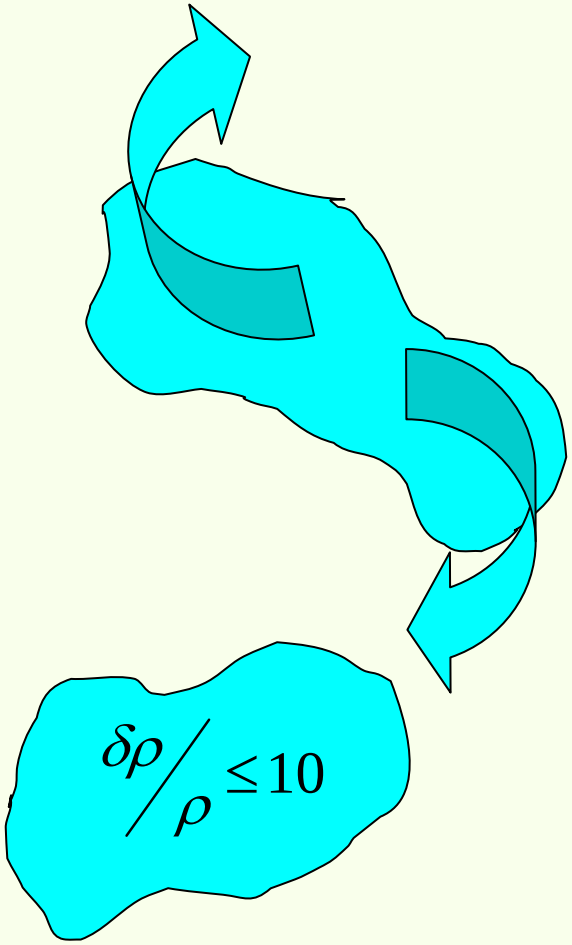

$\lambda = 0.05 \rightarrow 5\%$ of motion in angular momentum.

The measured distribution of "spin" parameter in CDM halos

$\lambda = 0.05 \rightarrow 5\%$ of motion in angular momentum.
A disk has >50% of its energy in angular momentum.

Thus if the gas collapses by a factor of ten it will have the correct angular momentum.

The distribution of observed disk sizes (2-20kpc) may reflect the scatter in the angular momentum of the dark matter halos.

Hoyle etc...

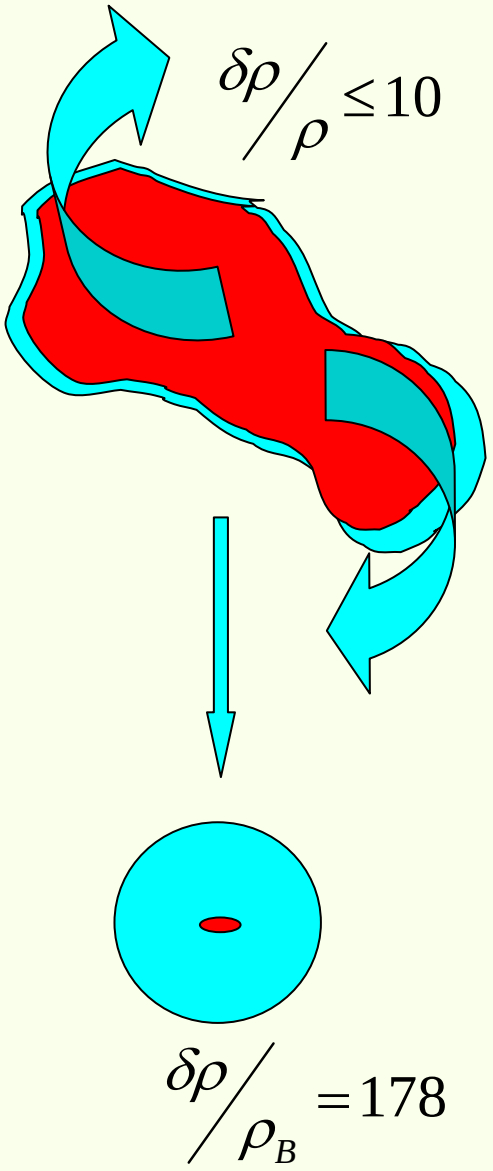

How do galaxies get their baryons?

The extra-planar neutral gas in the edge-on spiral galaxy NGC 891

Filippo Fraternali

Theoretical Physics, University of Oxford (UK)

Tom Oosterloo

ASTRON, Dwingeloo (NL)

Renzo Sancisi

INAF-Bologna (I) & Kapteyn Institute, Groningen (NL)

Rob Swaters

Department of Astronomy, University of Maryland (MD)

Abstract. We present neutral hydrogen observations of the nearby edge-on spiral galaxy NGC 891 which show extended extra-planar emission up to distances of 15 kpc from the plane. 3D modeling of the galaxy shows that this emission comes from halo gas rotating more slowly than the gas in the disk. We derive the rotation curves of the gas above the plane and find a gradient in rotation velocity of -15 km s^{-1} kpc^{-1}. We also present preliminary results of a galactic fountain model applied to NGC 891.

Longer/deeper observations…

2. HI observations

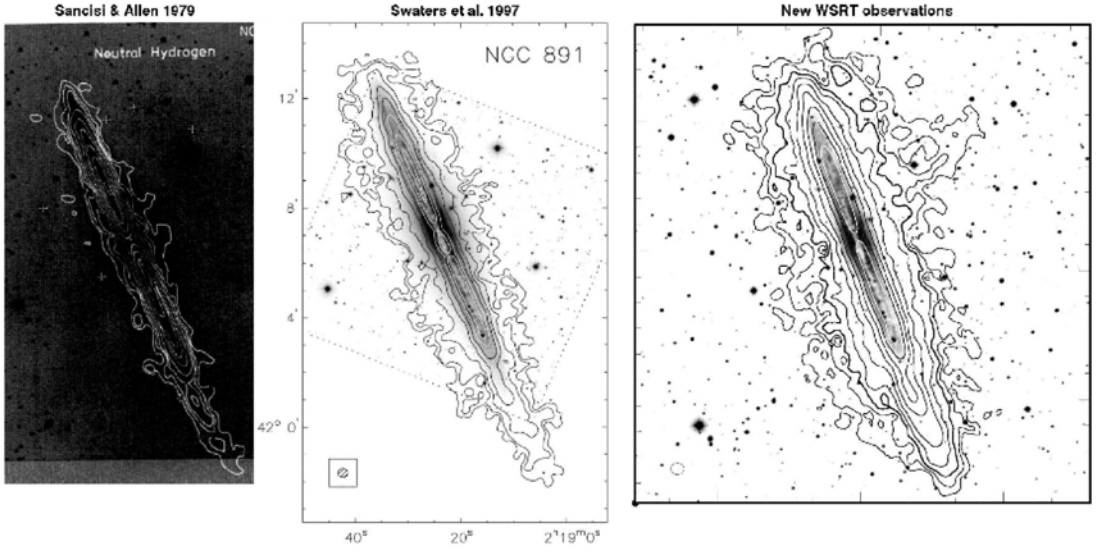

The extra-planar neutral gas in the edge-on spiral galaxy NGC 891

Filippo Fraternali

Theoretical Physics, University of Oxford (UK)

Tom Oosterloo

ASTRON, Dwingeloo (NL)

Renzo Sancisi

INAF-Bologna (I) & Kapteyn Institute, Groningen (NL)

Rob Swaters

Department of Astronomy, University of Maryland (MD)

Abstract. We present neutral hydrogen observations of the nearby edge-on spiral galaxy NGC 891 which show extended extra-planar emission up to distances of 15 kpc from the plane. 3D modeling of the galaxy shows that this emission comes from halo gas rotating more slowly than the gas in the disk. We derive the rotation curves of the gas above the plane and find a gradient in rotation velocity of -15 km s^{-1} kpc^{-1}. We also present preliminary results of a galactic fountain model applied to NGC 891.

Longer/deeper observations…

2. HI observations

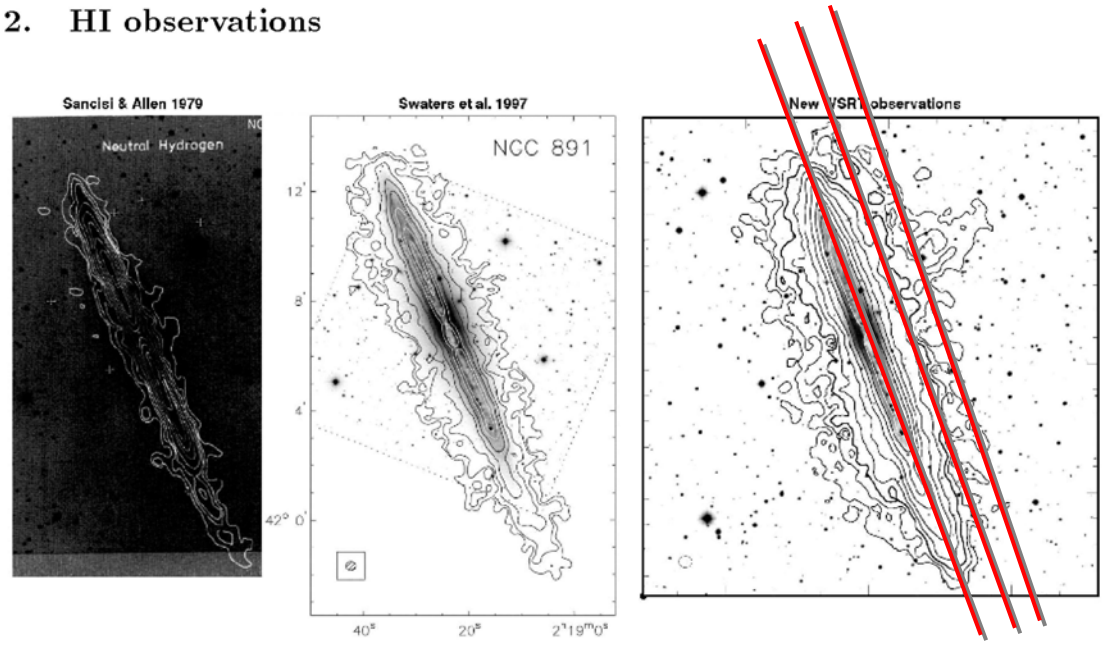

Cooling flows within galactic haloes: the kinematics and properties of infalling multi-phase gas

Tobias Kaufmann [1] *, Lucio Mayer [1], Joachim Stadel [1] , James Wadsley [2] and Ben Moore [1]
[1] *Institute for Theoretical Physics, University of Zürich, CH-8057 Zürich, Switzerland,*
[2] *Department of Physics & Astronomy, McMaster University, 1280 Main St. West, Hamilton ON L8S 4M1 Canada*

Accepted year Month day. Received year Month day; in original form year Month day

ABSTRACT
We study the formation of disks via the cooling flow of gas within galactic haloes using smoothed particle hydrodynamics simulations. A thermal instability results in the formation of numerous warm clouds that are pressure confined by the hot ambient halo gas. These accrete slowly onto the forming disk which grows from the inside out from material flowing preferentially down the angular momentum axis. The rotational velocity of the infalling cold gas decreases as a function of height above the disk, closely resembling that of the extra-planar gas recently observed around the spiral galaxy NGC 891.

Key words: methods: N-body simulations – galaxies:

Angular momentum transport and disk morphology in SPH simulations of galaxy formation

Tobias Kaufmann [1] *, Lucio Mayer [1,2], James Wadsley [3], Joachim Stadel [1] and Ben Moore [1]
[1] *Institute for Theoretical Physics, University of Zürich, CH-8057 Zürich, Switzerland*
[2] *Institute of Astronomy, ETH Zürich-Hönggerberg, CH-8093 Zürich, Switzerland*
[3] *Department of Physics & Astronomy, McMaster University, 1280 Main St. West, Hamilton ON L8S 4M1 Canada*

Accepted year Month day. Received year Month day; in original form year Month day

ABSTRACT

We perform controlled N-Body/SPH simulations of disk galaxy formation by cooling a rotating gaseous mass distribution inside equilibrium cuspy spherical and triaxial dark matter halos. We systematically study the angular momentum transport and the disk morphology as we increase the number of dark matter and gas particles from 10^4 to 10^6, and decrease the gravitational softening from 2 kpc to 50 parsecs. The angular momentum transport, disk morphology and radial profiles depend sensitively on force and mass resolution. At low resolution, similar to that used in most current cosmological simulations, the cold gas component has lost half of its initial angular momentum via various numerical and physical mechanisms. The angular momentum is transferred primarily to the hot halo component, by resolution-dependent hydrodynamical and gravitational torques, the latter arising from asymmetries in the mass distribution. In addition, disk-particles can lose angular momentum while they are still in the hot phase by artificial viscosity. In the central disk, particles can transfer away over 99% of their initial angular momentum due to spiral structure and/or the presence of a central bar. The strength of this transport also depends on force and mass resolution - large softening will suppress the bar instability, low mass resolution enhances the spiral structure. This complex interplay between resolution and angular momentum transfer highlights the complexity of galaxy formation even in isolated haloes. With 10^6 gas and dark matter particles, disk particles lose only 10-20% of their original angular momentum, yet we are unable to produce pure exponential profiles due to the steep density peak of baryons within the central kpc. We speculate that the central luminosity excess observed in many Sc-Sd galaxies may be due to star-formation in gas that has been transported to the central regions by spiral patterns.

Cosmological simulations do not form disk dominated galaxies…

(each gas particle is 10^6Mo… resolution effects?)

Tobias Kaufmann etal (2005).

Study cooling of gas within CDM triaxial haloes.

Explore convergence in numerical parameters, spurious angular momentum loss, disk properties, how the gas gets to the disk.

Set up initial conditions…

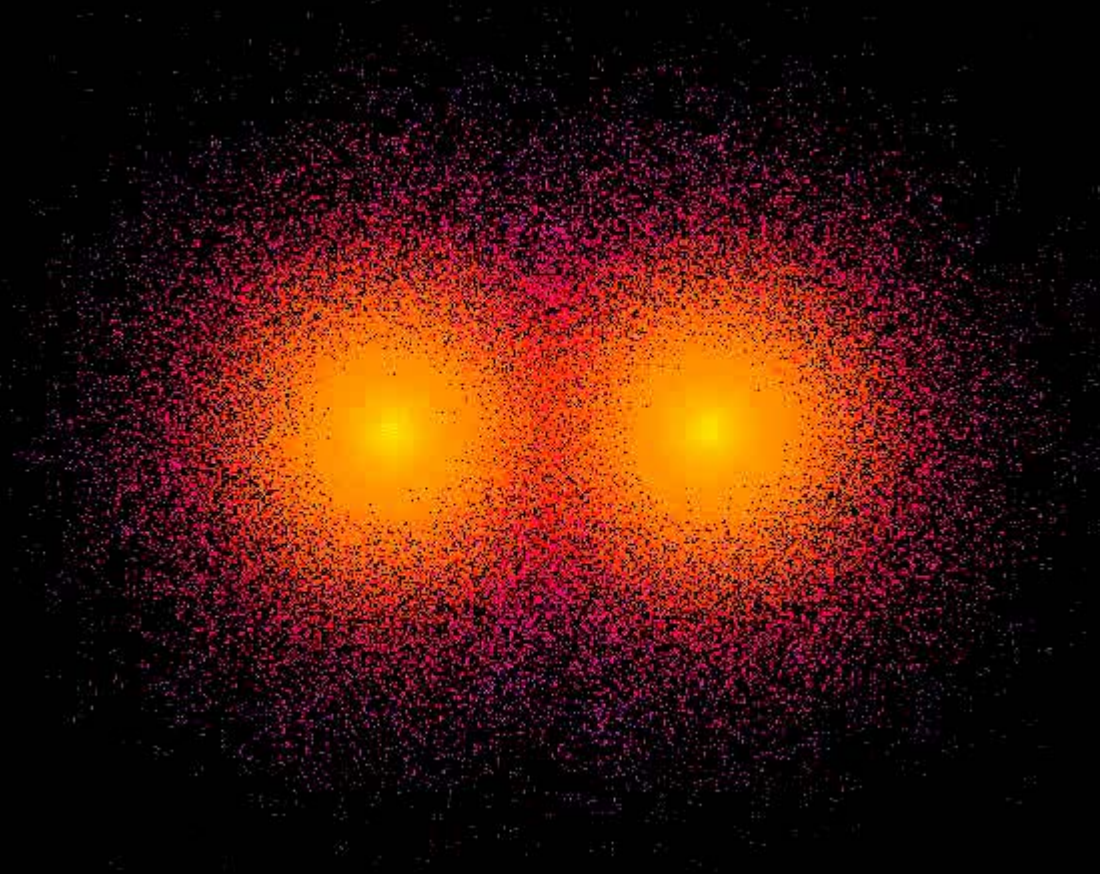

Now allow the gas to cool. Look at the face and edge on projections.

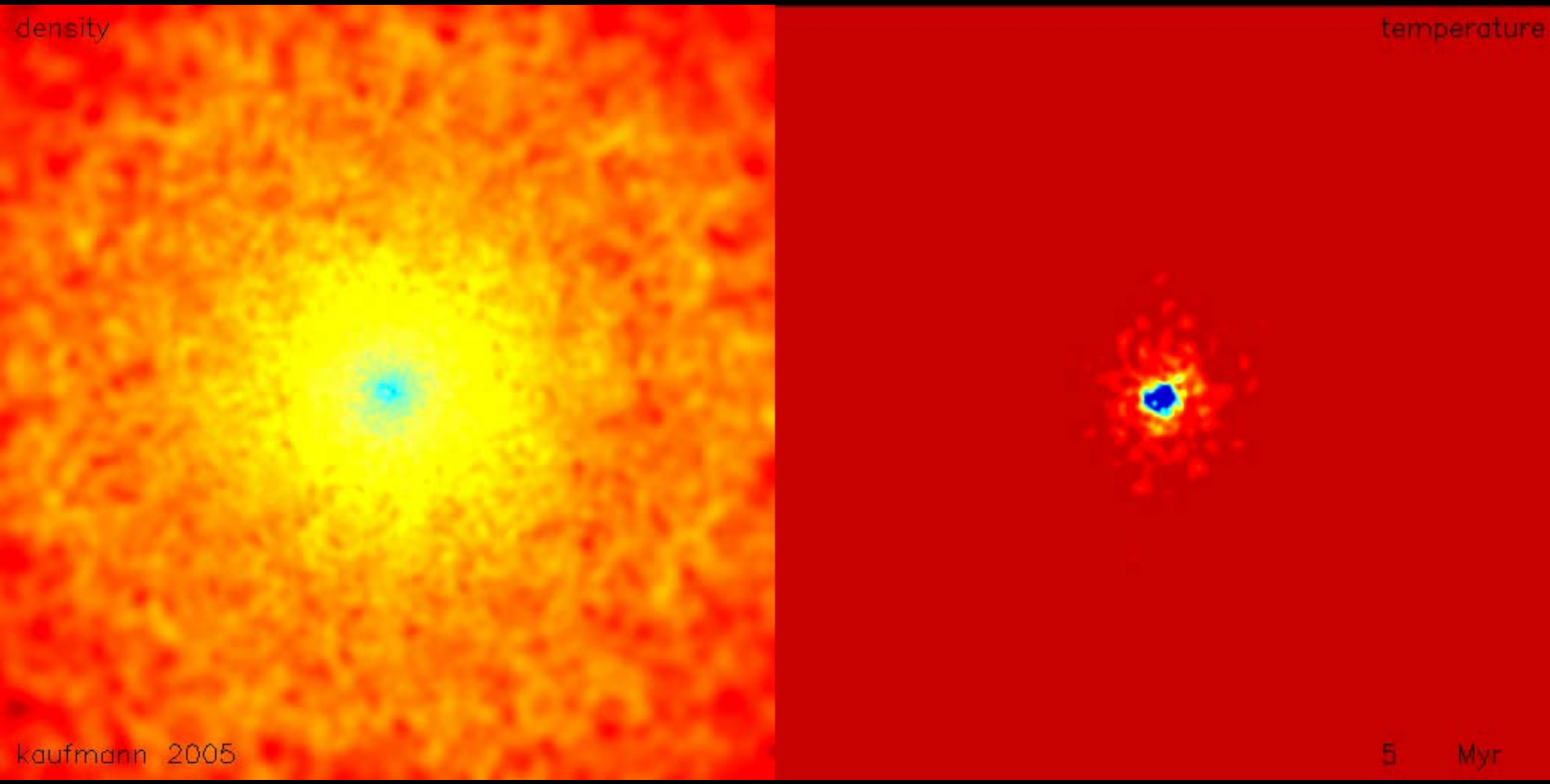

4 million SPH particles, 2 million dark matter particles, 100pc force resolution.
Need particle mass < 10^5Mo to resolve formation of two-phase medium.

- Disk forms from inside out as expected
- Low angular momentum material quickly accretes from the poles
- Gas forms unstable clouds which fall subsonically onto the disk

Kazantzidis etal (2004)

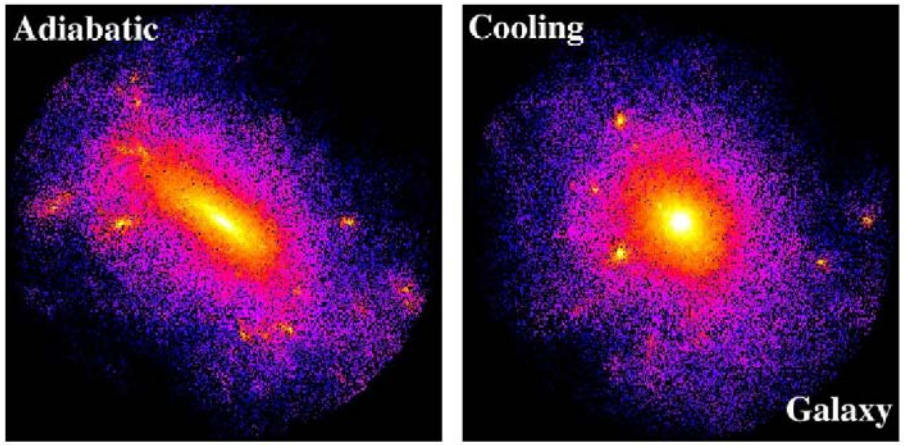

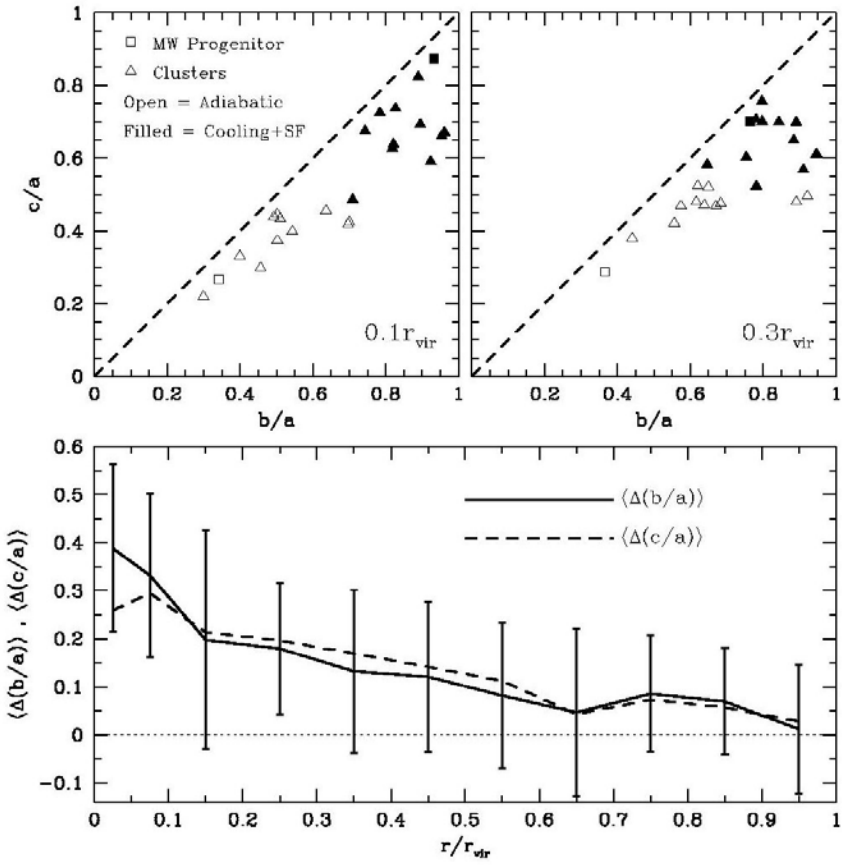

FIG. 1.— *Top panels:* Axis ratios c/a vs. b/a for halos in cosmological simulations. Open symbols show adiabatic simulations and solid symbols correspond to simulations with gas cooling and star formation. The galaxy simulation is shown by a square and the clusters by triangles. *Bottom panel:* the average difference between axis ratios in cooling and adiabatic runs as a function of radius. The error bars show the 1σ scatter in $\Delta(b/a)$ the mean in each bin. The scatter in $\Delta(c/a)$ is similar.

As baryons cool within dark matter halos, the central potential becomes more spherical. The box orbits which support the triaxial shape are destroyed and the entire system becomes more spherical – even at radii 10x beyond the baryons

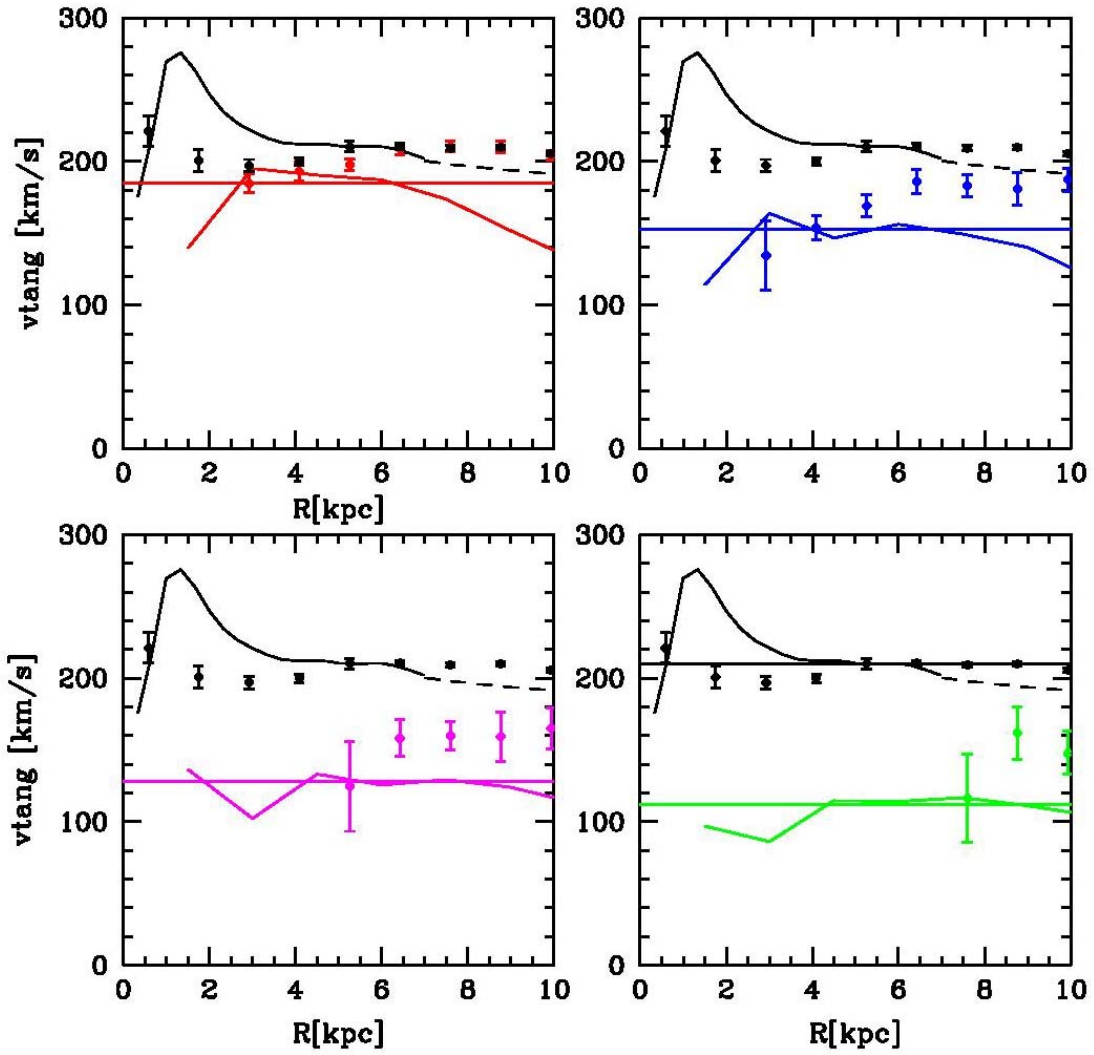

Further above the disk the gas is rotating more slowly, with a dv/dz=-15km/s.

This is similar to what we find as the gas sinks via dissipation and rotates faster by conservation of angular momentum.

The gas accretes onto the disk in cold clouds.

The disk forms from the material cooling preferentially along the angular momentum axis.

Is this evidence for multiphase cooling flows providing the cold gas for galactic disks?

Cold gas fraction

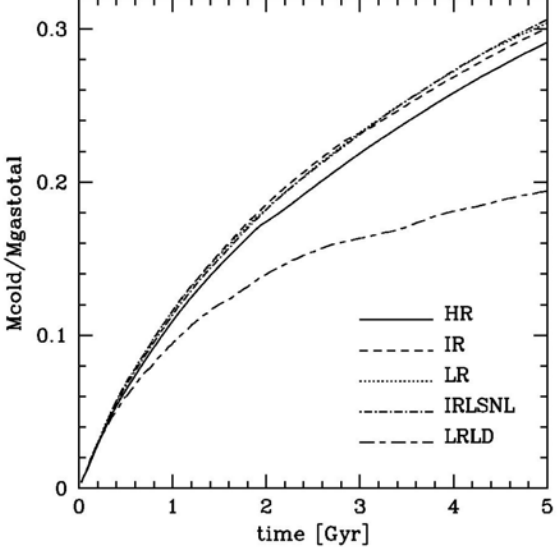

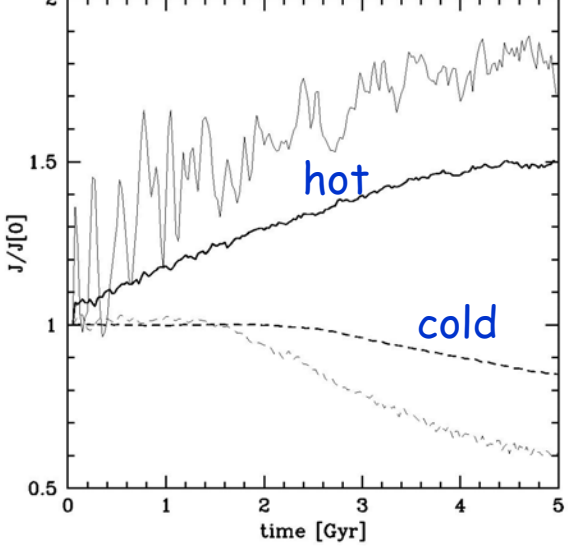

Total Ang. Mom.

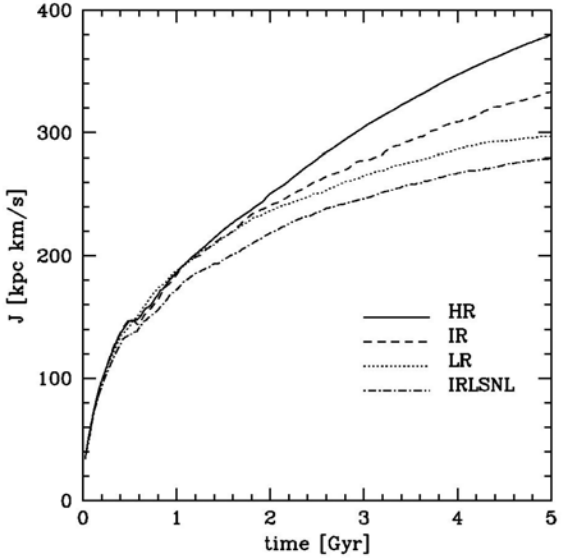

Ang.mom loss within a shell of initial radius 30-40kpc.

Resolution tests

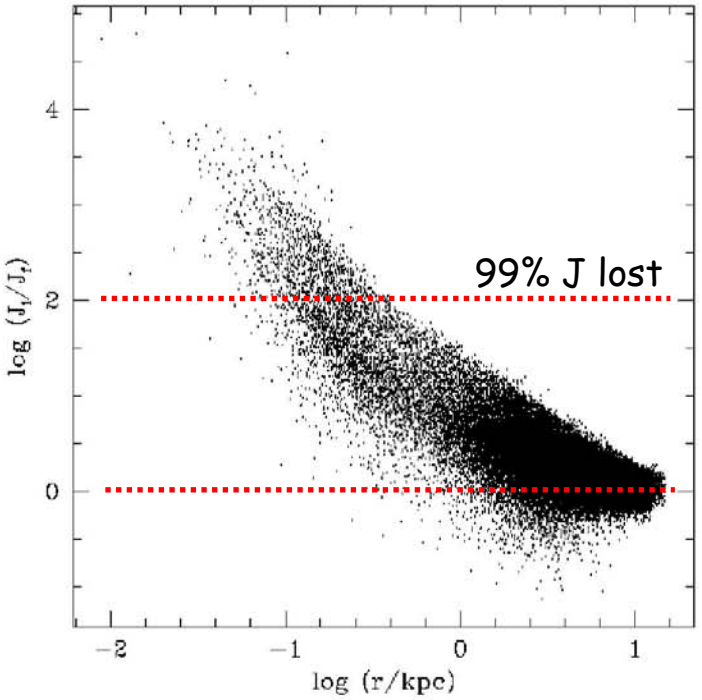

Figure 5. For the gaseous disk particles in the M33A model we plot the initial specific angular momentum over the final (measured at 4.8 Gyr) versus radius. The angular momentum loss in the centre can be very large.

Angular momentum loss is large for particles that end up near the centre

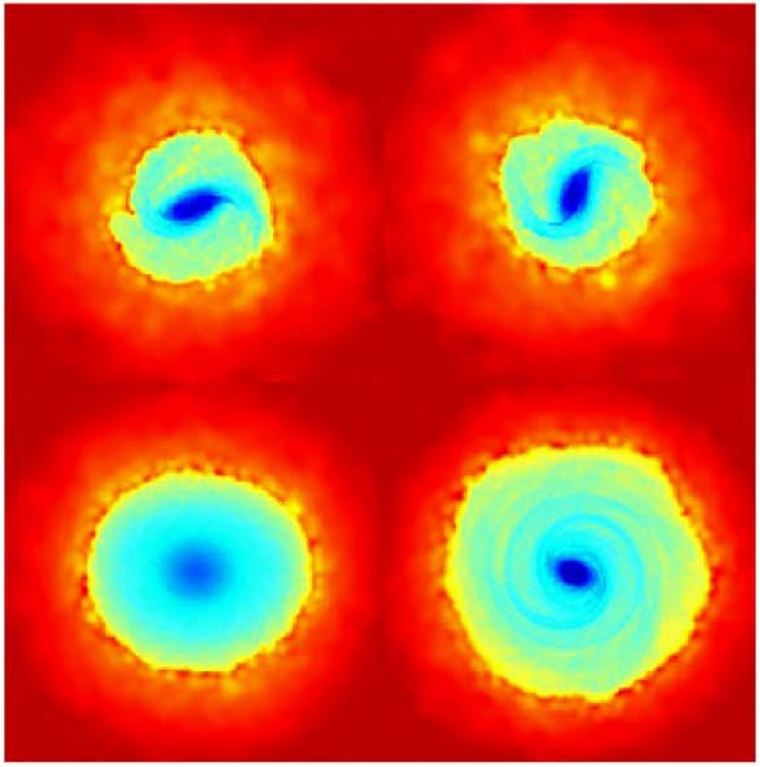

Figure 8. Density maps of gas in a slice through the centre of the Milky Way gas disk which show how bar formation can be suppressed by a large softening. On the left the HR run is shown, on the right the HRLS run. Upper panels show a snapshot after 1 Gyr, lower panel one after 5 Gyr. Boxes are 20 kpc on a side. The density is colour coded as in Figure 3.

Large gravitational softening suppresses bar formation

Formation of nucleus by angular momentum transfer

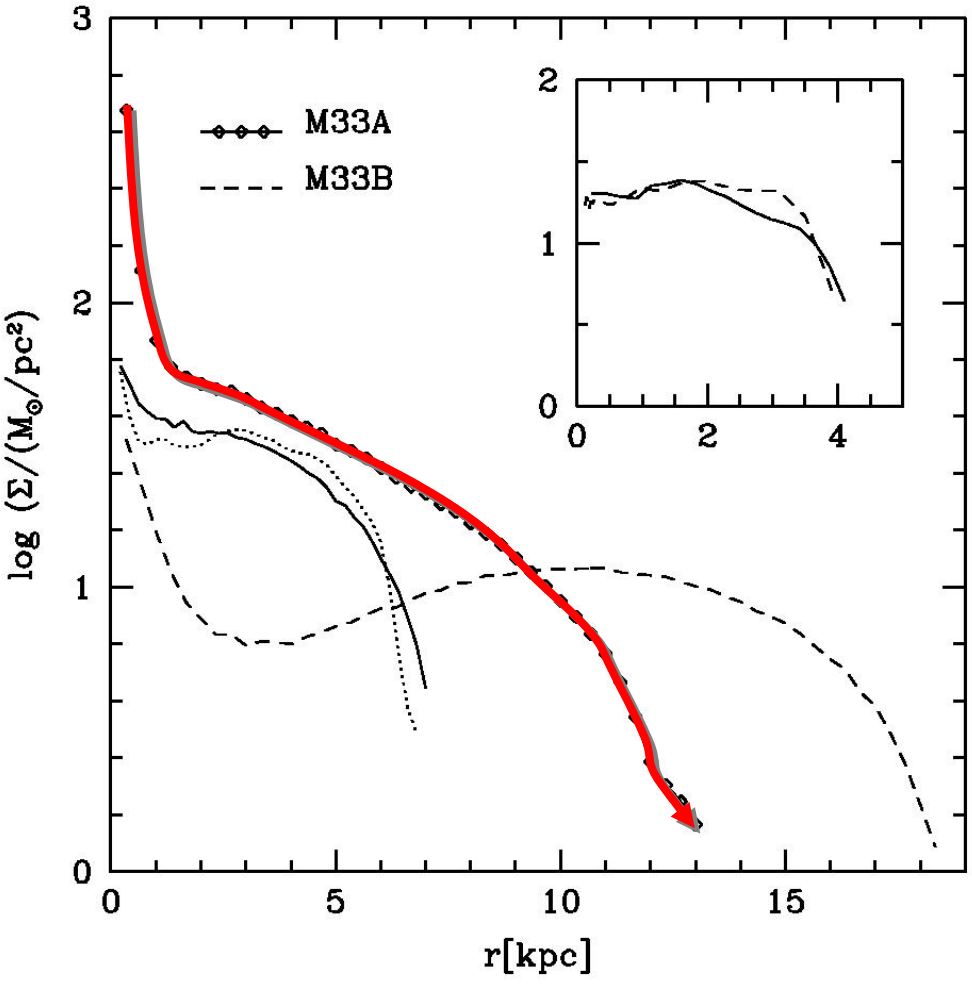

Figure 16. The logarithmic surface density of the M33 gas disk after four Gyr for different models: M33A (solid with open symbols), M33B (dashed line). The solid line shows M33A after one Gyr and the dotted line shows the refined model of M33A at the same time. Inset: logarithmic surface density of the standard and refined M33A (solid and dashed, respectively) run after 0.25 Gyr. All the M33 models showed at later stages a nucleus in the centre.

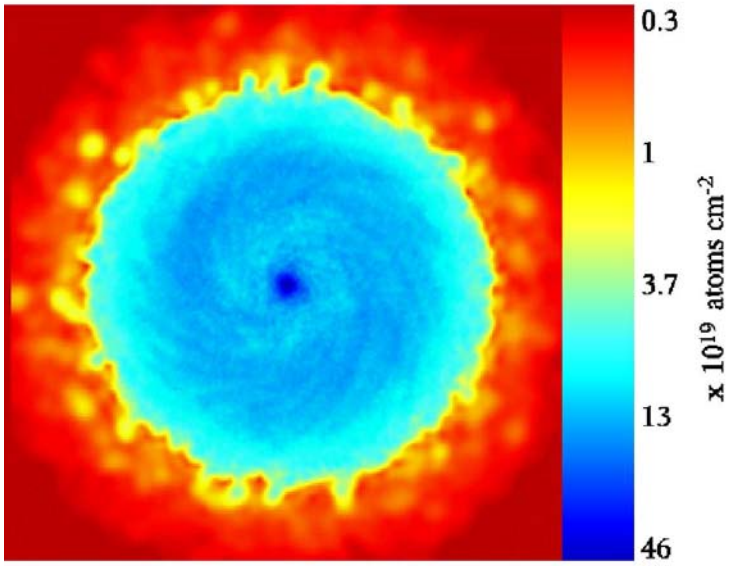

Very high resolution mass splitting run:

50pc force resolution

150Mo per particle

- **Cold accretion and the origin of polar ring galaxies**

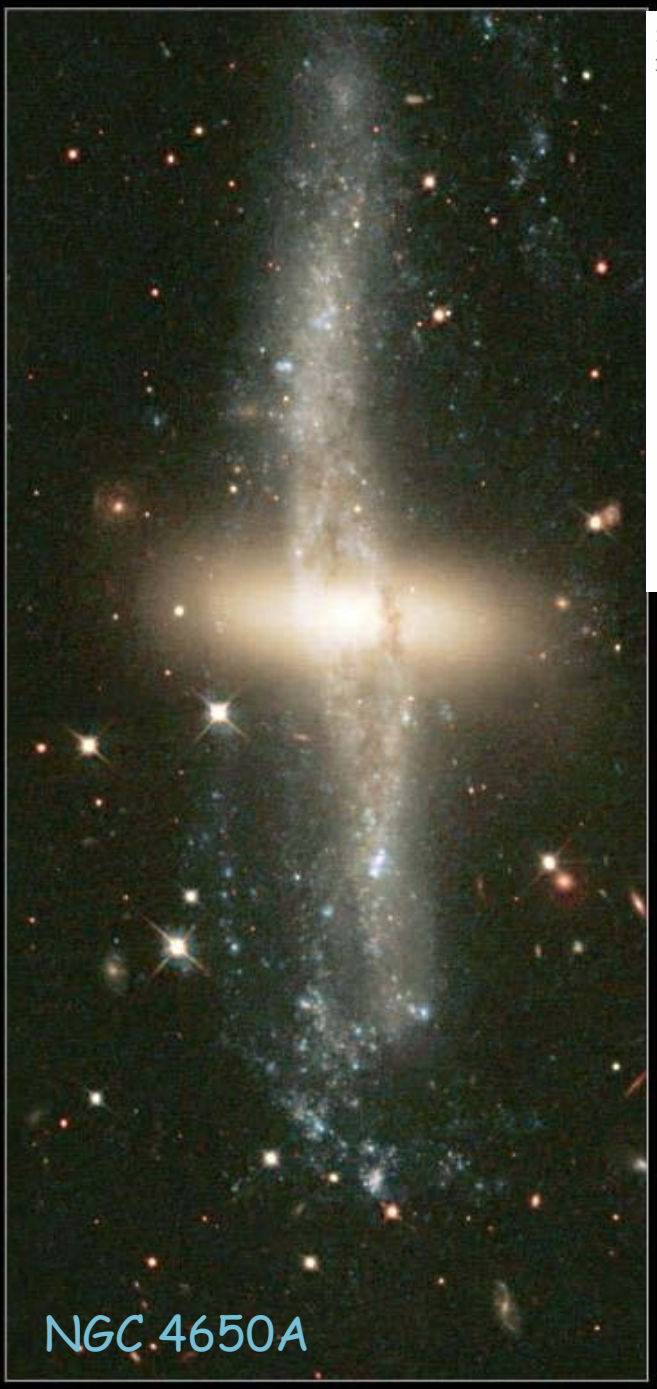

The Astrophysical Journal, submitted

Preprint typeset using LaTeX style emulateapj v. 11/12/01

THE ORIGIN OF POLAR RING GALAXIES: EVIDENCE FOR GALAXY FORMATION BY COLD ACCRETION

ANDREA V. MACCIÒ[1], BEN MOORE[1] & JOACHIM STADEL[1]

The Astrophysical Journal, submitted

ABSTRACT

Polar ring galaxies are flattened stellar systems with an extended ring of gas and stars rotating in a plane almost perpendicular to the central galaxy. We show that their formation can occur naturally in a hierarchical universe where most low mass galaxies are assembled through the accretion of cold gas infalling along megaparsec scale filamentary structures. Within a large cosmological hydrodynamical simulation we find a system that closely resembles the classic polar ring galaxy NGC 4650A. How galaxies acquire their gas is a major uncertainty in models of galaxy formation and recent theoretical work has argued that cold accretion plays a major role. This idea is supported by our numerical simulations and the fact that polar ring galaxies are typically low mass systems.

Subject headings: cosmology: theory — galaxies: formation — methods: numerical

Andrea Maccio etal (2005) serendipitous detection of a polar ring galaxy in a cosmological hydro-simulation.

Evidence for cold accretion on sub-L* scales.

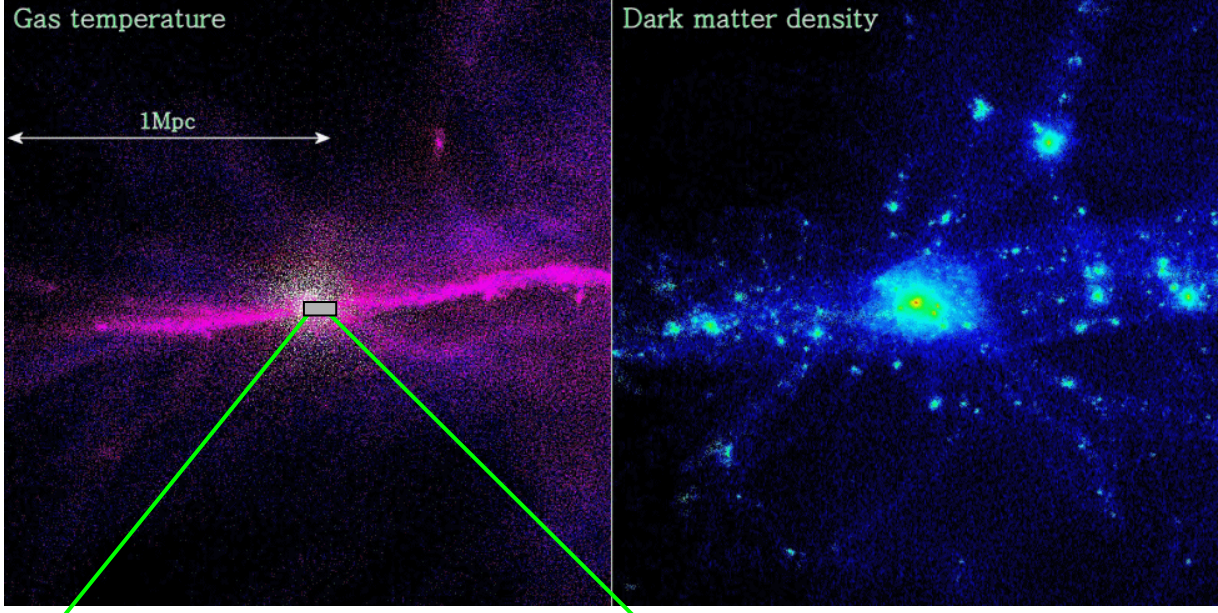

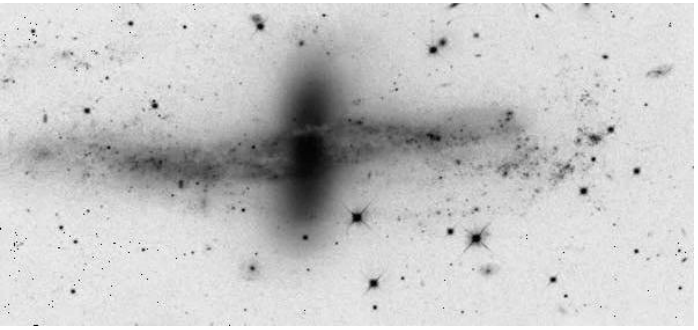

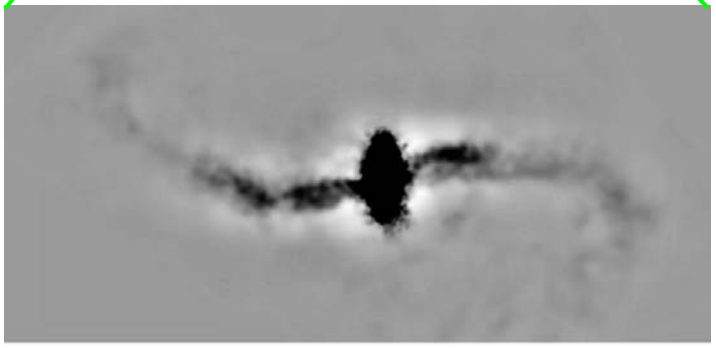

All polar ring galaxies are sub L* = expected from Keres etal, Birnboim etal.

Long lived in polar orbit.

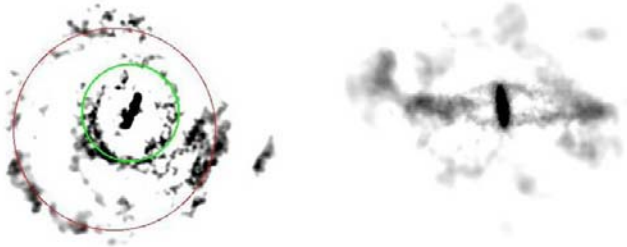

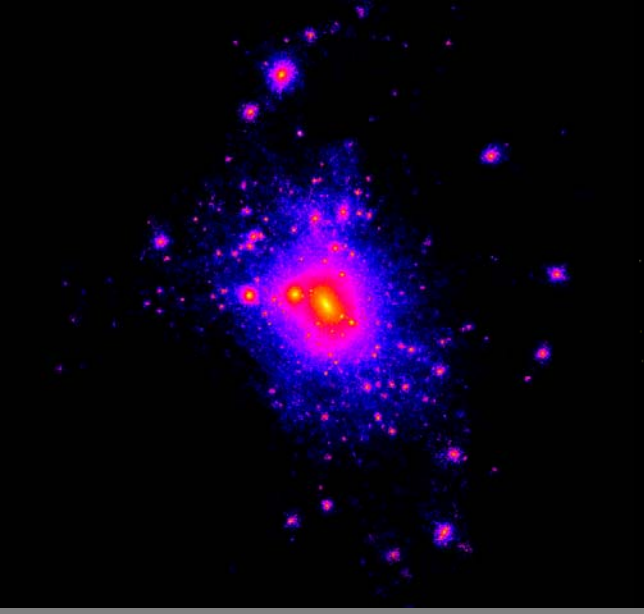

Dark matter density

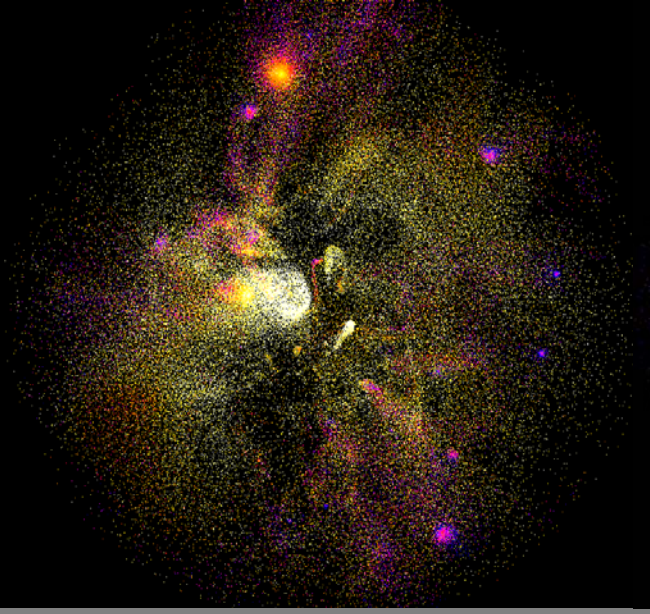

Cold gas < 300,000k

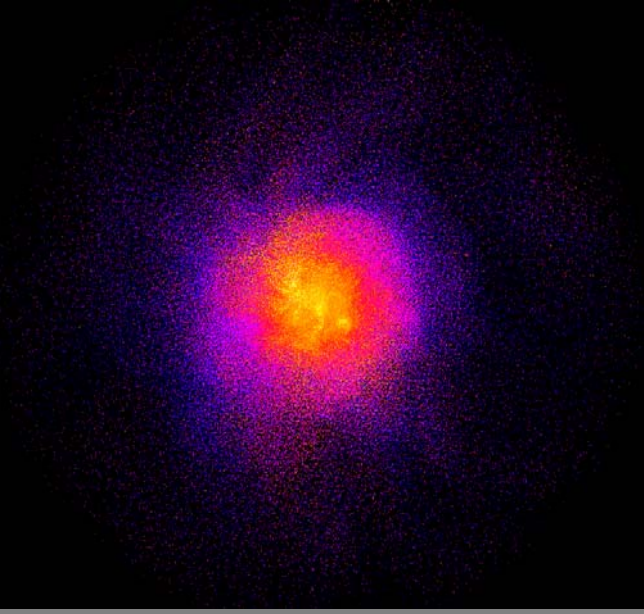

Hot gas > 1,000,000k

Andrea Maccio et al (2006)

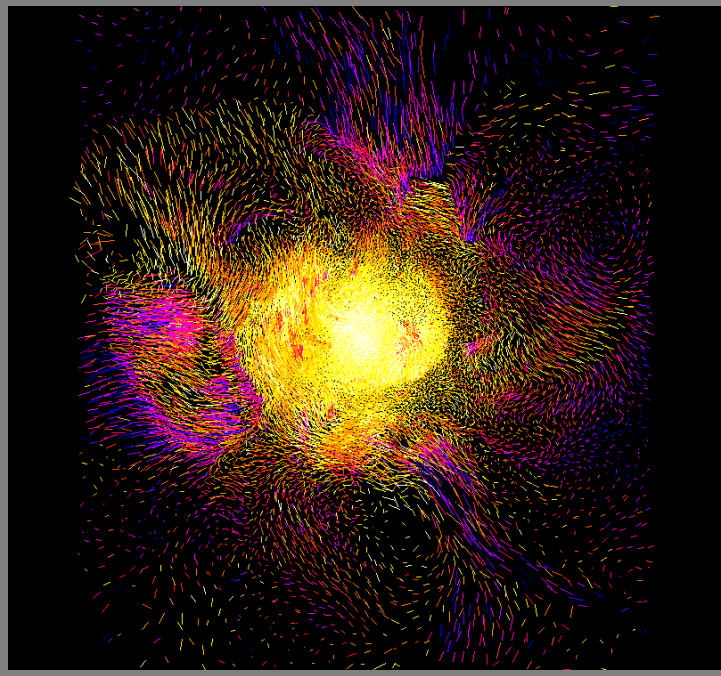

- **Simulating fluids – grids versus sph**

Oscar Agertz

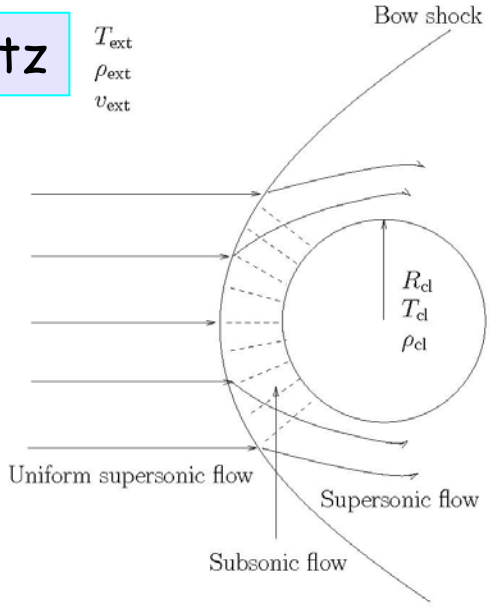

Figure 1. Illustration of the problem setup. The external medium, which initially was in pressure equilibrium with the cloud, travel with a supersonic velocity creating a detached bow-shock in fron of the cloud. The postshocl flow is subsonic until the smooth flow accelerates and again obtains supersonic speed on the lateral sides of the cloud.

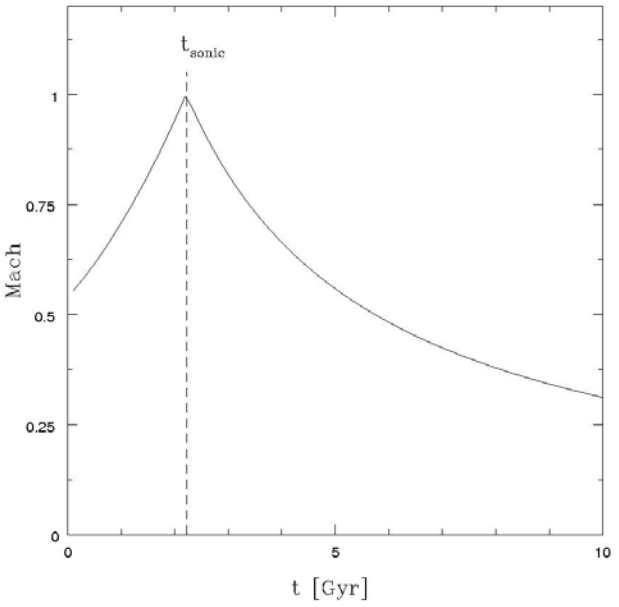

Figure 2. Mach number for flow directly in front of the cloud. The flow speed increases due to the weakened shock strength up to $t_{\rm sonic}$ where the relative motion of the cloud and wind turns subsonic. After this, the mach number is simply goverened by the acceleration of the cloud.

shock and 2 downstream. Formally we need to take the obliqueness of the bow shock into account but for simplicity we will only consider the flow that enters at the symmetry axis of the cloud.

The cloud acceleration can be approximated by considering the maximum area that can obtain momentum from the ambient flow. This implies that all gas in a cylinder in front of the cloud transfers momentum leading to an acceleration

$$a \sim \frac{\rho_{\rm ext} \pi R_{\rm cl}^2 v_{\rm ext}^2}{M_{\rm cl}} \qquad (3)$$

Thacker et al. 1998 considered this and solved for the velocity

$$V(t) = l/(t - t_l), \qquad (4)$$

cloud and reaches supersonic speed at the points indicated in Fig. 1. Beyond this region we expect to see a turbulent boundary layer forming (in constrast to laminar in subsonic cases) which transports material of the surface. The cloud will compress along the line of motion due to an internal shock wave generated by the external gas. From Bernoulli's theorem we know that the pressure is low on the lateral sides which causes an overspilling of the cloud due to the high inner pressure of the compressed cloud.

The fundamental reason for a cloud to loose its gas is due to *ram pressure stripping*. This occurs when the pressure of the surrounding wind of size $\sim \rho_{\rm ext} v^2$ overcomes the thermal pressure of the cloud. Because we neglect gravity we expect his mechanism to be very effective. Turbulence and KHI will greatly facilitate the material transportation and large KHI and RTI modes are expected to develop resulting in a total destruction of the cloud.

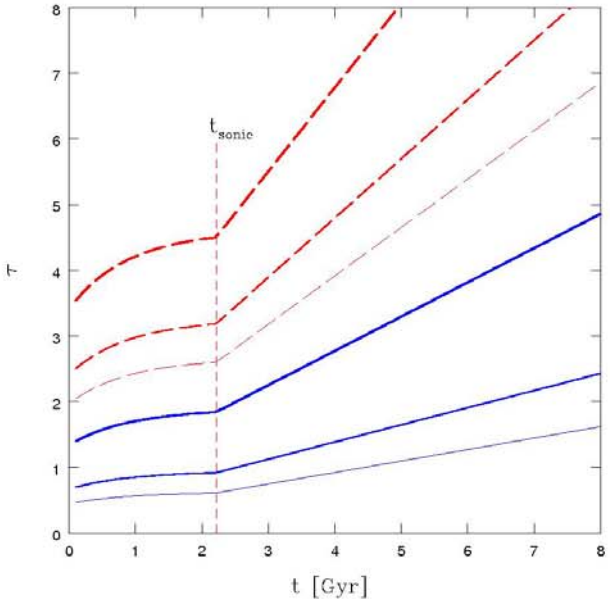

Figure 3. The time dependence of KH (solid, blue lines) and RT (dashed, red lines) growth rates. The lines represent different sizes of perturbation wavelenght: $R_{\rm cl}$ (thick), $R_{\rm cl}/2$ (middle) and $R_{\rm cl}/2$ (thin).

for an incompressible fluid is (Chandrasekhar 1961)

$$w = k\frac{(\rho_{\rm ext}\rho_{\rm cl})^{1/2}U}{(\rho_{\rm ext}+\rho_{\rm cl})}, \qquad (5)$$

where U is the relative velocity of the background and the cloud *at the interface* and k is the wavenumber of the instability. Following the argument above we can set $k = 2\pi/R_{\rm cl}$ which gives us a characteristic growth time for the cloud destruction

$$\tau_{KH} \equiv \frac{2\pi}{w} = \frac{R_{\rm cl}(\rho_{\rm ext}+\rho_{\rm cl})}{(\rho_{\rm ext}\rho_{\rm cl})^{1/2}U}. \qquad (6)$$

By inspection of this equation we see that the characteristic growth time is highly time dependent due to the evolution of densities and relative velocity.

3.2 The Rayleigh-Taylor instability

The cloud is accelerated with respect to the background and we expect RTI to develop. The RTI has a linear growth rate (Chandrasekhar 1961)

$$|w^2| = k'a\left(\frac{\rho_{\rm cl}-\rho_{\rm ext}}{\rho_{\rm cl}+\rho_{\rm ext}}\right), \qquad (7)$$

where k' in 3D is given by $k' = \sqrt{k^2+l^2}$, where k and l are the wave vectors descibing the perturbation. The acceleration on the surface, a, can be approximated by Eq. 3. Note that it is very difficult to analytically determine the effective acceleration on the surface of the cloud which depends on the effectiveness of the momentum transfer from the external medium onto the cloud. This should however give an upper limit.

Fig. 3 shows the characterisitc growth times for RTI (red, dashed lines) of size $R_{\rm cl}$ (thick), $R_{\rm cl}/2$ (middle) and $R_{\rm cl}/3$ (thin). We see that $\tau_{\rm KH} < \tau_{\rm RT}$ for all considered sizes of instabilities. The largest mode grows very slowly and is probably not important in this type of problem. We do believe that a fast growing small-scale RTI should develop on the cloud front, especially on the axis of symmetry the flow rams into the stagnation point. Complicated mixtures of KHI and RTI during later evolution is also expected until the cloud becomes fully comoving with the flow.

4 NUMERICAL SIMULATIONS

Before describing the outcome of numerical simulations there are some general comments on the assumed gas physics. First of all, we are only solving the Euler equations which means we neglect physical viscosity and radiative processes in all of the tests. Furthermore, the tests are performed as adiabatic. This means the gas can only undergo heating and cooling by adiabatic compression or expansion as well as irreversible heating by shocks. In other words, we allow conversion of kinetic energy into thermal energy. In order to see the differences in hydrodynamic solvers only we also neglect selfgravity the simulation.

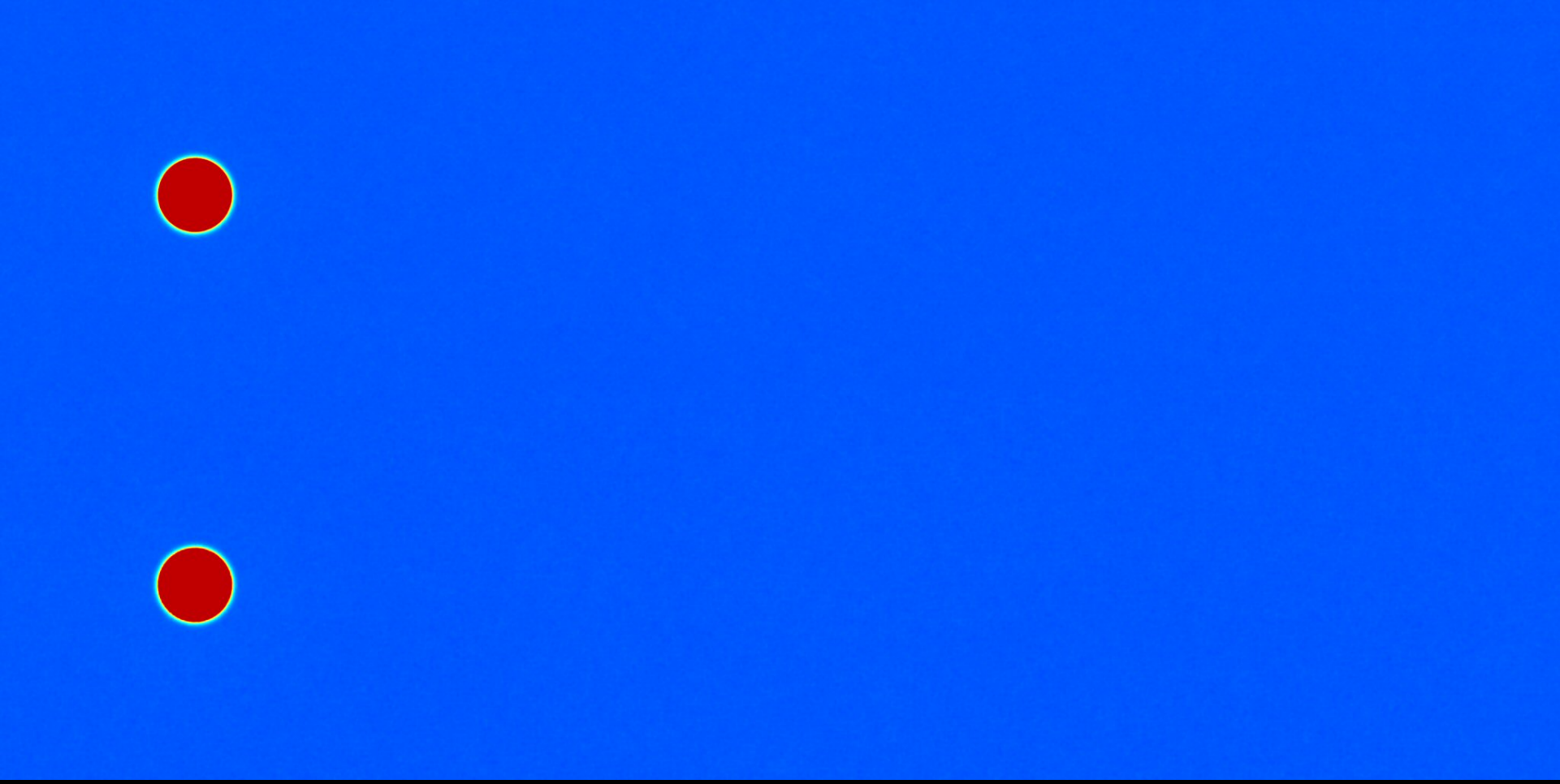

Oscar Agertz + many (2006)

A code comparison sph/grid on turbulent stripping of an infalling cloud

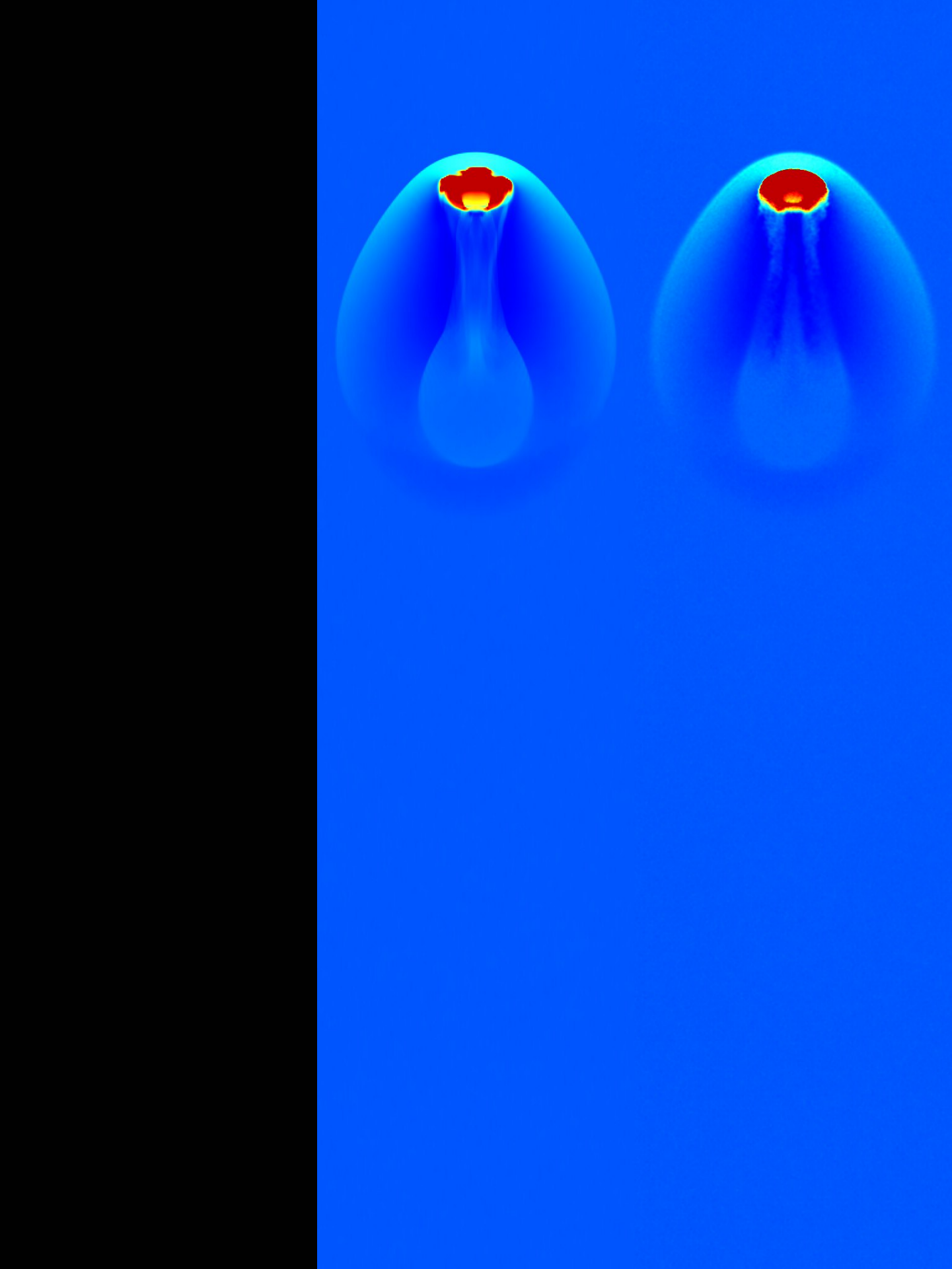

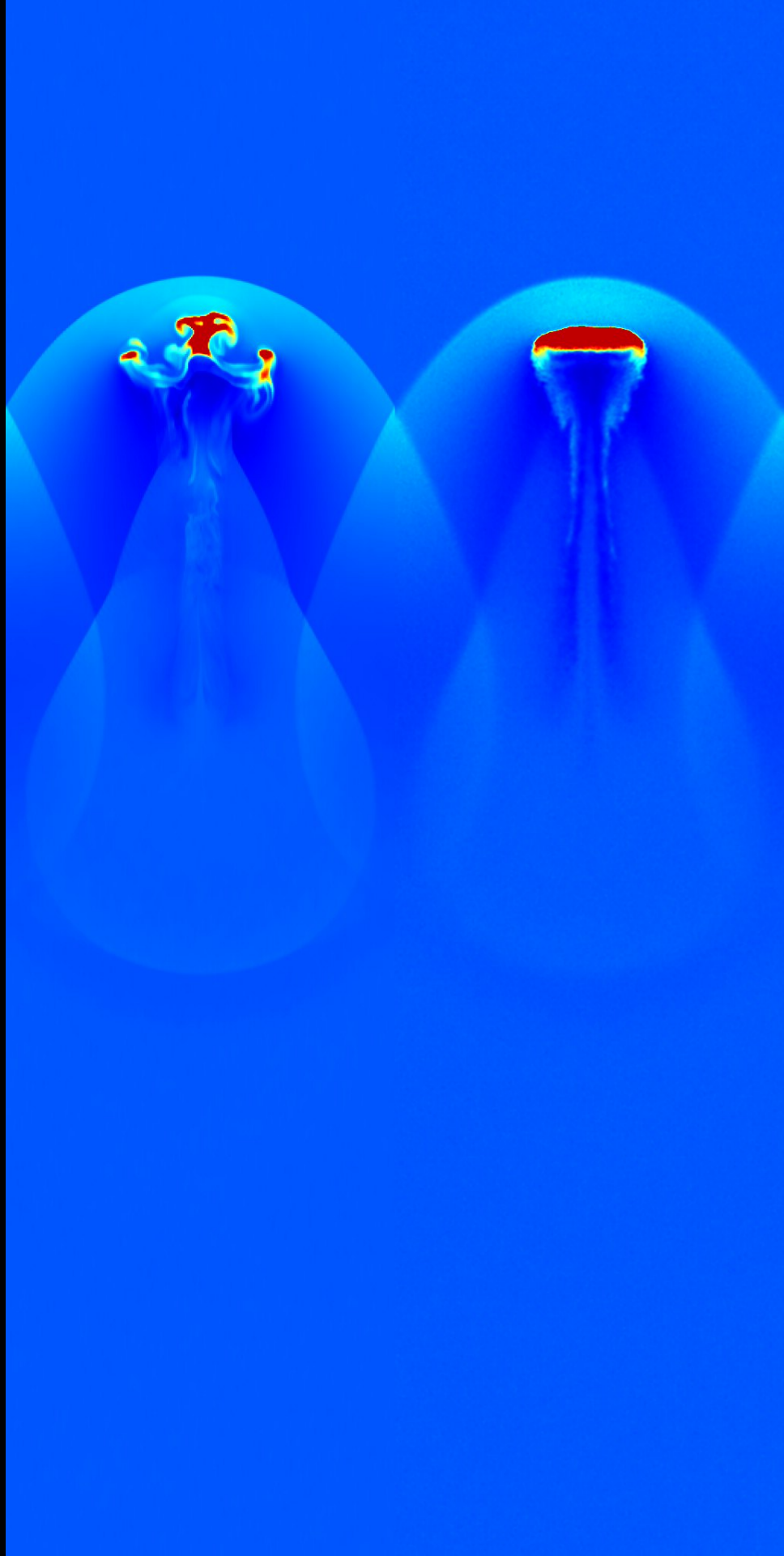

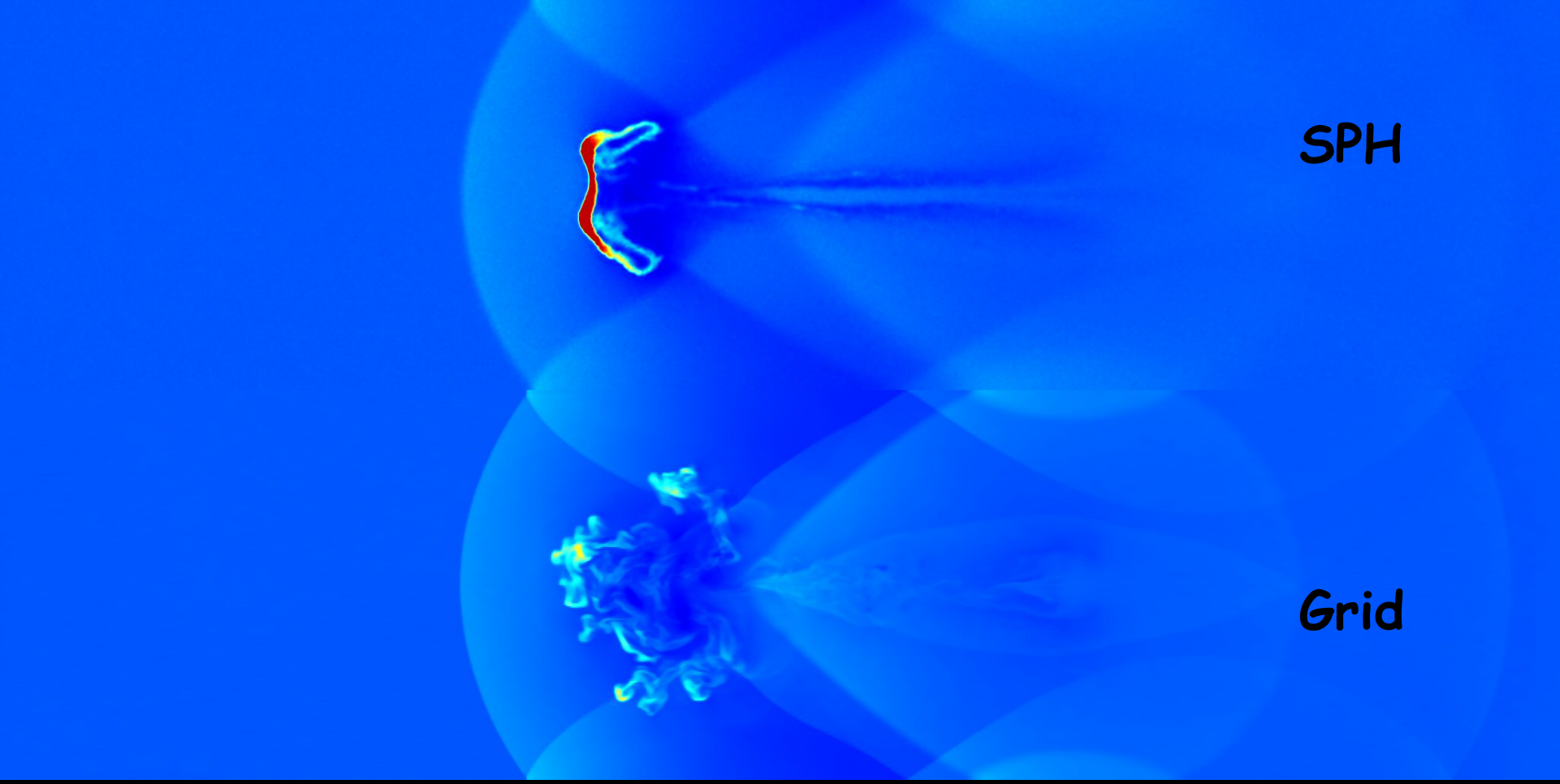
SPH
Grid

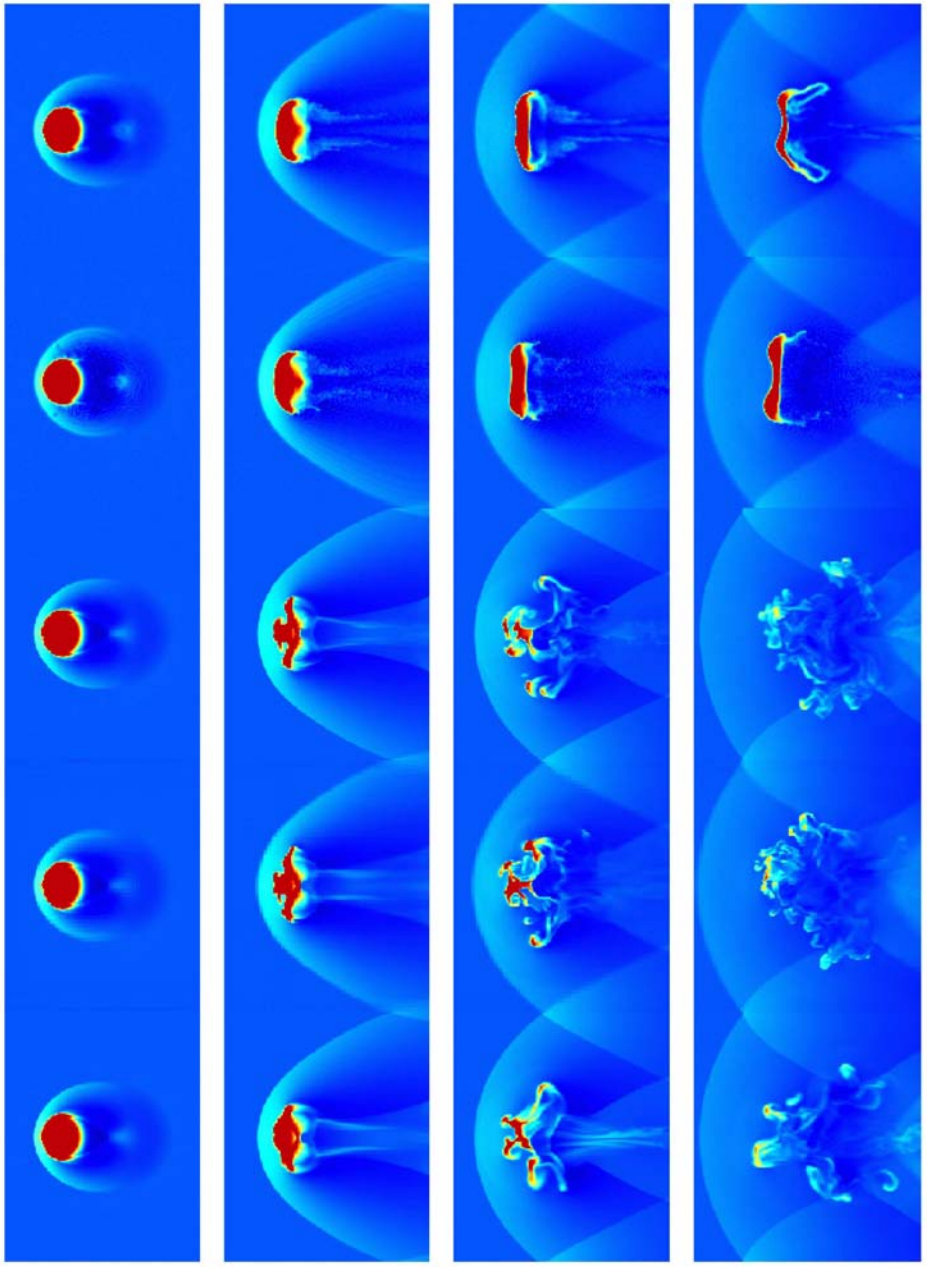

Figure 4. Central density slices roughly centered over the cloud at $t = 0.5, 2.0, 3.5$ and $5.0\,\mathrm{Gyr}$. From top to bottom we have Gasoline (Gas_10m), GADGET-2 (Gad_10m), Enzo (Enzo_256), FLASH (FLASH_256) and ART-Hydro (ART_256). While the grid simulations clearly show dynaimcal instabilities and total fragmentation, the SPH runs do not produce any of this and basically only looses gas due to ram-pressure stripping.

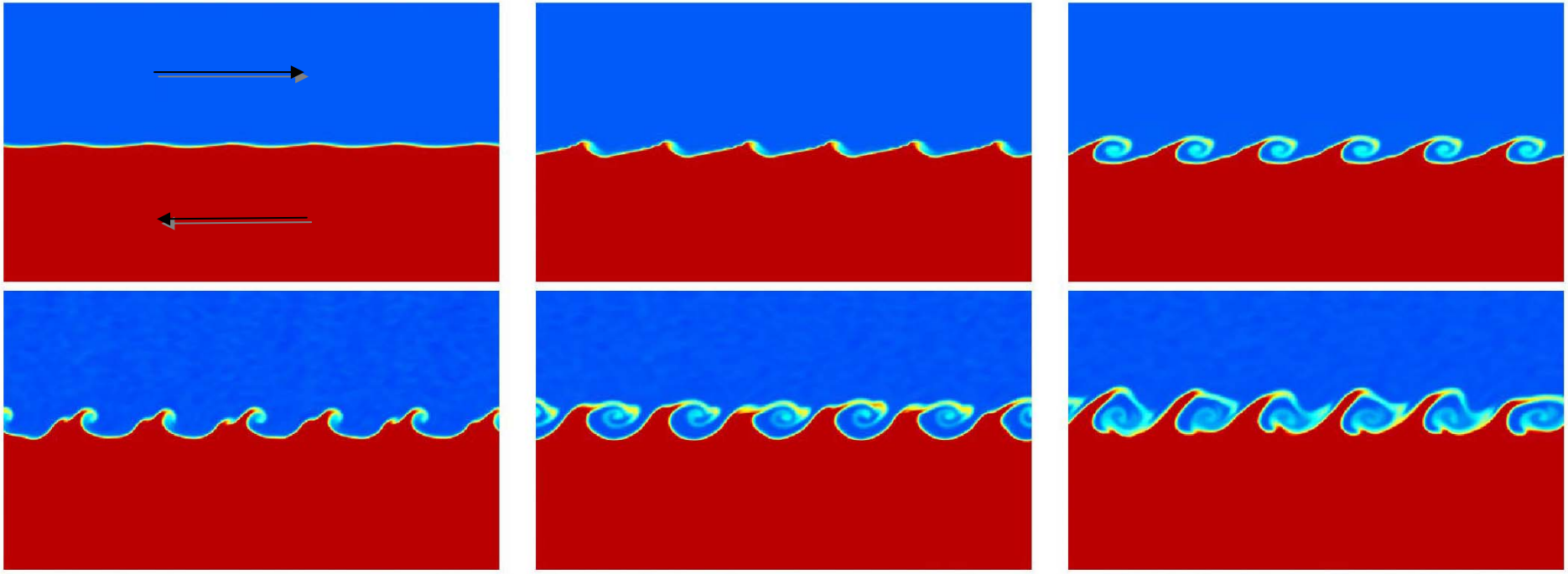

Grid code

SPH code

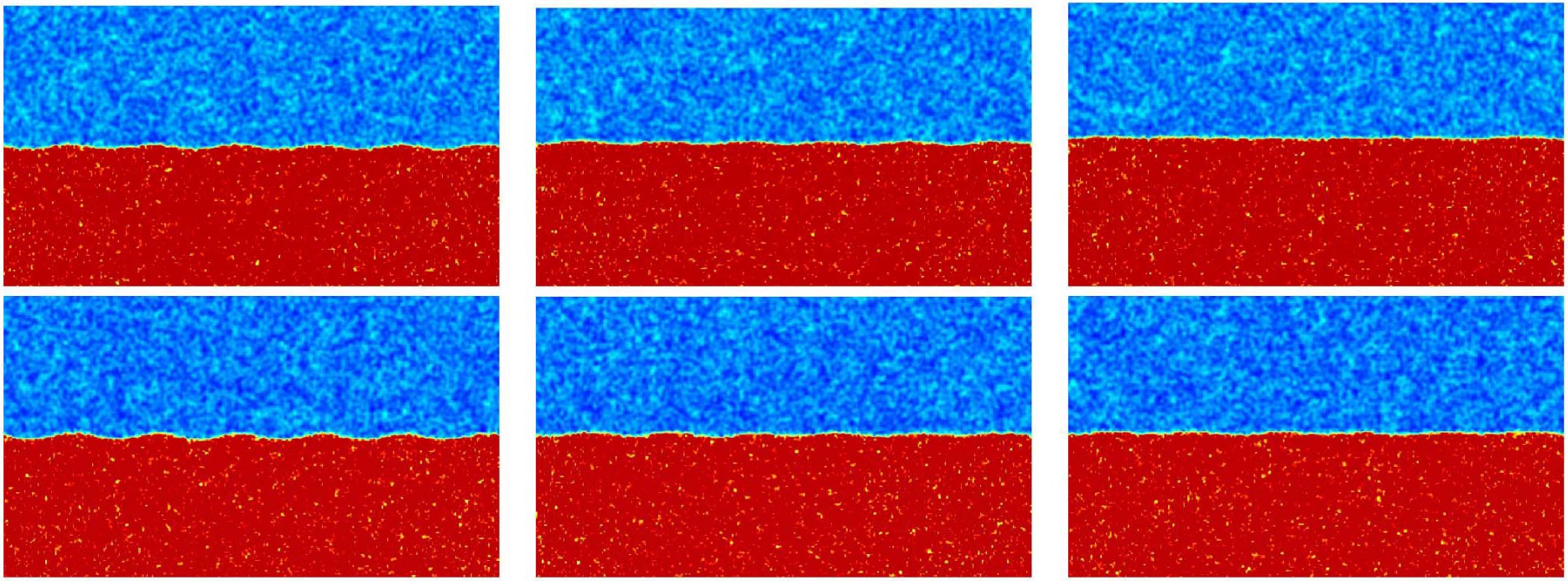

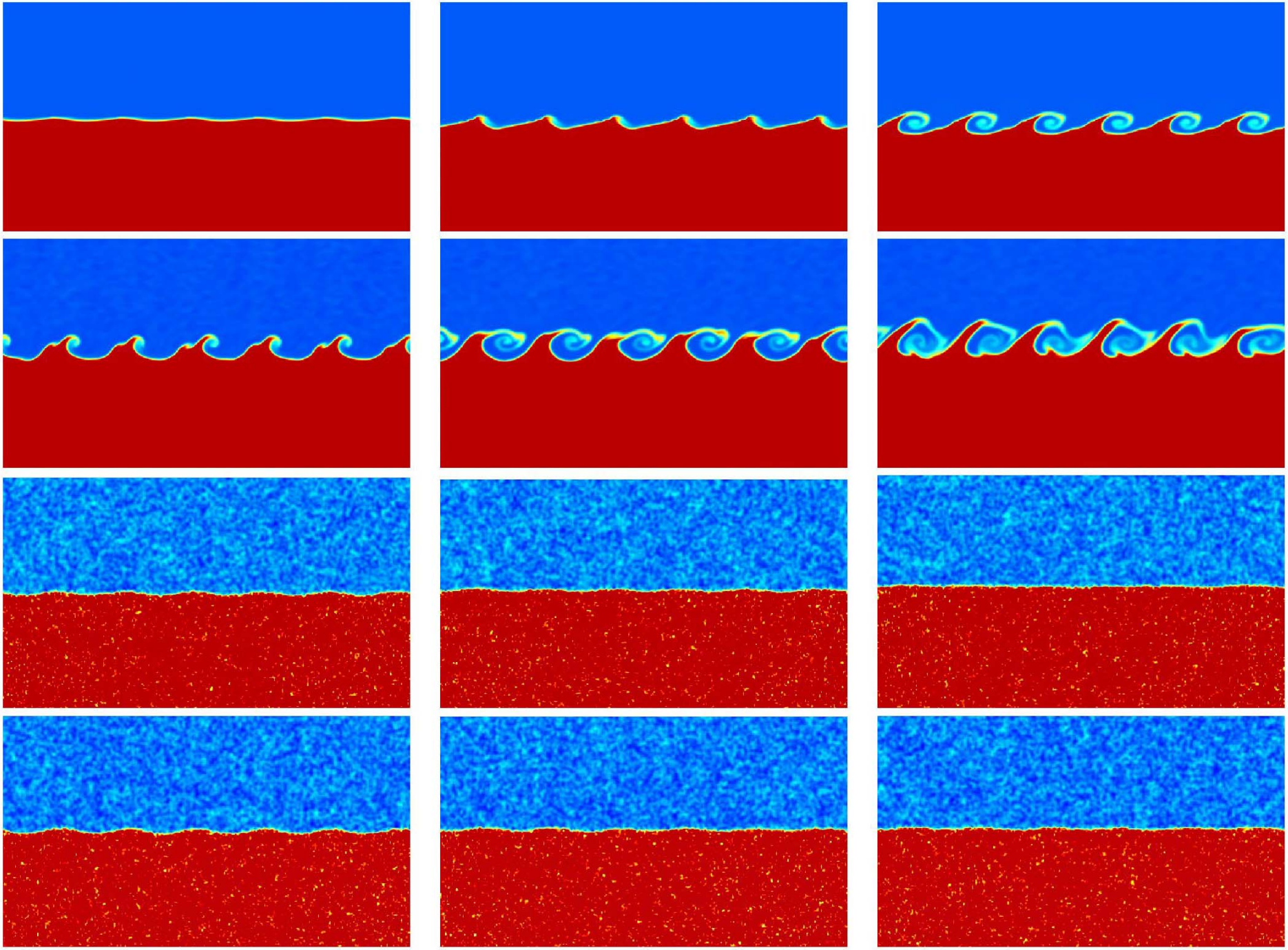

Oscar Agertz et al (2006) "mind the gap"

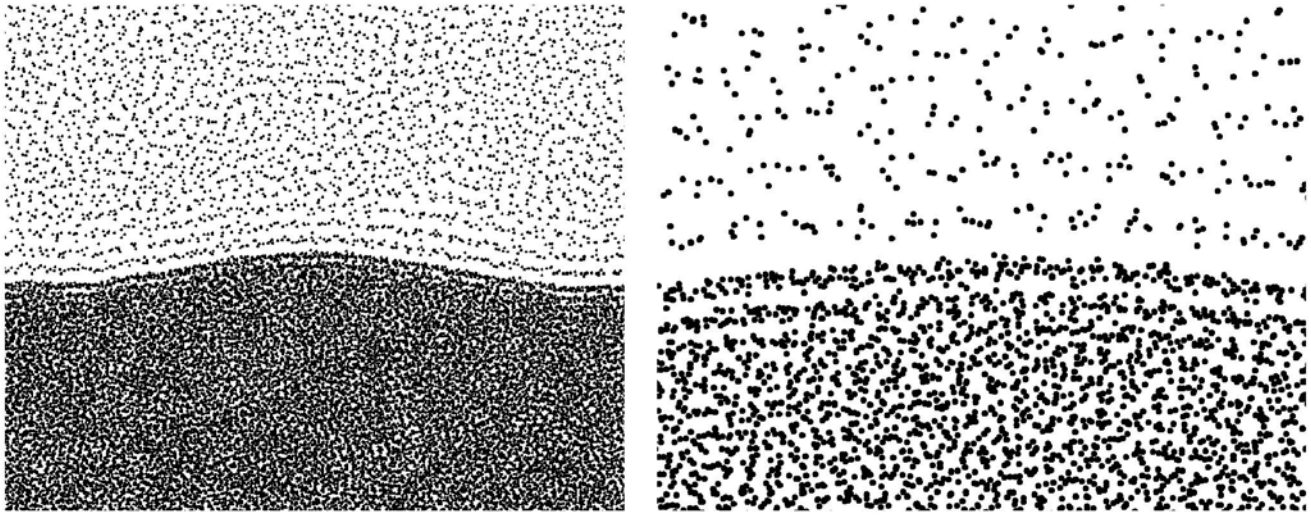

Figure 10. KHI.

Summary

- Gas accretion and evidence for a Galactic cooling flow
- A direct measurement of the spin parameter of the Halo
- Cold accretion and the origin of polar ring galaxies
- SPH can't model gas accretion/interaction